

**RESEARCH ON THE HUMAN PHYSIOLOGIC RESPONSE TO PROLONGED
ROTATION AND ANGULAR ACCELERATION**

A. Engineering Activities

**W. E. ROTHE
EDWARD E. POPE**

B. Physiologic Activities

**SAMUEL T. LIM, M.D.
JOHN G. FLETCHER, Ph.D.**

FOREWORD

This work was accomplished under contract No. AF 41(609)-2897 and task No. 793003, from January to December 1966. The paper was submitted for publication on 24 May 1967.

W. E. Rothe of Systems Research Laboratories was project manager. Dr. Sidney D. Leverett, Jr., Biodynamics Branch, USAF School of Aerospace Medicine, was monitor, and Dr. Robert Cramer was co-monitor.

Section A presents details of structure and original performance of the vehicle; of the engineering program leading up to flight testing; and of the telemetry system installed to allow observations to be made continuously during manned rotation.

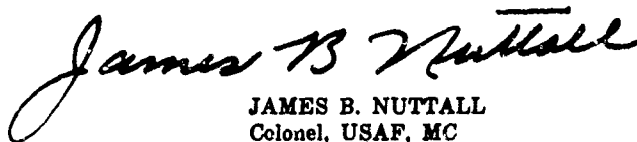
Section B describes the safety program, the experimental plan, and the program with physiologic and environmental observations. In all, 138 experiments were made on 7 men, and the records given are typical of those obtained at rpm's up to 16— in pitch, roll, or random axis rotation—in flights lasting 1 to 30 minutes. These investigations were performed by Webb Associates under subcontract.

The authors are grateful for the help of the following: Dr. Paul Webb, Vincent Blockley, and H. C. Rothe, who served as consultants; Rufus Fairchild, Technical Sergeant Herbert Gannon, William Bowie, and Jamy L. Jaggars, who gave technical support; Major William K. Brown, Captain Jerry F. Meyer, Major Robert M. Olson, Captain James D. Rogge, and Captain Hugh F. Stegall, who were medical monitors.

Special recognition should be given the subject panel: Airman Third Class R. A. J. Dottore, Technical Sergeant J. C. Nichols, Technical Sergeant E. R. Osbon, Lieutenant V. Reynolds, Technical Sergeant A. Rost, Airman First Class A. Sepulveda, and Airman First Class W. T. Springfield, Jr. The subjects cooperated magnificently in a strenuous environment and under adverse conditions.

Extended flights and flights at higher rpm will be attempted as soon as structure, control, instrumentation, and safety engineering permit.

This report has been reviewed and is approved.



JAMES B. NUTTALL
Colonel, USAF, MC
Commander

ABSTRACT

The first phase of a physiologic research program was conducted to explore the responses of humans to rotation and acceleration. The test vehicle was the Rotational Flight Simulator, an air bearing suspended sphere with unrestricted rotational freedom propelled by internally mounted inertia rings and, in the later phase, complemented by a single axis external drive assembly. Engineering efforts established the dynamics and improved the control of the test vehicle. Instrumentation was provided for the readout, display, and recording of significant data serving for physiologic evaluation and medical monitoring. The data were telemetered; pictorial display of the subject and two-way communication links were provided. A total of 138 experiments yielded valid physiologic and human performance information in a rotational environment from fractional to 16 rpm and for several minutes to a maximum of 30 minutes. The subject panel consisted of 7 young, healthy males (USAF personnel) that served previously as subjects in the centrifuge.

Results of the study indicated: The Rotational Flight Simulator properly used and instrumented represents a valuable and unique test vehicle. Changes in heart rate and ECG readings depended on body position with respect to gravity. Electro-oculogram, subjective sensations, incipient nausea, and ability of the pilot to right the stationary sphere after tumbling were all dependent on the rate, duration, and axis pattern of rotation.

CONTENTS

	<i>Page</i>
Section A	
I. Introduction	1
The Rotational Flight Simulator	1
Capabilities of the RFS	2
Earlier work on the RFS	3
II. General Preparations	3
Other considerations	4
Safety measures	4
III. Engineering Efforts	4
RFS dynamic testing	4
Internally and externally controlled drive systems	6
Inertial instrumentation (instantaneous position and rate readout)	6
TV system	8
RFS intercom system	9
Environmental control of RFS	9
Basic instrumentation setup	9
Development of physiologic instrumentation	11
Special instrumentation	17
References	19
Addendum 1. The Motion of a Rotating Sphere Under the Influence of a Body-Fixed Torque	21
Addendum 2. RFS System and Equipment Layout	26

	<i>Page</i>
Section B	
I. Introduction	31
II. Summary and General Conclusions	31
III. Materials and Methods	32
Safety problems	32
Equipment	33
Subject preparation	33
Cardiovascular response	33
Hot and cold ambient air temperatures	35
Water immersion	35
Performance decrement and disorientation	36
IV. Results	36
Cardiovascular system	36
Hot and cold temperatures	39
Water immersion	39
Disorientation and performance decrement	45
V. Discussion	49
Cardiovascular system	49
Effects of ambient air temperature	75
Effects of water immersion	75
Pilot performance and motion sickness	75
Bibliography	76
Appendix 1. Personal Data	79
Appendix 2. Methods for Instrumenting Subjects	80
Appendix 3. Scheme of Experiments	87
Appendix 4. Experiment Protocols	89

RESEARCH ON THE HUMAN PHYSIOLOGIC RESPONSE TO PROLONGED ROTATION AND ANGULAR ACCELERATION

A. Engineering Activities

I. INTRODUCTION

In aerospace studies it is important to learn how man responds physiologically to rotational and angular accelerations. We wished to examine cardiovascular, respiratory, oculomotor, and subjective sensations to movement in various planes of rotation. The Rotational Flight Simulator (RFS) at the USAF School of Aerospace Medicine was the facility to be used in accomplishing these studies. The engineering work was to support the test plan by determining and improving the dynamic response and control of the RFS facility.

The physiologic experiments required a step-by-step development of basic and specific physiologic sensing instrumentation, the installation, checkout, and maintenance of the telemetry, display, and recording system, and the necessary dynamic and physiologic instrumentation.

The Rotational Flight Simulator

The RFS facility was designed as a device capable of simulating the rotational flight control problems expected to be encountered in manned flights. It consists of a fiber glass sphere (10 ft. in diameter) comprising power control and telemetry elements. The sphere is supported by a pressurized air bearing provided by a stationary cylindrical pedestal and fed by a compressor/air supply system and external control console. Display, recording, monitoring, and control consoles, as well as TV display and two-way communication systems, are stationed nearby.

Structure. The sphere is constructed of a 2-in. layer of nylon honeycomb with fiber glass faces on each side. It is coated with abrasion-resistant polyester (0.1 in. thick). A vertical bulkhead in the sphere supports the seat and other equipment, and divides the two compartments—the subject compartment and the instrument (hydraulic control system) compartment. Two doors are located approximately 180° from each other.

Air bearing. The original air bearing system relied on the single cup "hole in center" principle and required large quantities of air (1,200 std. c.f./min. at 20 p.s.i.) to achieve free floating conditions. (This type of air bearing imposed restrictions on the maximum safe rotational speed and a contract was let to remedy these shortcomings.)

Air-conditioning. An air-cooling system allows the sphere to maintain approximately a 70° temperature during runs not to exceed 1 hour. This system was supplemented by a special window-type air-conditioner for certain tests. Cooling is achieved by a replenishable ice supply. Ice water is circulated through a heat exchanger and the warm water is returned to the ice tanks where it is again chilled.

Propulsion drive system. Rotation of the simulator is achieved by driving three large inertia rings located in the three principal planes of the ball. Driving of a ring in one direction causes the simulator to rotate in the opposite direction.

The rings are energized by activation of the "joy stick" by the subject within the sphere

or by control switches at the outside control panel.

Hydraulic system. The rings are propelled by friction drive wheels connected, through a solenoid-operated magnetic clutch, to a hydraulic motor. The pressure driving the hydraulic motor is controlled and regulated from the main system pressure through a servo control system. The hydraulic system originally presented a severe safety hazard. It was rebuilt by Government personnel for utilization of nonflammable hydraulic fluid.

The main system pressure is supplied by a hydraulic pump driven by an electric motor (60 v., d.c.) which, owing to its design, was another limiting factor for long-term high-acceleration test runs and reliability.

Main battery and charger system. Seven 12-v. storage batteries are mounted inside the sphere and provide power for operations. Five of the batteries serve the hydraulic system. Two batteries supply power for all other instrumentation and telemetry of the simulator.

Radio control. The Rotational Flight Simulator's drive control system is operated externally by control switches on the radio control transmitter located in the external console. The amount of radio command acceleration is adjustable throughout the total capability range of the drive system. Adjustments are made by setting the gain potentiometers at the control amplifier in the sphere.

Telemetry system. The sphere has unrestricted rotational freedom and all information to and from it is transmitted via a telemetry transmitter system located in the simulator.

Television system. Observation of the simulator subject by the external operator is provided by a compact portable television system of broadcast quality.

Voice communication. Direct voice communication between the subject and the external console operator is provided by three commercial "push-to-talk" transceivers.

Air bearing supply system. Air pressure is provided by a remotely located low pressure/high flow compressor (800 std. c. f./min.) and a jet starter (1,200 std. c. f./min.). This system is subject to overhaul in the subsequent phase of the program.

Capabilities of the RFS

Dynamic and control characteristics. The RFS represents a unique test vehicle that in its dynamic response closely resembles a space vehicle with respect to rotational motion—except for the presence of gravity, of course. The RFS is a vehicle of unrestricted angular motion, featuring only negligible damping. It is propelled by three inertia rings which are arranged in three mutually perpendicular planes and produce body-fixed torques which themselves are rotating with the sphere. Since the external drive system was installed, propulsion is accomplished by torques that are earth-fixed and nonrotating—not fixed to the sphere.

In the assessment of the dynamic and control characteristics we have to differentiate between two modes of operation which are governed by the initial conditions: (a) An angular acceleration is applied to the system while it is at rest or spinning only about the axis around which it is accelerated. (The sphere has no angular momentum about any other axis.) (b) An acceleration acts on the system which has an angular momentum in a direction that does not add or subtract from the original angular momentum.

These two conditions cause radically different dynamic responses. Furthermore, in the case of *b* above, the dynamic response of the sphere differs because of torques applied by the *inertia rings* (body-fixed and rotating) in contrast to those produced by the external drive system (earth-fixed and nonrotating).

Attitude and motions of sphere accelerated from the initial rest position. Assuming the configuration at rest as the initial condition, the sphere will, not considering air bearing turbine torques, react with a spinning motion in opposite direction of the inertia rings

energized, or in the direction of the torque applied by the drive wheels of the external drive system. The direction of the rotation axis can be predicted by the rules of simple vector compounding.

The sphere assumes the characteristics of a gyroscope with consistently increasing angular momentum as long as an acceleration prevails. As soon as the acceleration stops and a rate prevails, the angular momentum remains fixed.

For a sphere not equipped with external drive system the spin axis of the sphere describes a small cone angle if the spin axis is not coincidently the axis of the greatest or smallest moment of inertia of the sphere. Owing to the viscous damping of the air bearing the sphere, in that case, it slowly moves to align its axis of the greatest moment of inertia with the axis, about which the acceleration was supplied. The amount and angular speed of these nutations depend on the difference of the moment of inertia and on the viscous damping. It is assumed that the damping provided by the external drive system will successfully cope with this phenomenon and the nutations be attenuated to negligible magnitudes.

Attitude and motions under dynamic conditions. The dynamic response of the sphere changes radically if an angular momentum prevails at a time when an acceleration is applied which does not directly add to or subtract from the inherent angular momentum. Addendum 1 discusses a typical case for the system when governed by inertia rings only, and addendum 2 gives the case of a sphere equipped with the external drive system. In these cases dynamic responses occur which are governed by the gyro precession torques ($M_d = I \times \omega$) and the moment of inertia torques, and require for accurate determination a computation of differential equations. In a case of purely inertia ring control, an input was applied to the Y ring with a spin vector at 90° to the plane of rotation. The resulting motion was a spiraling of the spin axis which opened up to a certain maximum cone angle and then decreased again. See figure 1, addendum 1.

The frequency and magnitude of this spiraling effect is a function of the ratio of the moment of inertia of the two axes involved. In the case that the moment of inertia about both axes becomes equal, the spiral increases until the motions induced fall in the plane of the original rotation. The obvious reason for this wobble is that the acceleration applied occurs about a sphere-fixed axis, which itself rotates with the sphere so that the torque assumes positive and negative values if observed from the outside. A case was investigated in which the sphere was propelled by the external drive system. In these calculations damping was not considered and it was found that the sphere would respond with a series of short oscillations of relatively small amplitude around the originally selected axis (fig. 2, addendum 1). This excursion would shortly subside and the sphere would mainly follow the gyro law and precess in direction of the third coordinate. This precession interestingly will not be performed in a uniform fashion but at retarded-accelerated rates caused by the superimposed excursions mentioned above.

Earlier work on the RFS

The technical personnel of the Government brought the RFS system to a reasonable operational and safe status. The TV system was improved, a jet starter was added in the air supply system, and a fire hazard presented by inflammable fluid used in the hydraulic system was removed. The latter activities involved complete refurbishing of the hydraulic system and rewiring of the sphere.

II. GENERAL PREPARATIONS

The generation of a meaningful test plan required a reasonable knowledge of the capabilities and the dynamic response of the test vehicle. The information available was incomplete, outdated, and in part contradictory to theoretical engineering investigations.

Severe restrictions were realized: (a) in procedures that required the setup and maintenance of a clear axis of rotation; (b) in procedures that required rotational speed in excess of 12 rpm; (c) in procedures that required the

maintenance of medium rotational speeds for longer periods of time (in excess of 10 minutes); and (d) in general performance and environmental conditions bearing directly on the safety of the subject.

Informed as to these findings, we devised an acceptable physiologic test plan that retained a necessary amount of flexibility.

A number of remedial engineering actions relied in part on rudimentary operations (e.g., low-speed single-axis rotation was at times produced manually and later on by means of a temporary and adjustable external drive system). Subsequently the supporting instrumentation, telemetry, physiologic instrumentation, display, and recording systems were installed, refined, or newly developed and supplemented in accordance with demands from the medical monitor or the physiologist.

An external drive system had to be designed and procured. Detailed drawings of subassembly and system assembly were prepared. The system was designed to provide rotational speeds up to 50 rpm and maximum accelerations of 0.200 rad/sec.²

Other considerations

The air bearing and unsphericity of the RFS resulted in a very high noise level, making external operation communications very difficult. The external console arrangement was limited in that it did not have sufficient space for system operation, dynamic output data, and physiologic data and maintenance. The internal RFS arrangement reflected inadequate safety and maintenance considerations for such a highly experimental test vehicle.

Safety measures

The novelty of the test vehicle and its history necessitated a methodic review of safety hazards that could occur during the experimental test phase. Extensive efforts were made to assure maximum safety for the subjects undergoing physiologic experiments. Applicable Air Force Regulations were used as guidelines, and a comprehensive safety plan

was devised as shown in figure 1, displaying the foreseen events and the precautionary measures taken. The complete physiologic test plan was submitted to the subjects who were to undergo the tests. To assist in the actual operational procedures, a safety checkoff list and specific assignments were given everyone participating in the experiments. Subsequently, a number of safety drills were performed. It was found that a subject, in the event of a catastrophic failure, could be removed from the sphere within 18 seconds. Within these activities, also, the restraining harness for the subject was modified by the Air Force personnel. An independent breathing air supply system and mask were installed and instrumentation was relocated to assure free access to the subject.

III. ENGINEERING EFFORTS

(Note: No differentiation is made in this section between tasks performed by the team of Government technical personnel and those of SRL engineering personnel which worked as an integrated team on essentially all instrumentation described hereafter. Addendum 2 discusses the composite system and equipment layout.)

RFS dynamic testing

Preliminary performance predictions of the RFS were made and fundamental tests performed as a basis for the physiologic test plan.

Within these activities a test program was designed for maximum utilization of the RFS with an ambitious aim of 3 to 4 dynamic runs per day. Operation of the rings by the external manual control switches was augmented by an automatic control system (ACS). This system was designed from a mathematical estimate as to the desirable input pulses to the rings which would normally be accomplished by intermittent operation of the external control switches and now would be a preset operation rate controlled by an automatic control system. The intermittent duty cycle of the hydraulic motor dictated relatively short inputs to the rings in the 0- to 10-second range. The automatic control system made repeatability possible and thus minimized the complex dynamic characteristics of the RFS.

The test program revealed the extremely low MTBF (mean time between failure) of the RFS facility. Difficulties included frequent malfunctions of the jet starter, unreliability of the auxiliary control system, and not having a continuous fuel supply, to mention only a few. The latter problem was resolved by increasing the jet fuel storage capability at the place of activity.

Finally the hydraulic motor proved to be the prime limiting factor. Because of overheating, its duty cycle was restricted to less than 18%. Considerable effort was made to provide for additional cooling and some improvement was noted. The duty cycle was carefully monitored by a special motor duty cycle and temperature instrumentation system developed specifically for this test program.

The ACS ultimately permitted RFS single axis rates above 12 rpm for 30 minutes. The RFS attitude control problems remained during the longer runs, and the limitations imposed by the hydraulic motor limited the system to single ring operations.

The combination of RFS imbalance, unsphericity, and air bearing inefficiency prevented accurate attainment and maintenance of low rates and attitude by means of inertial ring control. The threshold for this uncertainty was at 3 to 5 rpm.

Time limitation and excessive maintenance problems precluded further dynamic analysis and subsequently a flexible and modest physiologic test plan was formulated.

Internally and externally controlled drive systems

The original RFS featured an internal drive system which could be activated internally or externally. The lack of supporting dynamic data precluded any but a theoretical estimate of the actual RFS dynamic performance. The marginal design of the electromechanical components required consistent maintenance and resulted in time losses. Rudimentary modes were devised that assured a reasonable systems

reliability. In radical cases, for example, a pair of suction cup axials were attached to retain a desired axis of rotation and the sphere was propelled by hand (fig. 2). Later a basic single axis external drive assembly was designed and installed (fig. 3). This system proved to be very effective.

Inertial instrumentation (instantaneous position and rate readout)

The inertial RFS instrumentation for the assessment of speed consisted of only an open loop readout system relying on three external rate meters. Each meter represented the respective rate in rpm of the inertia rings. The rate signal is derived from a tachometer generator mounted on the drive wheel of each respective ring and represents rates of the drive wheel, the inertia ring rpm (less slippage), and only in a relative manner the true rates of the RFS itself. The internal instrumentation included a three-axis attitude indicator and meters to assist the subject in orienting himself. It was necessary to have an inertial reference system to provide information as to the orientation of the subject. For this reason a three-axis, subject-oriented rate gyro system and a three-axis accelerometer system were incorporated. The accelerometers are used as gravity sensors to indicate subject orientation relative to gravity (figs. 4A, B, and C).

The rate gyro units (figs. 5A and B) consist of a U. S. Time Corporation subminiature precision rate gyro, model SD-400, and the related electronic circuits (1, 2).

The accelerometer package consists of bridge excitation circuitry for the accelerometers and a differential amplifier to condition the accelerometer output for the voltage control oscillators (VCO). The accelerometers are referenced to the subject/sphere axis so that a subject orientation relative to gravity is indicated at any given time and can be extracted from recordings. (The superimposed centrifugal forces are comparatively small at the rotational speeds experienced.) The accelerometer units (fig. 6) consist of a Statham model F-2-350 linear accelerometer excited



FIGURE 2

The application of suction cups to retain single axis rotation.

and calibrated according to manufacturer's instructions, with the low level output amplified by a Philbrick PP65AU operational amplifier in a differential configuration. R_c was adjusted to give a calibrated signal equal to 1 G. The balance potentiometer can be set to read + 1 G, 0 G, or -1 G as desired without affecting the basic 1 G calibrated signal.

TV system

This instrumentation was considered essential for the safety and physiologic evaluation during test runs. Although the present system was operational, it showed poor resolution and instability. The video transmitting system was modified to include a front end

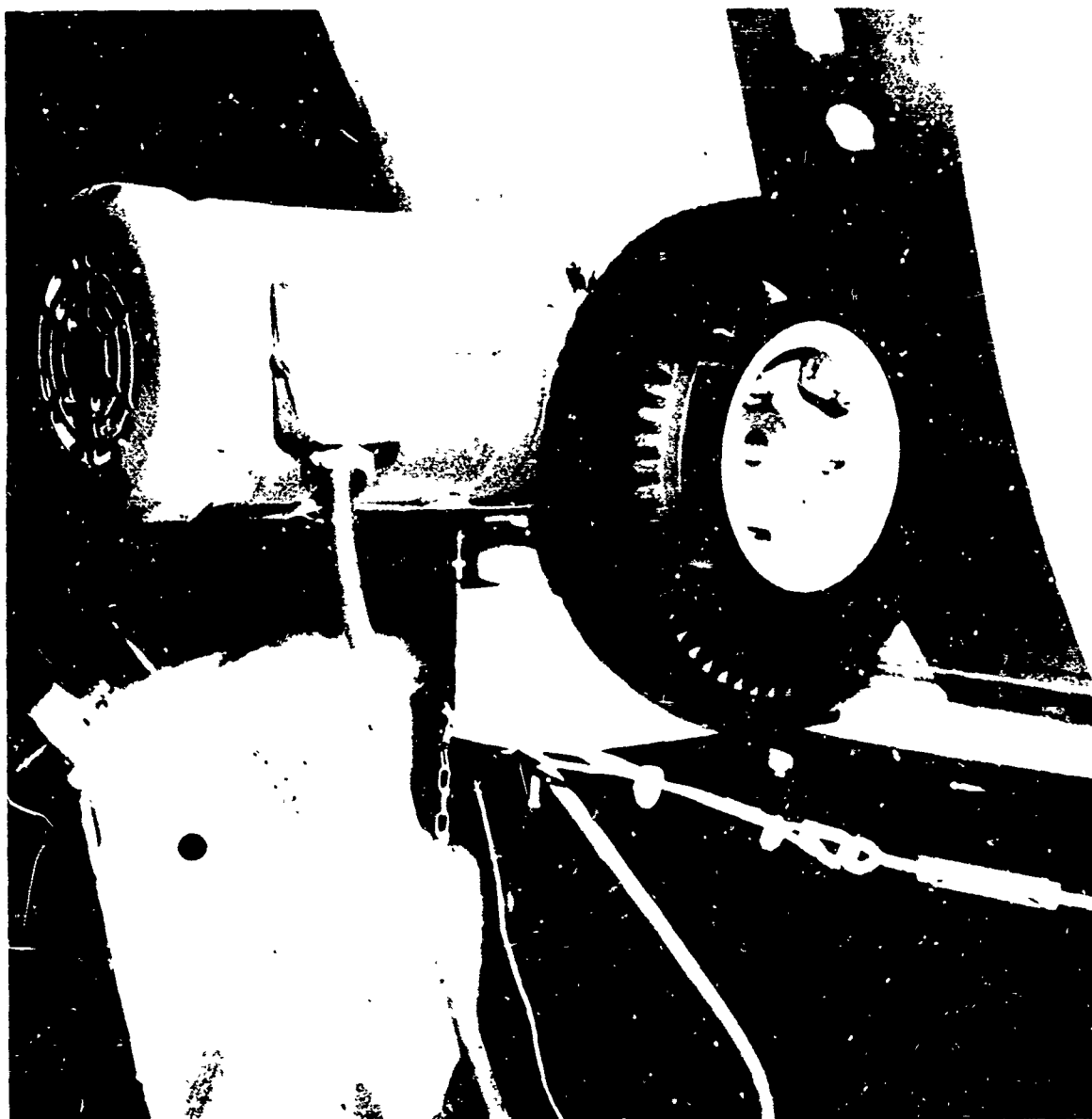


FIGURE 8

The mounting and arrangement of the single axis external drive system.

video amplifier with an emitter-coupled modulator. This significantly improved the quality of the picture and the stability of the basic synchronization pulses. A spare GE No. 4TE9A3 camera replaced the marginal Dage No. 340B camera unit. The TV mount was modified to accommodate this camera, and special connections of the external power plug were provided.

The new TV system performs remarkably well except for momentary fading when the antenna revolves in the air bearing cup.

RFS intercom system

The RFS external communication survey showed that a standard aircraft intercom system would be satisfactory. The system finally decided upon was an AN/AIC-10 USAF intercom system which would be modified to accommodate the special control function of the RFS facility and the FM telemetry link for communication with subject.

The system was designed for maximum growth potential and flexibility. It was installed and modified to meet RFS specific needs. To improve the signal-to-noise level and provide for automatic frequency control, a new external FM receiver was installed.

Environmental control of RFS

In the later phases of the test program, work was started toward controlling the internal environment of the RFS. The existing system provided only for cooling the RFS. The limit was about 70° F. A commercial room air-conditioner was connected to the RFS and thereby reduced its static temperature to 50° F.

There was no provision for heating the RFS. By use of small electric space heaters powered by the external a.c. line power, the RFS temperature was raised to 100° F. for static conditions. Since the RFS is a good thermal insulator, the static temperature could be held for short runs.

For future prolonged runs and dynamic temperature control a more sophisticated thermal system will be required.

Basic instrumentation setup

The RFS has a space- and power-limited environment. The basic sources are 24-v. direct current and 115-v. at 400 Hz. Power consumption is a constant consideration. The RFS is an electrically insulated sphere resting on an electrically grounded base. Because of its self-contained nature, the RFS resembles, in many ways, the environment of an airborne system. All RFS systems must be capable of performance in an aircraft-type environment.

Telemetry system. The telemetry system (fig. 7) consists of a Bendix TXV-100 telemetry transmitter (TX) with center frequency at 235.5 msec./sec., 12 TOE-305 voltage controlled oscillators (VCO) and one TAA-305 mixer amplifier (3). The TX is loaded into an AT-256A/ARL standard UHF aircraft antenna.

The same type of antenna is used to recover the signal from the RFS. The FM receiver (RX) is a Nemes Clarke model 1412. The 12 subcarrier discriminators are Vector model AD-10B. Table I is a listing of the IRIG subcarrier frequencies (3).

The input to the VCO's warrants special attention. This system has an input requirement of ± 1.5 -v. maximum into a 100K-ohm load. The voltage and frequency requirements mean that all dynamic and physiologic parameters have to be conditioned to meet those requirements. This imposes the burden of having a special instrumentation package inside the RFS.

At first we wondered if data could be transmitted from the RFS because it was so close to the grounded pedestal and because the internal antenna would be randomly rotated in 3° of freedom. Fortunately, the recently installed aluminum hydraulic panel was mounted on the approximate rear hemisphere of the RFS and this panel was used as an RFS ground reference. On the panel was mounted the standard aircraft VHF/UHF antenna (AT-256A/ARC). In spite of the limited internal antenna space and constant random antenna

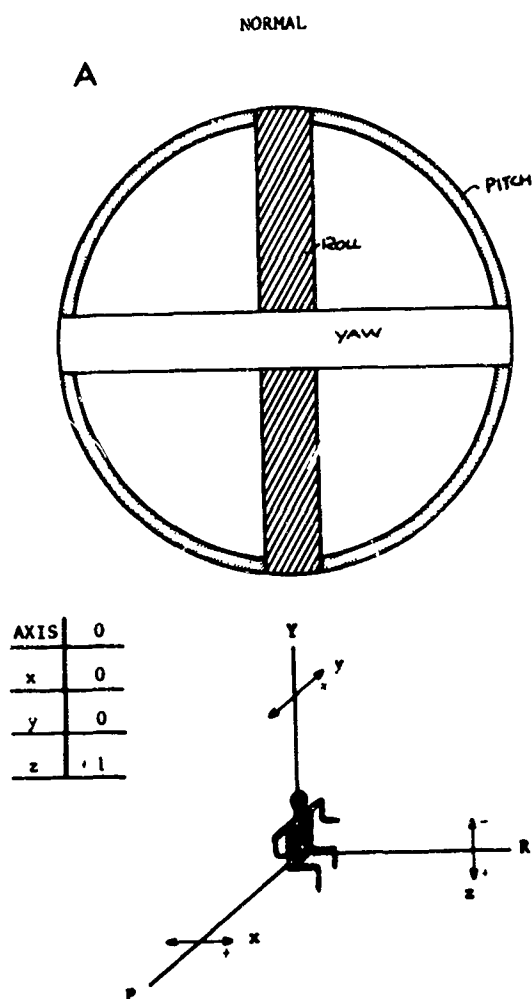


FIGURE 4A

Figures 4A, B, and C display the output of the accelerometer in relation to the subject's attitude as function of G .

orientation, fully satisfactory reception and signal levels were realized. This was due in part to the relatively high transmitter output (5 w.) for the relatively short distance (25 ft.). It was anticipated that with the necessity for several different transmitting systems, the resulting internal reflections would cause serious instrumentation problems. However, such problems proved to be well within reasonable limits.

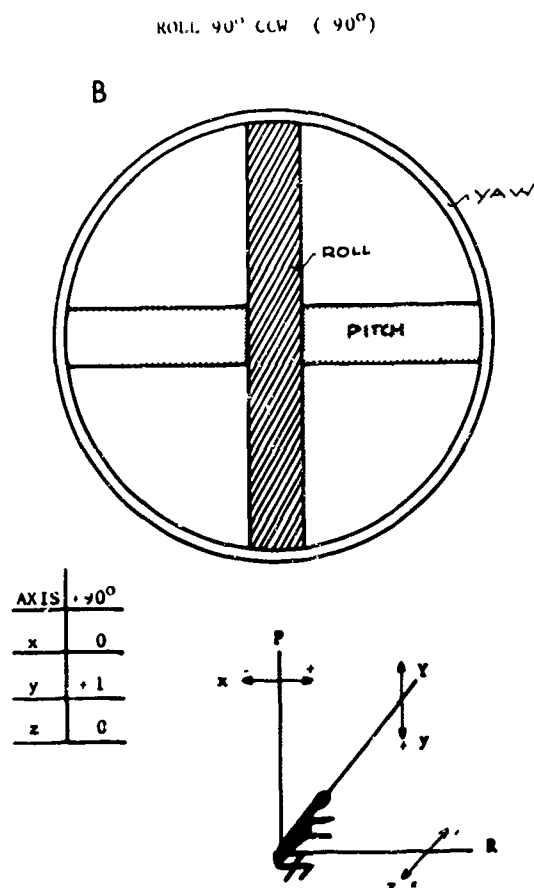


FIGURE 4B

The instrument package used had initially been designed for aircraft use and was modified for the specific needs of the RFS. The package consists of 16 jacks for 8 amplifiers and 8 special circuit boards. The boards are glass epoxy with a 12-pin connector (Vector No. 2811WE). All boards are wired for standard power (± 10 v.), input, and output connections.

Because of the stringent space and power requirements of the RFS, it was necessary that all electronic circuits be reduced or modified to fit the standard instrumentation circuit board. The use of circuit boards provided standardization and overall system flexibility. To change a basic system parameter either dynamically or physiologically requires only the replacement of the respective circuit board

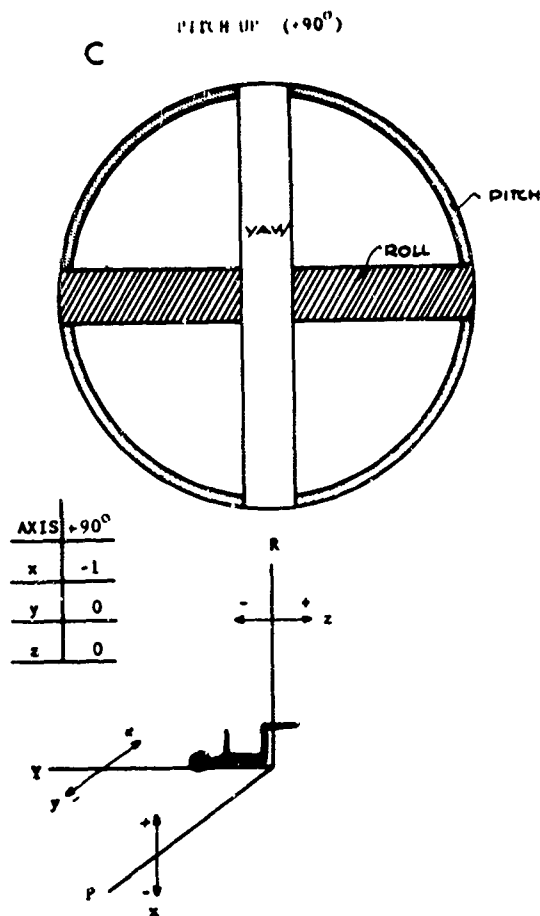


FIGURE 4C

in the internal instrumentation package. The system included a special plug which was modified to provide a safety feature for quick disconnection of the subject's harness.

To increase the signal-to-noise ratio, the subject's cable was replaced by one with special shielding and two additional signal leads. The original power supply was modified by providing a regulation feature. Further improvements included a rearrangement of the patch panel and the addition of a special power test panel independent of the power supply located in the attic area of the RFS (fig. 8). The internal patch panel provides for complete patching flexibility from subject input plug to VCO input, including all the intermediate amplifier and conditioning circuits. In addition a special

power test panel was incorporated to provide for maintenance testing of power supply performance at the internal patch panel. This was desirable because, owing to space limitations, the power supply had to be located in the awkward attic area of the RFS. In addition, special output load jacks were installed to provide for a dummy resistance load for maintenance purposes to simulate the input requirements of the VCO's.

All external interconnections are made through a system patch panel (fig. 9). This panel contains the discriminator outputs, the strip chart recorder input, the medical monitor scope inputs, and a special 8 circuit board conditioning panel. This panel features input and output jacks and a ± 15 -v. supply for use with active circuits and affords conditioning of signals after they are received from the RFS.

In developing the instrumentation system for the RFS the emphasis was placed on developing a system with maximum flexibility, minimum setup time, and calibration time. This effort was realized by designing almost all systems with internal calibration circuits. The three-axis accelerometers and rate gyro can be calibrated by a single three-axis switch. The temperature systems can be calibrated for full range by a unique two-switch configuration at the top of each respective circuit board. The blood pressure ramp can be calibrated from the external console.

Data recording and physiologic monitoring. All data reception, recording, and monitoring were done at the RFS recording facility. The recorder consisted of an 8-channel real time Beckman ink recorder. Although the telemetry system has a 12-channel capability, 8 channels of data were sufficient for the testing. The medical monitor scope was an 8-channel Sanborn 700 series.

Development of physiologic instrumentation

The initial configuration of the RFS was completely void of any physiologic instrumentation. The TV system was satisfactory for safety and general subject conditions, but the camera lacked sufficient resolution for it to be useful in photographing physiologic data.

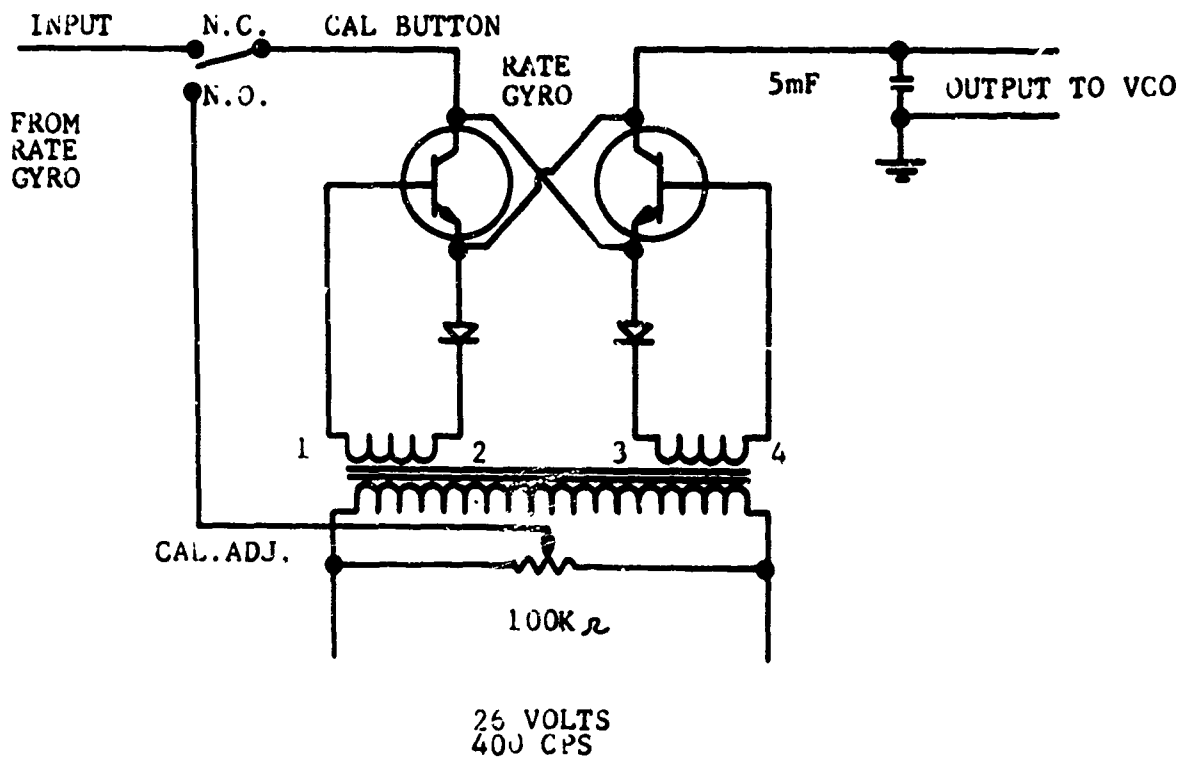
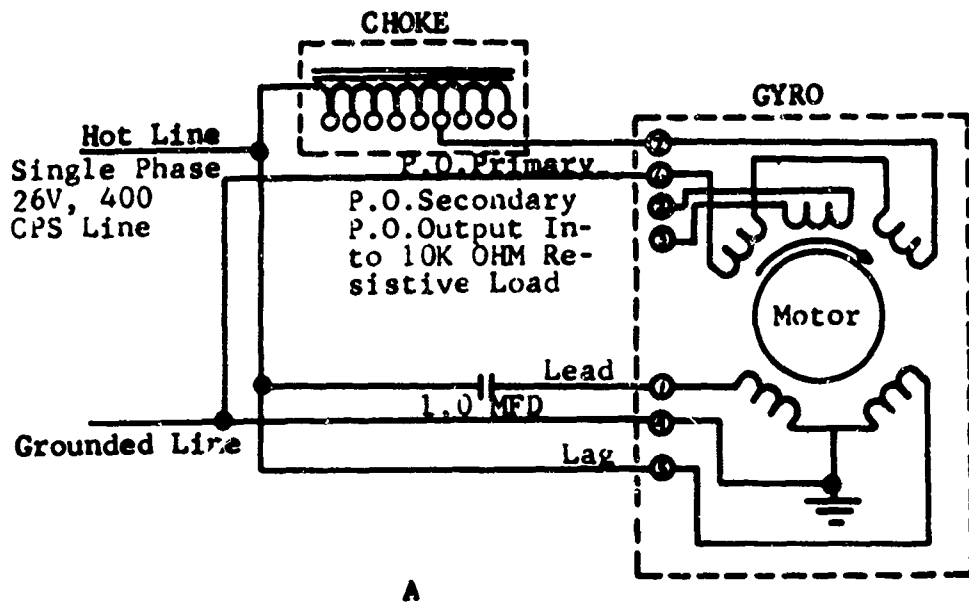


FIGURE 5

A. Diagram of excitation of the gyros.

B. The demodulation circuitry.

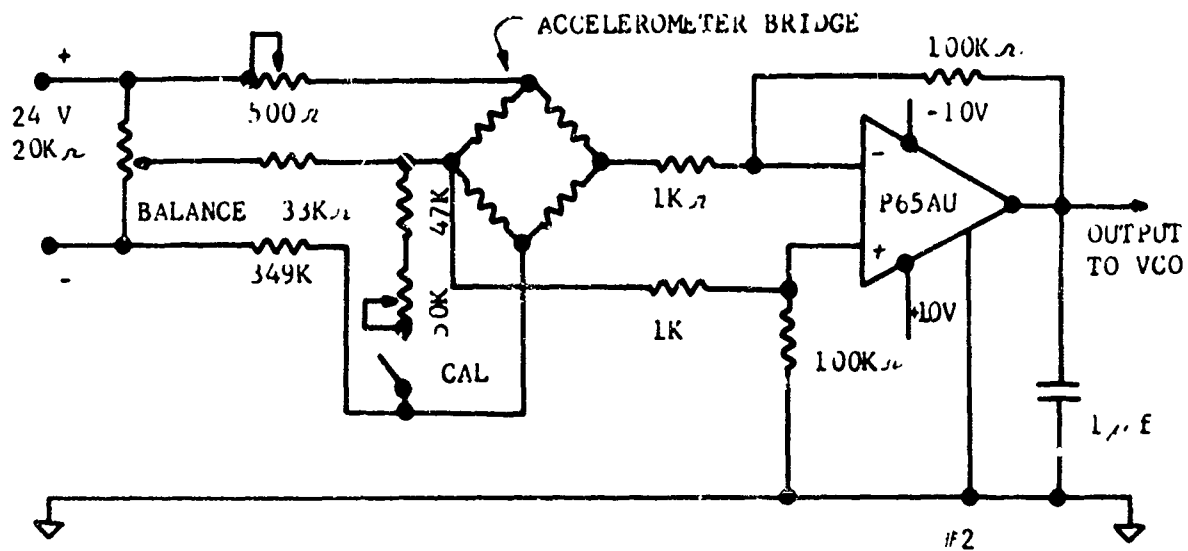


FIGURE 6
The accelerometer electrical circuitry.

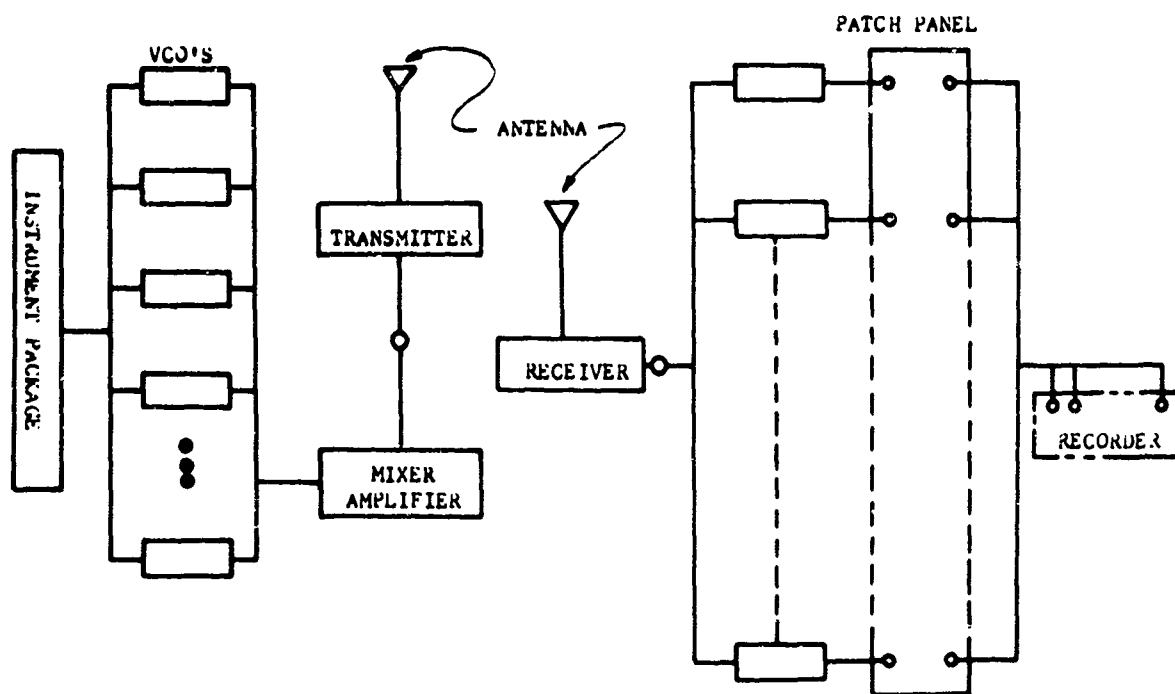


FIGURE 7
The overall information processing and transmission.

TABLE I
Subcarrier bands

RFS No.	IRIG band No.	Center frequency (Hz)	Lower limit (Hz)	Upper limit (Hz)	Maximum deviation (%)	Frequency response (Hz)
1	2	560	518	602	7.5	8.4
2	3	730	675	785	7.5	11
3	4	960	888	1,032	7.5	14
4	5	1,306	1,202	1,399	7.5	20
5	6	1,700	1,572	1,828	7.5	25
6	7	2,300	2,127	2,473	7.5	35
7	8	3,000	2,775	3,225	7.5	45
8	9	3,900	3,607	4,193	7.5	59
9	10	5,400	4,995	5,805	7.5	81
10	11	7,350	6,799	7,901	7.5	110
11	12	10,500	9,712	11,288	7.5	160
12	13	14,500	13,412	15,588	7.5	220

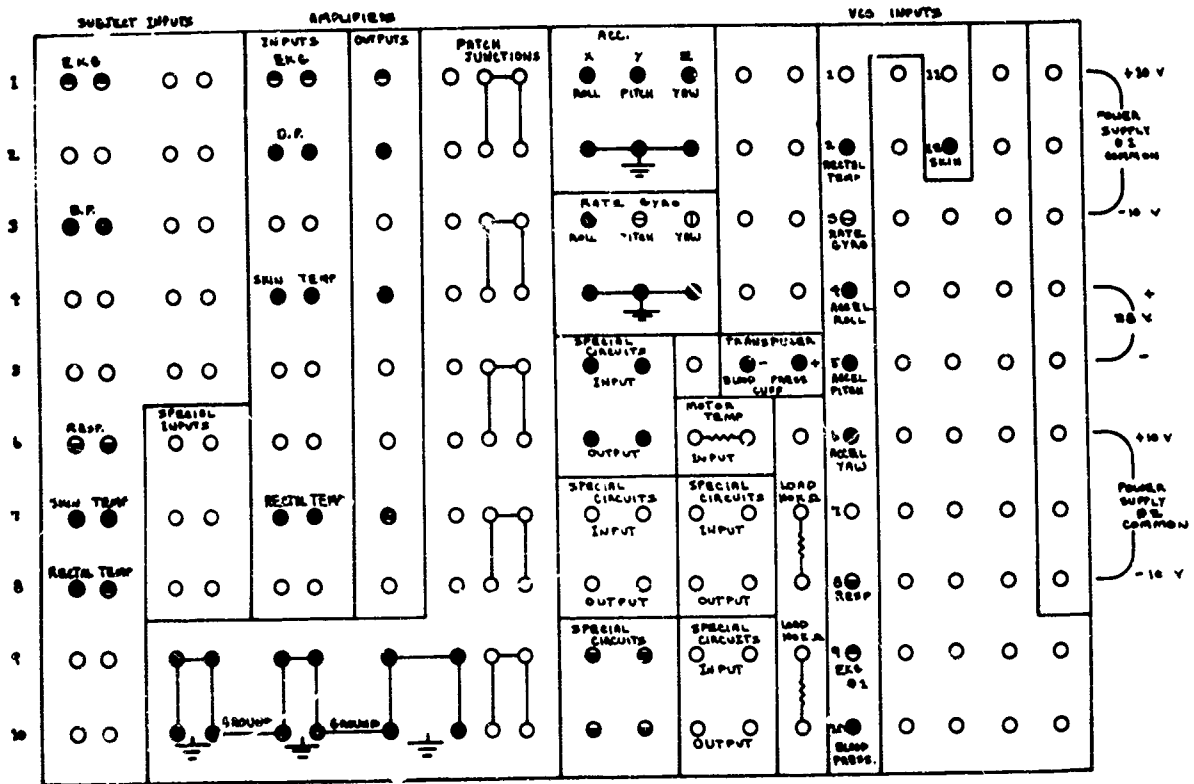


FIGURE 8

The coordination and arrangement of the patch panel located within the sphere.

Electrocardiogram (fig. 10). Each ECG system uses a basic three-lead silver chloride electrode configuration with a Mennen-Greatbatch 621A high gain differential amplifier to condition the ECG signal for the VCO inputs. The output is adjusted not to exceed ± 1.5 v. into a 10K-ohm load. Considerable interference was noted because of RFS rotation. Several approaches to this problem were investigated. The most promising one and the one which proved to provide an excellent ECG signal was to put RF filters in both the positive and negative ECG leads from the subject.

Respiration (fig. 11). Considerable effort was expended to improve the respiration system. The initial system used a thermally saturated thermistor in a bridge configuration

with respiration flow used to cool the thermistor and give a corresponding bridge output. This system recorded respiration rate but did not distinguish between inhalation, exhalation, and rest period. To achieve this objective, we used thermistors to measure actual breath temperature. In such a system the thermal mass of the thermistor must be held to a minimum and thermal heating due to circuit current must be minimized. An extremely small bead thermistor (VECO-55A5) served reasonably well for this purpose, but because of its size, presented packaging problems. Finally the nose-clip type of probe was replaced by a modified oxygen face mask; all the oxygen intake hoses and valves were removed and a plastic respiration channel installed. The complete respiratory flow passed through this

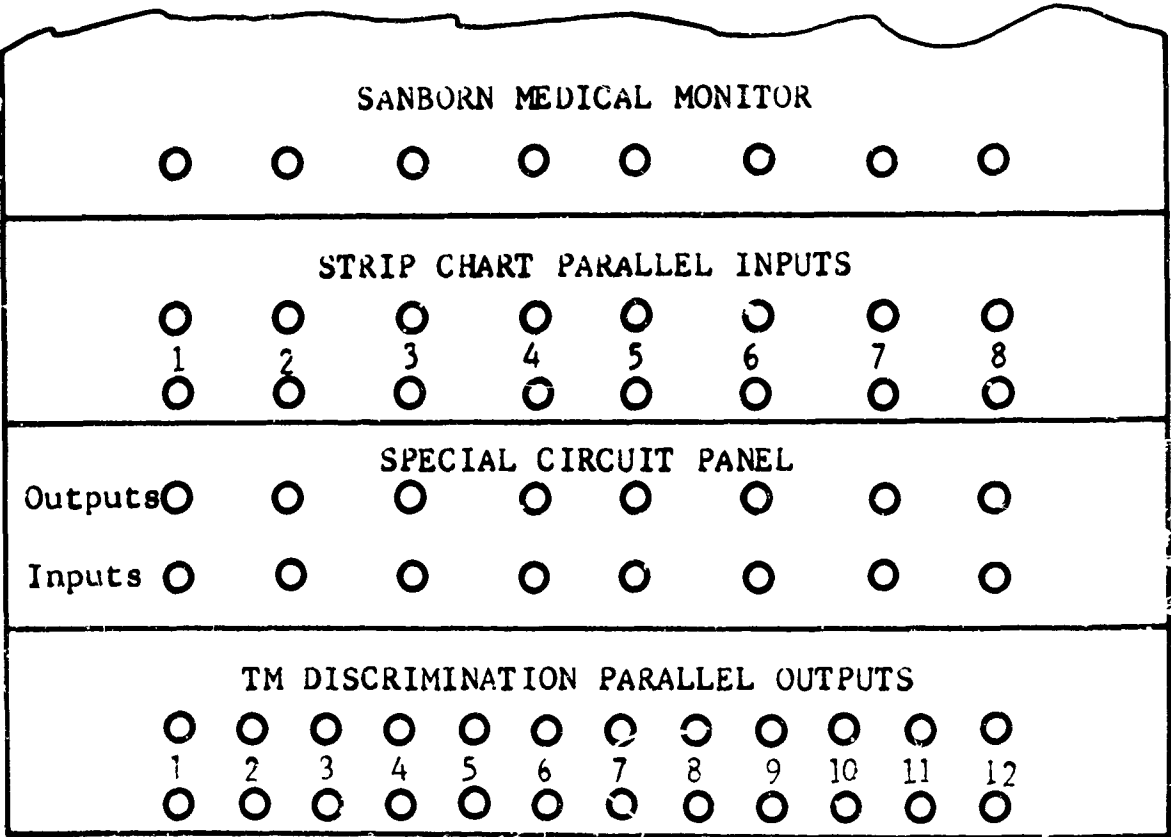


FIGURE 9
The patch panel arrangement at the operator's console.

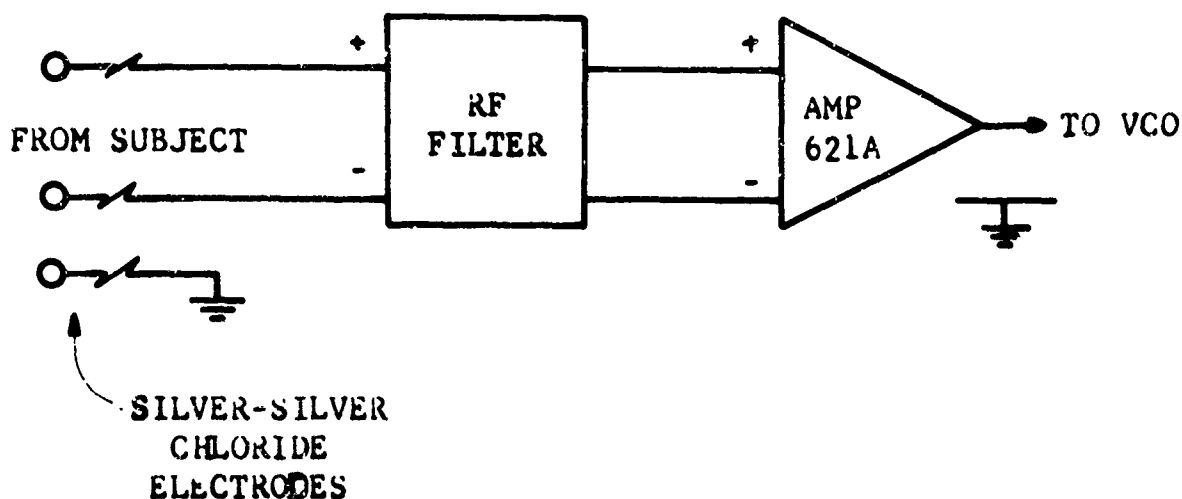


FIGURE 10
The basic ECG amplifier circuitry.

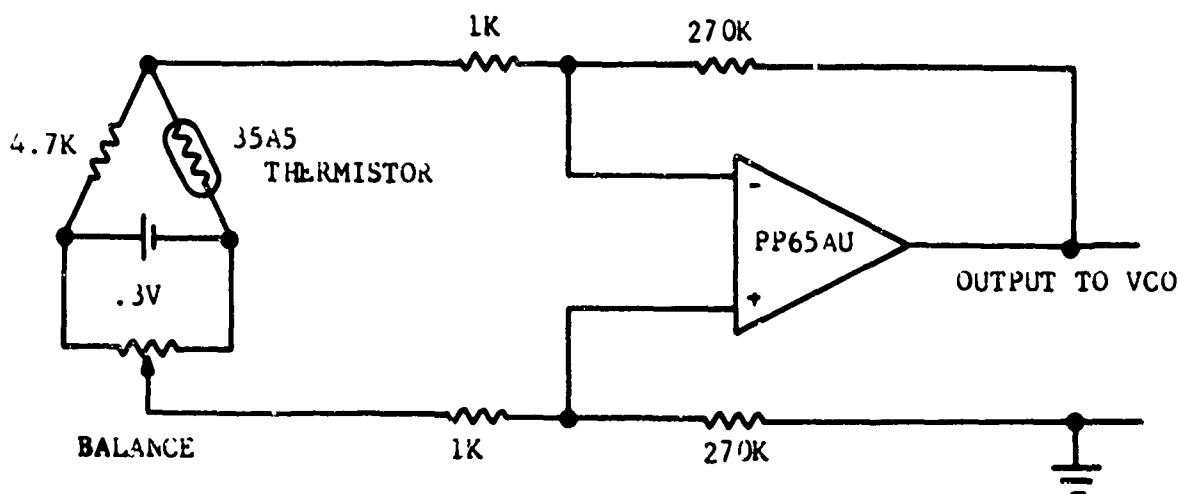


FIGURE 11
The basic respiration monitor circuitry.

channel with a minimum of effort. A standard 4-pin Cinch-Jones plug was modified to mount the thermistor in the mask and the threaded segment of the plug was installed in the side of the respiratory channel so that the thermistor was placed in the center of the air flow. This made detachment and replacement easy.

To insure a minimum of heating due to circuit current, a special circuit was designed

with a very low level bridge excitation current and a Philbrick PP65AU differential operational amplifier to condition the respiration signal for the VCO input.

Blood pressure. The cuff method of indirect blood pressure recording was used (fig. 12). The pressure bleed-off device was developed by SAM. The pressure transducer was Whittaker model P2-3136. The amplifier

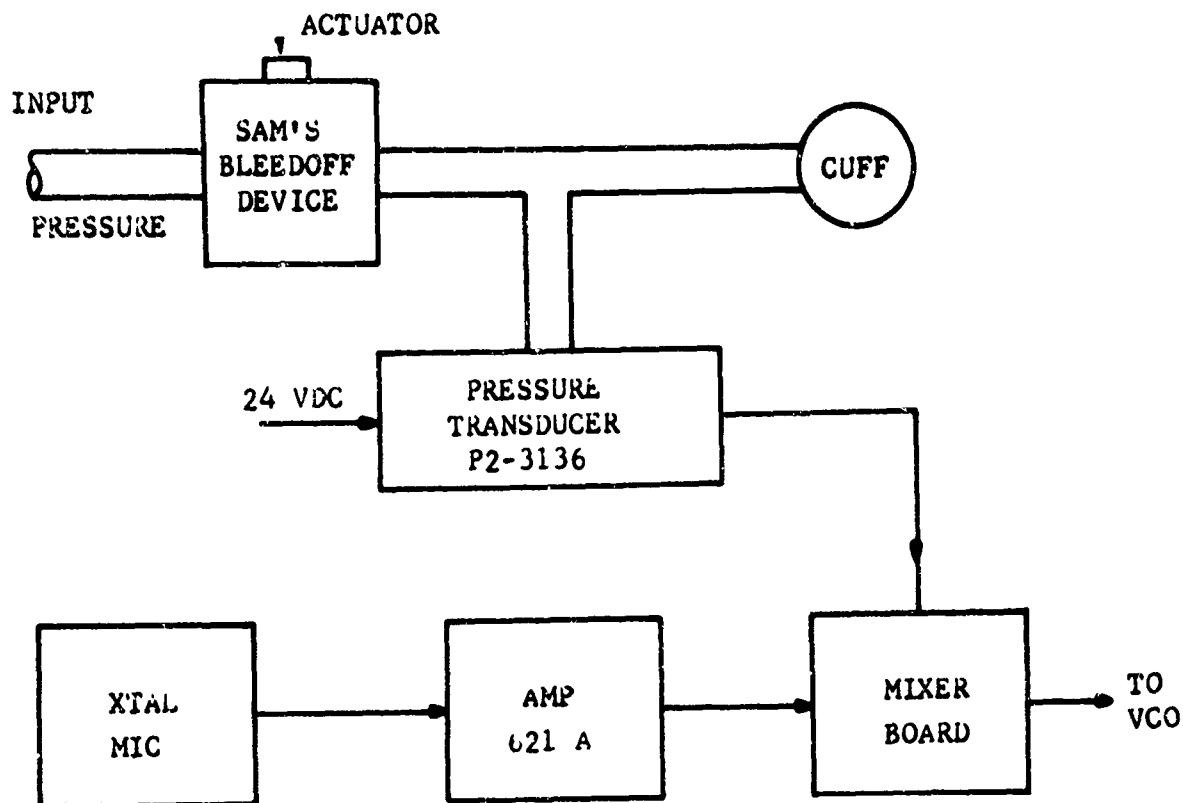


FIGURE 12

The basic blood pressure measuring circuitry.

was a Mennen-Greatbatch model 621A. The pickoff was a specially encapsulated XTAL microphone. The mixer board was designed to impose the Korotkoff sounds on the blood pressure ramp and condition the resulting compound signal for the VCO inputs.

A special external BP trigger system was designed (fig. 13). This system consists of an auto oscillator trigger input to a realistic TRC-5 transmitter. The auto trigger is received in the RFS by a modified walkie-talkie. The RX output triggers a solenoid that activates the SAM bleed-off device.

Special instrumentation

Electronystagmogram. The first parameter developed was the electronystagmogram

(ENG) (fig. 14). Two identical systems were designed and developed. The basic electronic problems came from amplifying the extremely small eye potentials to a level for the VCO's. It was demonstrated that pure ENG signals could be received from the RFS when the subject and the RFS were stationary. However, from the dynamic data generated, it was evident that RF energy and artifacts due to motions of the subject presented serious problems in acquiring any meaningful ENG data.

Cardiotachometer. A basic cardiotachometer system was developed for the RFS. The 8-channel Beckman had no cardiotachometer capability and an Offner cardiotachometer amplifier was externally wired to the 8-channel Beckman. This cardiotachometer required a high level ECG input as would be available

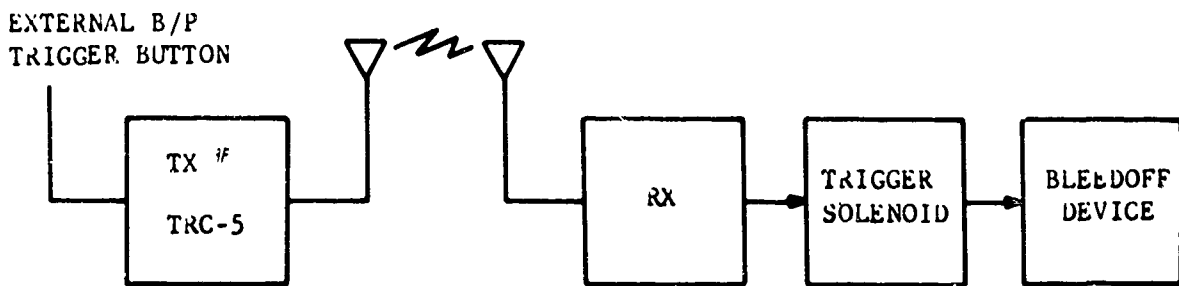


FIGURE 18

The triggering circuitry for the blood pressure measuring instrumentation.

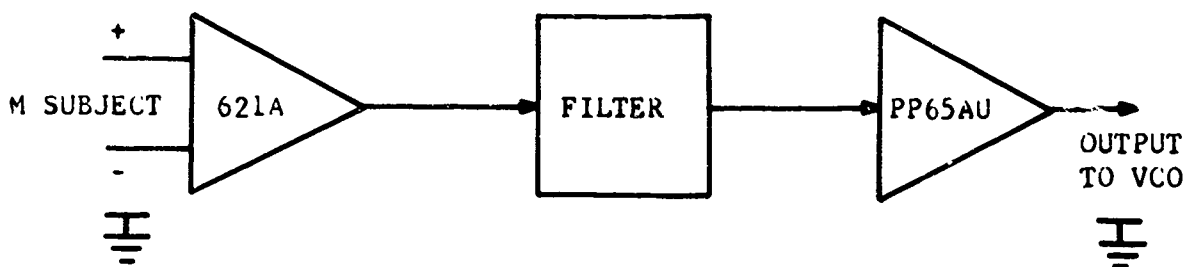


FIGURE 14

The electrical circuitry for the developed electrocnystagmogram.

from an Offner preamplifier. Since the discriminator output was not of this level, a small pulse amplifier circuit was designed and developed.

Limb girth. Work has begun on a Whitney-gage-type of limb girth system, designed to meet RFS requirements. This effort will be continued.

Temperature. Three temperature systems were developed—subject's skin temperature, his rectal temperature, and sphere temperature—

whereby all three systems utilized the same basic circuit (fig. 15).

With work continuing in the area of environmental RFS control, some artifacts traced to drift were evident in the temperature systems. An extremely high degree of accuracy is required to yield meaningful repeatable data of body temperature parameters. The overall system provided data well within 0.25° C. A further improvement is difficult to realize because of the range of temperature and the complex nature of the RFS instrumentation system.

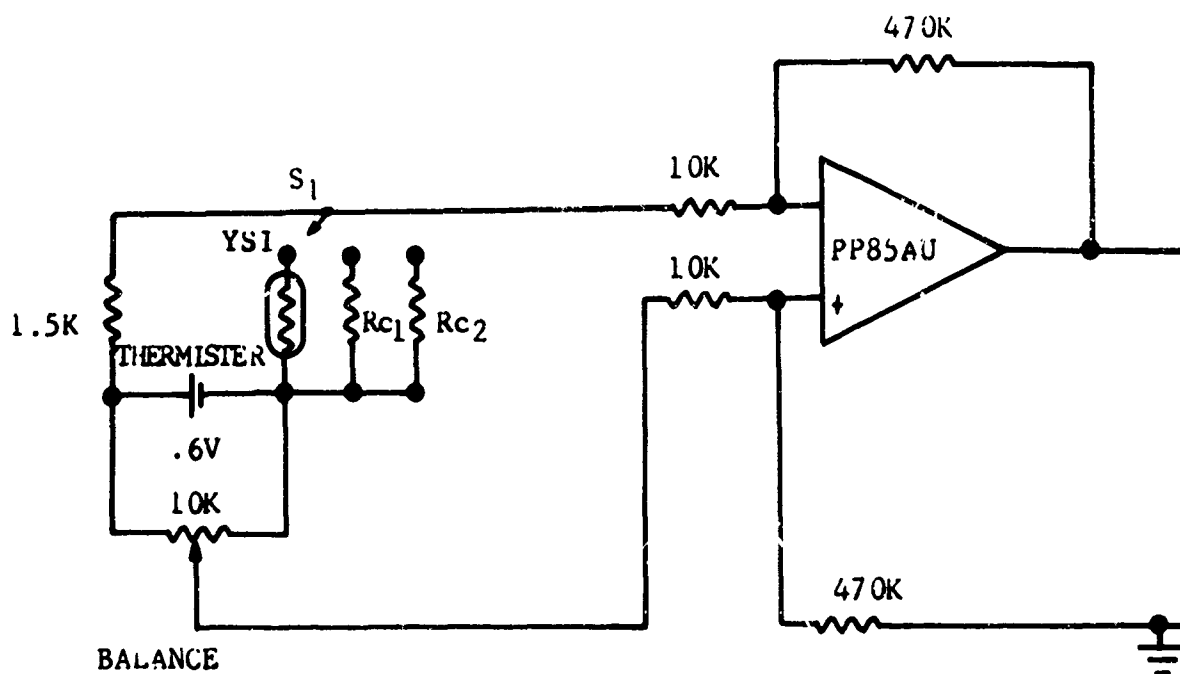


FIGURE 15

The electrical circuitry for the temperature measuring system used.

S_1 — Cal. switch.

R_{c1} — Lower Cal. temperature resistor.

R_{c2} — Upper Cal. temperature resistor.

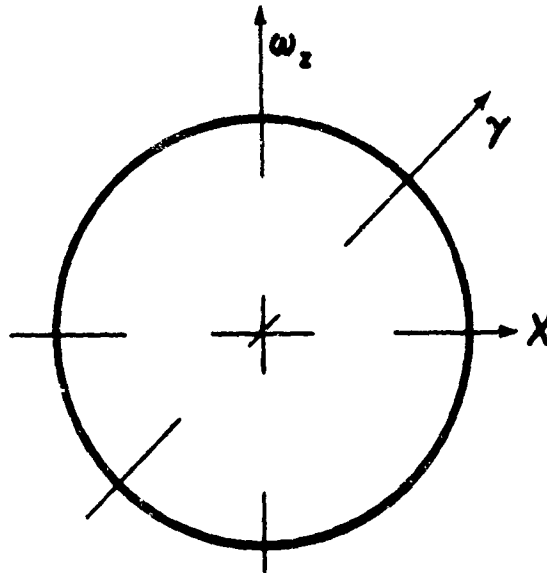
REFERENCES

1. Technical Data Handbook SA78A-4. Subminiature precision rate. Middlebury, Conn.: U.S. Time Corporation, 1954.
2. Landee, R. W., D. C. Davis, and A. P. Albrecht. Electronic designer's handbook. New York: McGraw-Hill, 1957.
3. Stiltz, H. L. Aerospace telemetry, pp. 1-28. New York: Prentice-Hall, 1961.

ADDENDUM 1

THE MOTION OF A ROTATING SPHERE UNDER THE INFLUENCE OF A BODY-FIXED TORQUE

Note: The viscous torque of the air bearing is very small in comparison to the angular momentum (less than 1 per mille) for the considered spin speed and can be overlooked.



Terminology: A = Moment of inertia about spin axis.
 B = Moment of inertia about X and Y axis.
 ω_z = Angular speed about spin axis.
 θ_x and θ_y = Angular displacement about X and Y axes (nonrotating space axes).
 $\dot{\theta}_x$ and $\dot{\theta}_y$ = First derivative with respect to time.
 $\ddot{\theta}_x$ and $\ddot{\theta}_y$ = Second derivative with respect to time.
 T_x and T_y = Torques about X and Y axes.

The torque due to the reaction system about both axes is equal to the gyro-precession torque plus the inertia torque.

$$B \cdot \ddot{\theta}_x + A \cdot \omega_z \cdot \dot{\theta}_y = T_x \quad (1)$$

$$B \cdot \ddot{\theta}_y - A \cdot \omega_z \cdot \dot{\theta}_x = T_y \quad (2)$$

By multiplying equation 2 by j ($\sqrt{-1}$) and adding both equations we arrive at:

$$B (\ddot{\theta}_x + j \ddot{\theta}_y) + A \cdot \omega_z (\dot{\theta}_y - j \dot{\theta}_x) = T_x + j \cdot T_y$$

$$B (\ddot{\theta}_x + j \ddot{\theta}_y) - j A \cdot \omega_z (\dot{\theta}_x + j \dot{\theta}_y) = T_x + j \cdot T_y$$

By calling the resulting angle $\theta_x + j \theta_y = \theta$ and the resulting torque $T_x + j T_y = T$, we get

$$B \cdot \ddot{\theta} - j \cdot A \cdot \omega_s \cdot \dot{\theta} = T$$

The torque T in our system turns with the sphere and can be expressed as a time function, starting at the time zero about the X axis

$$T = T_0 [\cos (\omega_s \cdot t) + j \sin (\omega_s \cdot t)]$$

$$T = T_0 \cdot e^{j\omega_s t}$$

The resulting differential equation:

$$B \cdot \ddot{\theta} - j A \cdot \omega_s \cdot \dot{\theta} = T_0 \cdot e^{j\omega_s t}$$

For the starting conditions at $t = 0$: $\theta = 0$ and $\dot{\theta} = 0$: if $A \neq B$ the solution for θ is:

$$\theta = \frac{T_0}{\omega_s^2 (A - B)} \left[\cos (\omega_s t) + j \sin (\omega_s t) - \left(1 - \frac{B}{A} \right) - \frac{B}{A} \left\langle \cos \left(\frac{A}{B} \omega_s t \right) + j \sin \left(\frac{A}{B} \omega_s t \right) \right\rangle \right]$$

If we separate the real and the imaginary values, we arrive at:

$$\theta_x = \frac{T_0}{\omega_s^2 (A - B)} \left[\cos (\omega_s t) - \left(1 - \frac{A}{B} \right) - \frac{B}{A} \cdot \cos \left(\frac{A}{B} \omega_s t \right) \right]$$

$$\theta_y = \frac{T_0}{\omega_s^2 (A - B)} \left[\sin (\omega_s t) - \frac{A}{B} \cdot \sin \left(\frac{A}{B} \omega_s t \right) \right]$$

The resulting motion is a wobble of the spin axis which opens up to a maximum cone angle and then gets smaller again. The frequency of this pulsation depends on the ratio A to B. If $A = B = I$, then the wobble continues to open up to a steadily increasing cone angle.

Figures 1 and 2 show a calculated example of $A > B$ up to the approximate maximum openings.



Figure 1. Responses of a rotating sphere as observed from the outside (earth-fixed) as a result from inertia ring input.

Conditions:

$$A = 35 \times 10^6 \text{ cm. gm. sec.}^2$$

$$B = 30 \times 10^6 \text{ cm. gm. sec.}^2$$

$$T = 2 \times 10^6 \text{ cm. gm.}$$

$$\omega_s = 1 = 10 \text{ rpm.}$$

Direction of original spin vector "Z."

Direction of torque applied "Y."

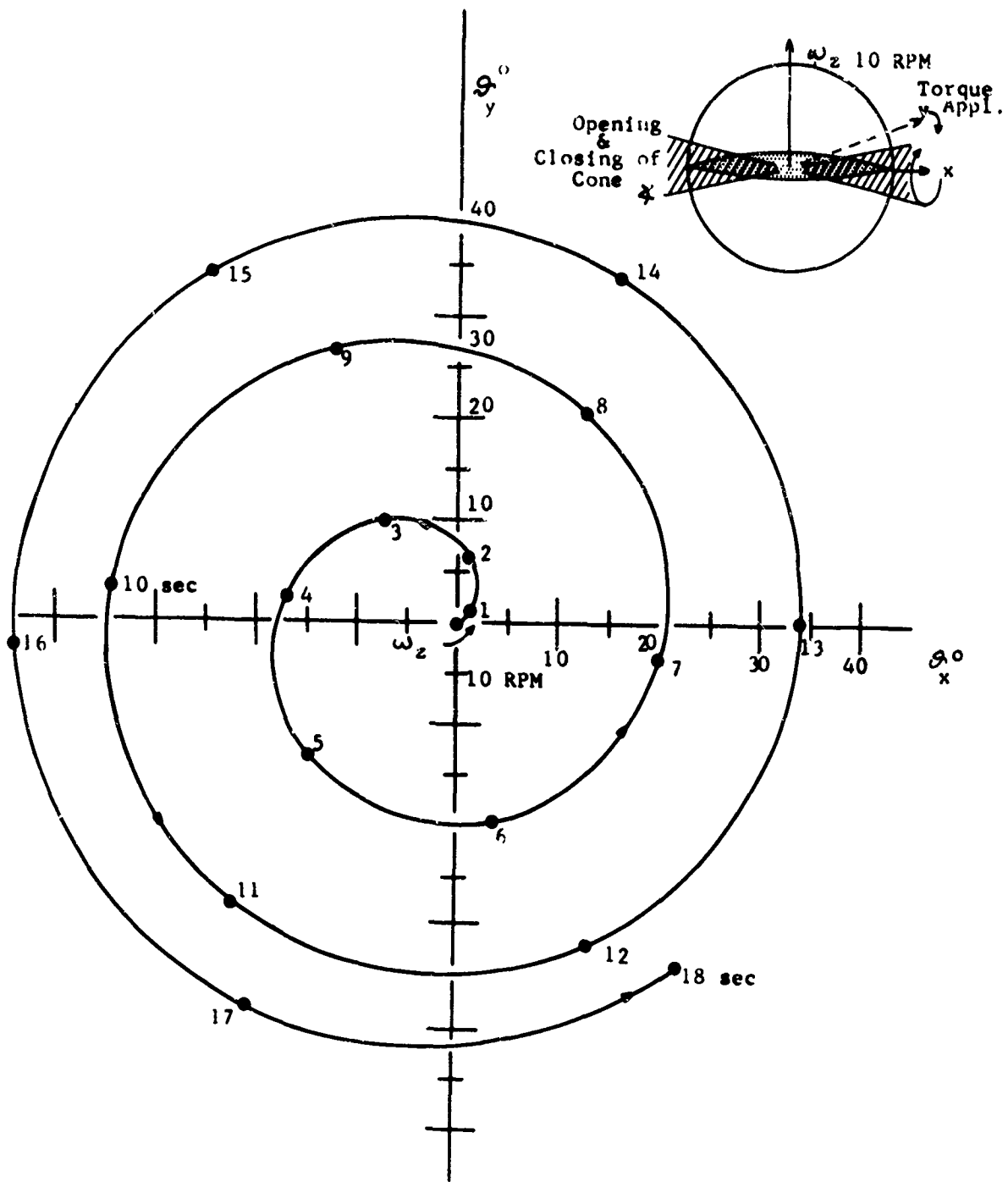




Figure 2. Responses of a rotating sphere as observed from the outside (earth-fixed) as a result from external drive system input.

Conditions:

$$A = 35 \times 10^6 \text{ cm. gm. sec.}^2$$

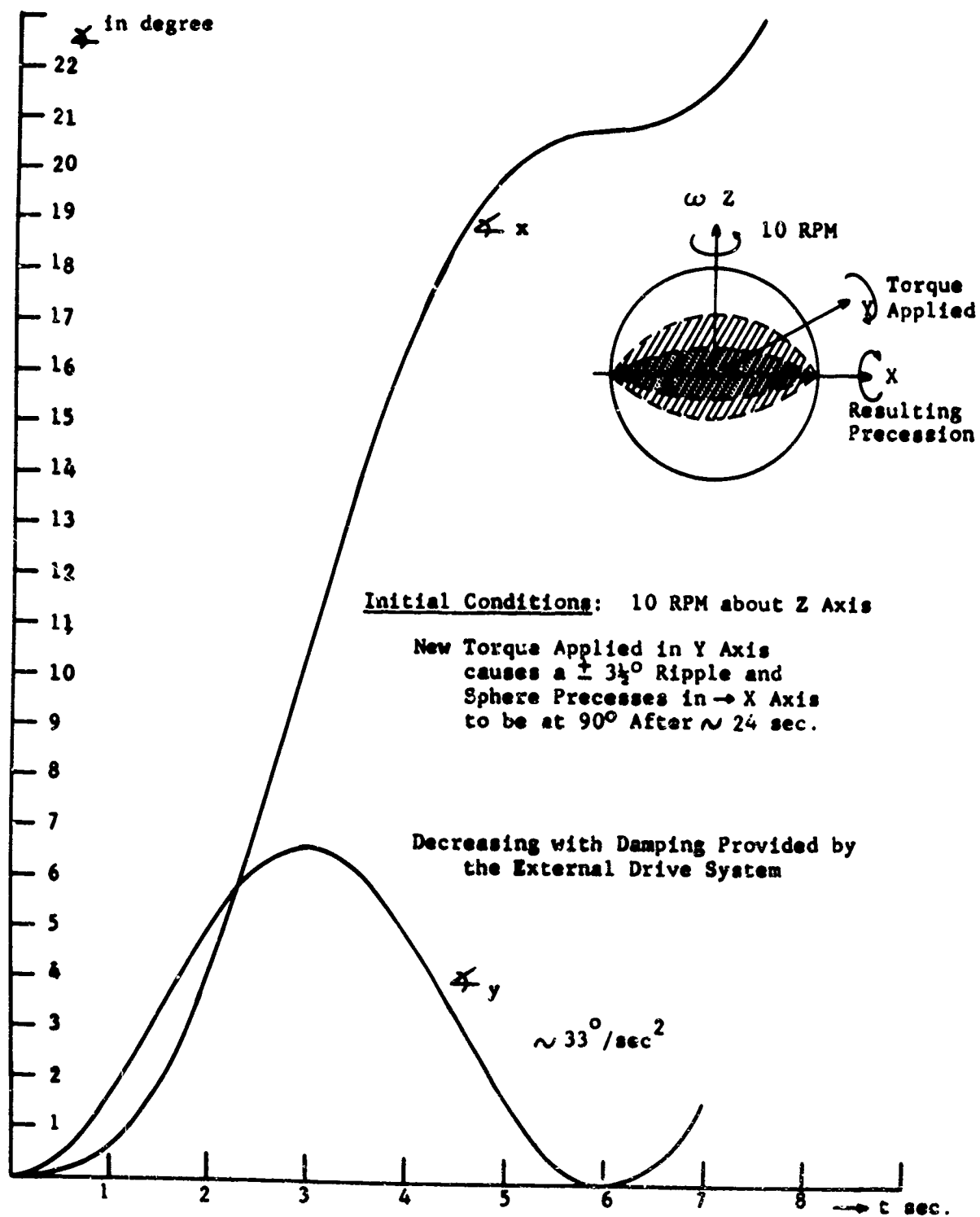
$$B = 30 \times 10^6 \text{ cm. gm. sec.}^2$$

$$T = 2 \times 10^6 \text{ cm. gm.}$$

$$\omega_s = 1 = 10 \text{ rpm.}$$

Direction of original spin vector "Z."

Direction of torque applied "Y."



ADDENDUM 2

RFS SYSTEM AND EQUIPMENT LAYOUT

The overall RFS system is shown in figure 1. The ball is as shown in the center of the figure with internal components defined. The external RFS console is presented on the left-hand side of the figure. The lower center portion of figure represents the basic air supply system.

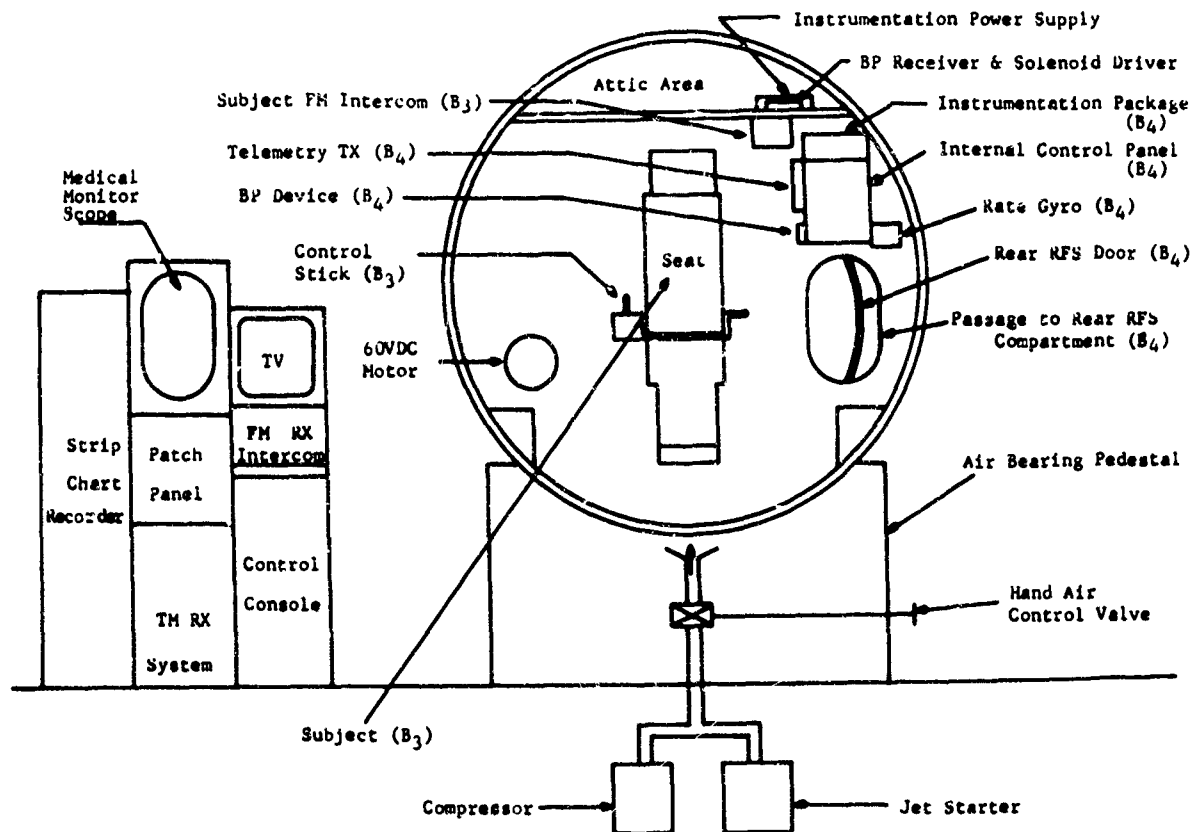


Figure 1. Layout of entire system.

Figure 2 is a view of the external control and instrumentation system as detailed in figure 1. Figure 3 is a view of the subject fully instrumented and ready for RFS operation. Figure 4 shows the composite arrangement of the RFS internal systems.

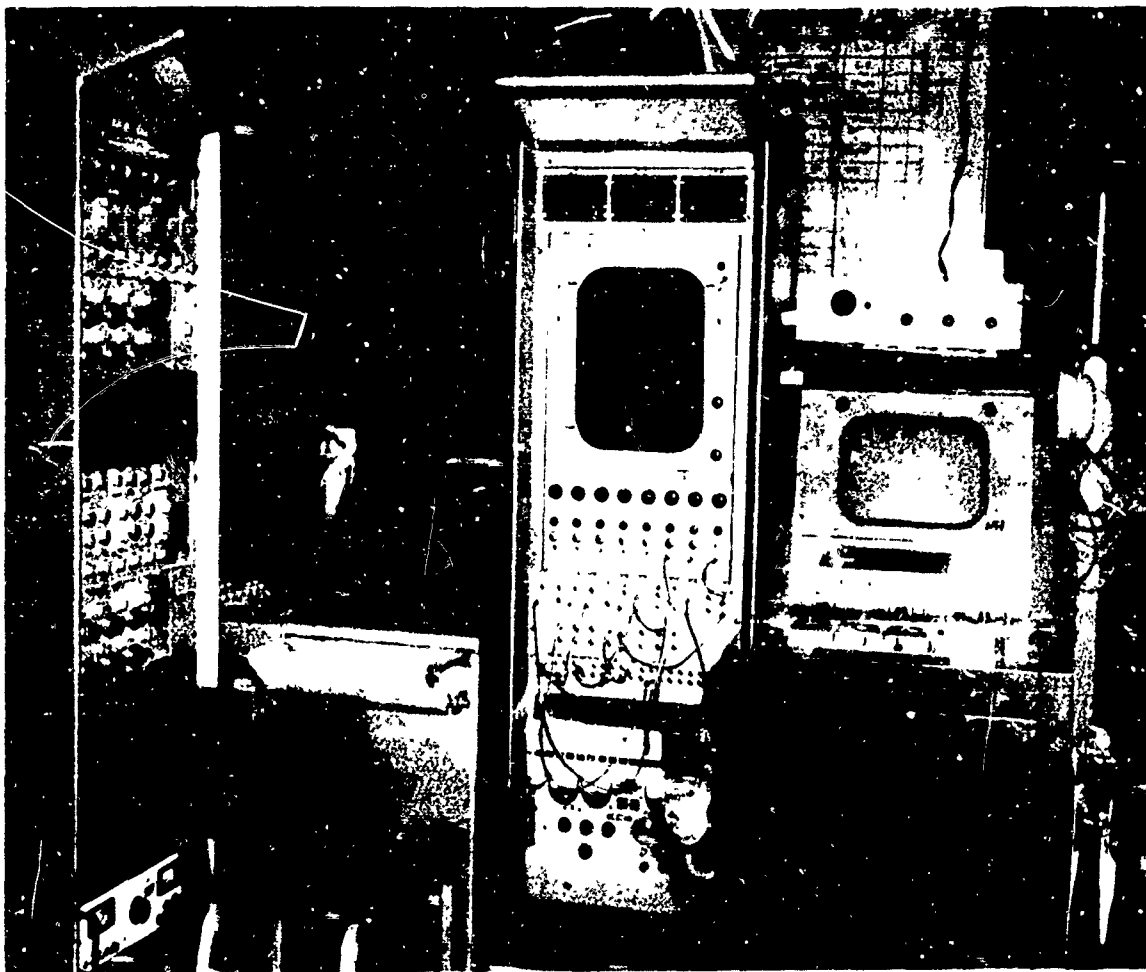


Figure 2. *Control recording and monitoring station.*



Figure 3. *Fully instrumented subject in the RFS.*

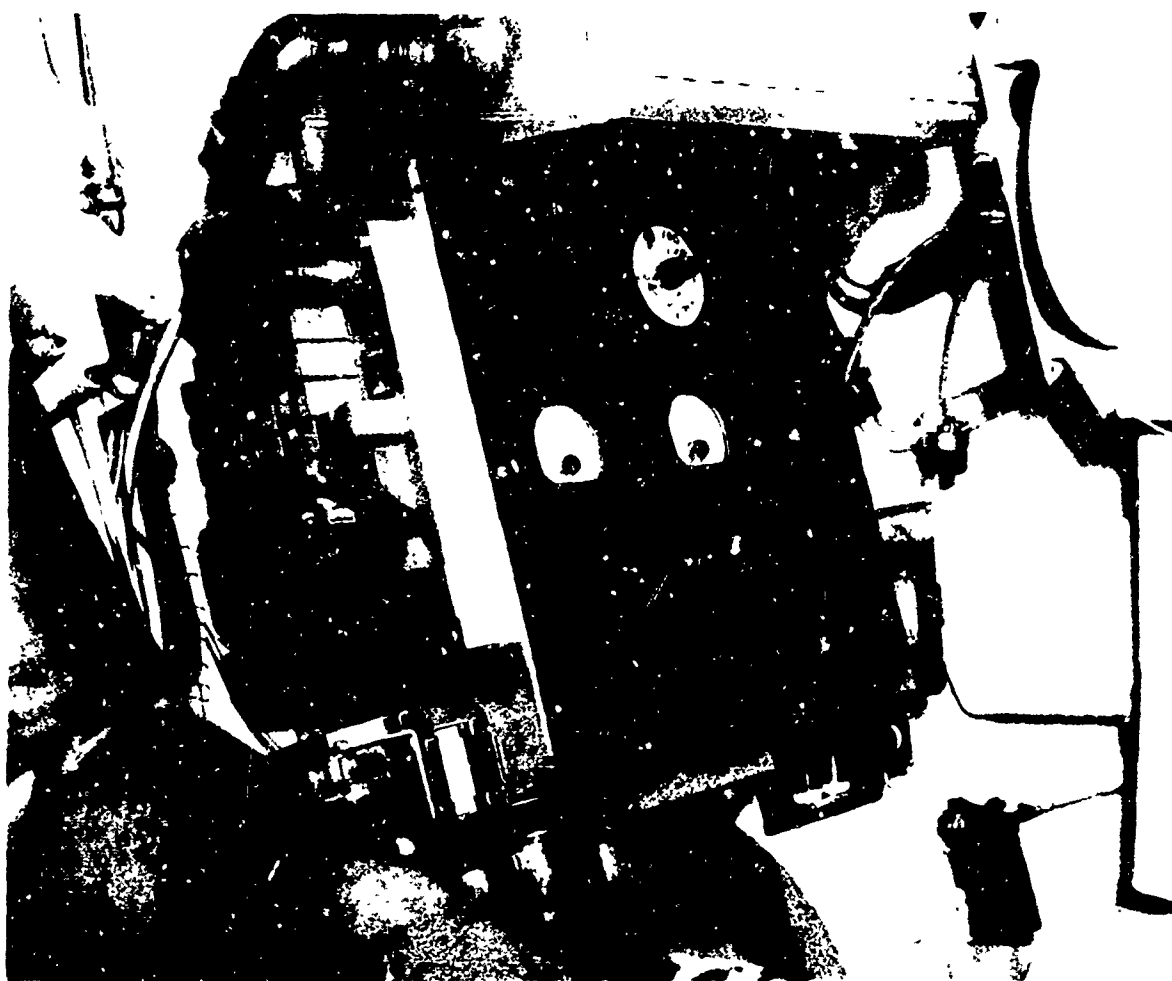


Figure 4. *Internal control console of the RFS.*

B. Physiologic Activities

I. INTRODUCTION

With the advance of present-day aerospace technology, man is being exposed to a wide spectrum of accelerative forces ranging from negative G and weightlessness to positive G and to different combinations and variations of these. Needless to say, it is important to learn man's response to these stresses. This study was undertaken to explore physiologic responses to certain patterns of slow rotation, where the center of rotation is through the iliac crest.

Many investigators have reported the human response to fast rotations. Urschel and Hood (44) studied the circulatory and vestibular response to fast rotations (up to 120 rpm) through the long axis of the body in the sitting position. Performance decrement and vestibular response were studied, by Useller and Algranti (45), in pilots rotated at rates up to 70 rpm about a resultant axis using the Multi-Axis Test Facility at NASA Lewis Research Center (Cleveland). Edelberg et al. (11, 12, 13, 52, 54, 55) studied, in both human subjects and animals, the effect of tumbling head-over-heels and horizontally at fast rates (up to 200 rpm) where the centrifugal forces acting in opposite directions through the body column were quite large. The Pensacola Slow Rotation Room has been used to study performance, disorientation, and adaptation in response to slow rotation where the axis of rotations was not necessarily through the body (6, 8, 15, 20).

The physiologic response to head-over-heels slow rotation at constant rates or random axes in men has not been investigated widely. The results of head-up and head-down tilt table studies done by many authors are, in a way,

applicable to some aspects of our study, but could not completely predict the results we obtained because the rates of tilt were not defined and the rotations were generally of short arc. A great deal of insight can, nevertheless, be derived from the results of the many variants of tilt table studies in understanding the circulatory response to slow rotation.

The Rotational Flight Simulator (RFS) is a vehicle that is capable of simulating various profiles of rotation and the forces associated with them. In the present investigation, blood circulatory responses to rotation were studied in 7 subjects at rates of 1.5 to 16 rpm in the pitch and roll axis, with center of rotation through the iliac crest. Preliminary study was also done in 3 subjects on the effect of initial ambient air temperatures of 38° and $12^{\circ} \pm 5^{\circ}$ C. (3 subjects) and of 6-hour water immersion (1 subject) on the heart rate response to 6 rpm pitch rotation. To investigate tolerance to and performance decrement resulting from random axis rotation, 3 subjects were exposed to a slow (4 ± 2 rpm) and fast (12 ± 4 rpm) random axis rotation.

It is hoped that the results and analysis presented will be of interest not only to acceleration physiologists, but also to those who have studied heart rate regulation using control theory concepts (21, 26, 40, 51).

II. SUMMARY AND GENERAL CONCLUSIONS

Subjective feeling and objective measurements both indicate that the human response to random slow tumbling in the RFS is an interesting one. There is no question that the reflex mechanisms controlling heart rate are

under continuously oscillating stimulation during slow rotation. Nor does any doubt exist that the subjects, however experienced they may be to centrifuge and other accelerations, are disoriented to some degree on the RFS when rotated at random axes. The precise nature of the disorientation is not yet known or measurable, but preliminary estimates of performance decrement have been made with the RFS controls. Results show, first, that improvement in handling comes quickly with repetitive training, and second, if random tumbling is continued long enough, that disorientation and performance impairment follow. It is very doubtful that any person with intact vestibular apparatus could continuously withstand the complex motions of the RFS when set into random motion.

It remains to determine what the body's response may be at higher rpm's—also, whether repeated exposure to many minutes of low-speed rotation or high-speed rotation confers greater tolerance. It is perhaps sufficient, at this point, to indicate that the RFS and its associated equipment have been developed to the point of utility as a physiologic research tool, and that a start has been made on basic investigations at the lower, short-duration spectrum of rotation.

III. MATERIAL AND METHODS

Safety problems

The operational and mechanical preparations for the safety of the subject in this test

program were discussed in part A, "Safety Measures." The areas of direct concern to the medical monitor and the investigators, discussed here, were based in part on reasonable predictions as to subject responses. In addition, the test runs were performed sequentially from less severe to more severe experiments and carefully observed at the physiologic and medical monitoring devices. In general, those unpredictable safety hazards due to possible mechanical deficiencies or accidents were guarded against by continuous voice intercommunication, TV observation, advance safety precautions, and the safety drills. The specific safety hazards from the physiologic point of view are listed in table I.

So far as low rpm, short-duration flights are concerned, only the following risks were considered: (1) vasovagal syncope with additional risk of RFS stopping in the head-up or head-down position; (2) asphyxiation caused by inhaled vomitus; (3) fire, especially of electrical origin; (4) broken restraint harness; (5) confinement due to blocked or jammed exit hatches; (6) smoke fumes due to overheating; and (7) acid/alkali burns due to damage of storage cells.

Accordingly, safety drills and procedures were developed for rapidly halting the RFS in any desired position (thus preventing prolonged head-down and prone unconscious positions), and for rapid stretcher removal of the unconscious subject with or without oxygen

TABLE I
Potential safety hazards

Physiologic origin	Vehicular origin
Asphyxiation	Fire
Fainting, unconsciousness	Loss of restraint harness
Vascular accident	Confinement
Tissue injury	Smoke or fumes
Impact injury	Electrocution
Self-inflicted injury	Acid/alkali burns

mask, tracheal suction, and artificial ventilation. Drills conducted at the start of the program showed that the operating team could halt the RFS and remove an unconscious subject from the vehicle in 18 seconds from the time an "emergency" was declared to the time the subject was carried on a stretcher outside the vehicle. The rate of rotation tested was about 6 rpm. In all the experiments the subject was continuously monitored by TV camera, 2-way intercom system, electrocardiogram, heart rate, respiratory rate, and indirect blood pressure measurement. The medical monitor was always present during human experiments so that medical attention could be given immediately to the injured subject.

Safety equipment available in the RFS site included: (1) a pressurized ambient air supply adequate for 12 minutes' use located near the subject's seat; (2) minuteman respirator (pressurized O₂) and suction installed outside the cabin; (3) stretcher; and (4) fire extinguisher. The medical monitor also had his stethoscope and sphygmomanometer during the experiments. An Air Force Medical Kit (containing narcotics, sedatives, and intravenous fluids) was always available for use during an emergency. The medical kit, stored centrally in the same building, was easily accessible.

Later, when high rpm flights become possible, special attention will be paid to: (1) body movements within the harness, especially to avoid tissue injury risk; (2) impact injury due to possible loss or breakage of restraint harness; and (3) possibilities of vascular accident.

In case of vascular accident it may be necessary to screen the subjects and seek appropriate medical advice.

Equipment

The development and operation of the different instruments and equipment used in the RFS for these experiments are discussed in the engineering section of this report. Details of the technic of instrumenting the subject and calibration of the instruments are described in appendix 2. Figure 1 illustrates the layout

of the RFS site, including the subject instrumentation area, physiologic and monitoring consoles, and the key personnel positions.

Subject preparation

Seven subjects experienced in the centrifuge were used in the different experiments performed. Appendix 1 tabulates their vital statistics, and the complete experimental protocol is tabulated in appendix 4.

The customary experimental procedure was to request the subject to be at the RFS site at least one hour before the run was scheduled to start. The required attire was either surgical "greens," or if not available, the suit trousers of his routine Air Force uniform and a tee shirt. The ECG (electrocardiogram) leads, ENG (electronystagmogram) leads or temperature probes (whichever were used for the particular experiment), and blood pressure microphone and cuff were then applied in that sequence. The subject was strapped on to the RFS seat by means of a harness that provided support of the shoulders and chest cage, the waist, the hips and feet (see appendix 2). This was followed by checking out and calibrating the telemetered signals, voice intercom, and TV picture. A final vacuum cleaning and inspection of the RFS cabin was then conducted by two personnel. The final check was given by the medical monitor, who was present in all the experimental runs. The door was locked and the RFS floated upon order from the physiologist to the different operators through the intercom.

Cardiovascular response

In the experiment to study the cardiovascular response, the telemetered data consist of the ECG, indirect blood pressure, respiration, X, Y, Z accelerometers, and a single-channel rate gyro, with the 8th channel of the strip chart recorder allotted for the cardiometer output. The external RFS drive tachometer also gave indication of rotational rate in one axis. After going through the general procedures for preparing the subject, a rest period of 10 to 15 minutes was given during which

the subject was instructed to relax while continuous recordings of his ECG and respiration were obtained. When the heart rate was stabilized for 3 minutes, rotation of the RFS was started.

Roll to the right and pitch forward were tested at constant rates ranging from 1.5 to 16 rpm in 7 subjects. The method of rotating the RFS is described in the engineering section of this report. Because of some imbalance of

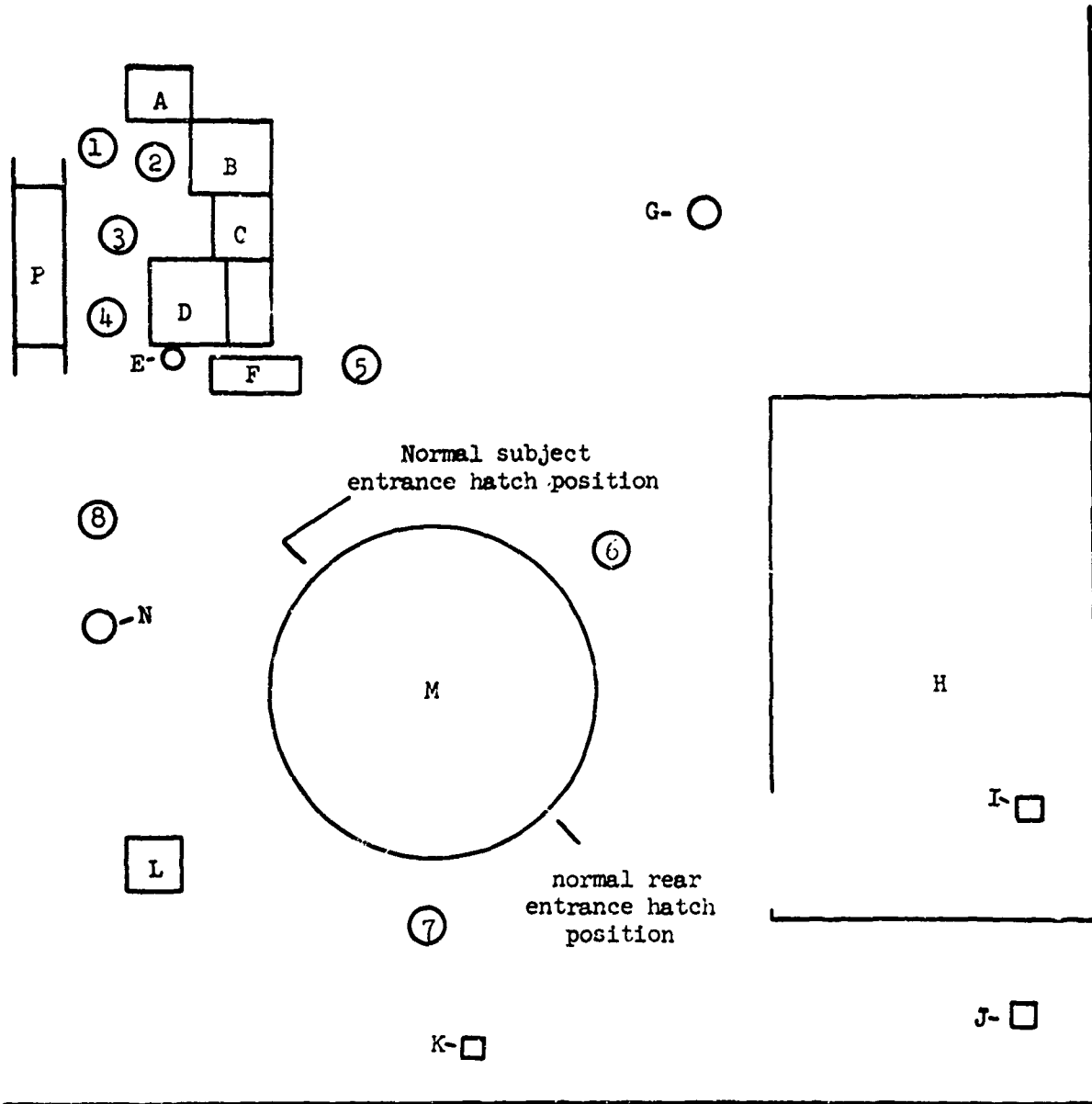


FIGURE 1

RFS site layout and personnel positions: 1, electronics technician; 2, medical technician; 3, medical monitor; 4, physiologist; 5, alternate position for external drive and jet starter operator; 6, external drive and jet starter operator; 7, RFS air compressor operator; 8, RFS technical foreman; A, amplifier bank for strip chart; B, strip chart; C, Sanborn medical scope; D, RFS control console and subject TV monitor; E, fire extinguisher; F, resuscitator and emergency O₂; G, fire extinguisher; H, subject instrumentation area; I, telephone; J, telephone; K, telephone; L, subject TV monitor; M, RFS; N, fire extinguisher; P, stretcher.

the RFS, the rotational rate below 4 rpm was such that turning to the head-up position was slightly slower than turning toward the head-down position. This slight asymmetry was, however, not considered significant. The duration of each rotation was 3 minutes and telemetered data were recorded continuously. Pre- and postrun blood pressures were taken. Rest periods of 3 to 5 minutes were allowed after each rotation during which the heart rate of the subject stabilized and another profile was chosen. For each session, one subject was usually subjected to three different profiles, and then a rest period of 1 to 2 hours was permitted, or another subject was used.

Hot and cold ambient air temperatures

Preheating of the RFS cabin was accomplished by installing two 1,650-w. hot wire fan-heaters—one in the front chamber and the other in the back chamber of the RFS. Heating of the RFS to 38° C. was achieved in 1 to 2 hours. The control and measurement of the RFS temperature are discussed in the engineering section. The subject instrumentation used included: ECG, respiration, blood pressure, skin and rectal temperatures, and cardiometer. Vehicle instrumentation involved: Z accelerometer and pitch rate gyro and the external drive tachometer.

The subjects were maintained in the RFS cabin at a temperature of 38° C. for 50 to 72 minutes, during which time the ECG, respiration, indirect blood pressure, medial thigh skin temperature, and rectal temperature were recorded continuously. Subsequently, the heater was turned off and the subject rotated at 6 rpm, pitch forward for 3 minutes. Continuous physiologic data were recorded during the rotation and for 2 minutes after the rotation. Pre- and postrun blood pressures were recorded. The RFS temperature dropped by 1.5° to 36.5° C. in all three runs performed. Subjects were sweating throughout the procedure.

Pre-cooling of the RFS was accomplished by using a 24,000 BTU/hr. air-conditioner mated to the rear door of the RFS. In one run the temperature achieved before subject (T.S.)

was inside the RFS was 11.5° C. and in the other run (subject A.S.) it was 10.5° C. It took 4 to 6 hours to attain this low temperature. After strapping-in the instrumented subject, check-out and calibrating the instrumentation, etc., the RFS temperature rose to 12.5° C. in the former and 11.5° C. in the latter, before actual rotation started. The subjects wore shorts during these experiments and were instrumented similarly as for the hot temperature run. Subject T.S. was in the cool RFS cabin for 55 minutes and subject A.S., for 60 minutes, before rotation was started. The profile in both runs was at 6 rpm, pitch forward for 3 minutes. The air-conditioner was detached during the rotations and in the run with subject T.S., the RFS temperature rose to 15.5° C. and in the run with subject A.S. it rose to 14.5° C. after the rotation. Physiologic data recorded were identical to that recorded in the hot temperature runs. Subjects reported feeling cool or cold throughout the procedure.

Water immersion

Subject J. N. was exposed for 6 hours to water immersion as a means of producing orthostatic deconditioning. He was then tested for 4 minutes at 6 rpm, pitch forward rotation to determine whether prior immersion caused any major modification to the tumbling response as compared to previous control experiment.

Water immersion was at 32° to 34.5° C. to a level covering the shoulder and with temperature regulation determined by the subject's comfort. During the 6-hour period he reclined comfortably within a water-impermeable suit used to prevent skin deterioration. He breathed air normally and was allowed to take a light lunch and beverage at midpoint. Periodic blood pressure was taken. Both water intake and urine output were recorded.

On termination of immersion, he was assisted from the bath to a stretcher, carried to the RFS, and assisted into the RFS after application of the electrodes. Twenty-two minutes elapsed from the time the subject came out of the bath to the time rotation was

started. ECG, respiration cardiometer, prerun and postrun blood pressure, Z accelerometer, and pitch rate gyro were recorded continuously.

Performance decrement and disorientation

Three subjects were used for this experiment. The subjects were instrumented for ECG, respiration, indirect blood pressure measurement, and lateral and vertical nystagmus. X, Y, and Z accelerometer and rate gyros¹ were used to monitor RFS position and rotation rate. In one subject, a learning curve was obtained for righting the RFS from the "right side" position by means of the internal "joy stick." In the other two subjects, a learning curve was obtained for righting the RFS from the "head-down" position. The RFS was first positioned in the initial position desired (on right side or head-down). The RFS was then floated and the subject in the RFS was instructed to bring the RFS to the upright position by means of the internal "joy stick." When the RFS had come to the upright position the RFS was then set down, and the time required by the subject to reorient the RFS (called "righting time" hereafter) was recorded. Each subject received as many trials as were required to get a consistent minimum "righting time."

The experiment consists of rotating the subjects using random axes introduced externally by energizing the inertia rings. Two sets of profiles were used: (1) a "slow random" rotation at 4 ± 2 rpm, and (2) a "fast random" rotation at 12 ± 4 rpm. In tumbling of this kind, the axis of rotation changes with no well-defined pattern and the rotational rate in each axis wavers, so that an exact characterization of the rotational profile is very complex. In the slow tumbling profile at 4 ± 2 rpm the rate of rotation never exceeded 6 rpm in any X, Y, Z subject axis and at no time were all X, Y, Z components slower than 2 rpm. In the fast tumbling profile at 12 ± 4 rpm the rate of rotation never exceeded 16 rpm in any subject axis and at no time were all X, Y, Z

components slower than 8 rpm. Appropriate rotational patterns were accomplished by energizing a randomly chosen inertia ring whenever the RFS moved too slowly, and by hand-braking whenever it moved too fast.

Rotation was scheduled to last for 2, 4, 8, 16, and 30 minutes and the ability to right the RFS was measured after stopping the RFS at the "right side" or "head-down" position (depending on the subjects' learning experience). All experiments went to completion unless the subject complained of symptoms of nausea. Sweating and subjective symptoms of disorientation were reported and recorded whenever they were present.

IV. RESULTS

Cardiovascular system

For this set of experiments, the rotational rates were held constant and the initial accelerating and final decelerating were held to a low level to avoid possible disorientation. With this kind of profile, there was no report from any subject of any symptoms that were interpretable as motion sickness. The subjective feeling of tumbling head-over-heels was not objectionable to the subjects at the rates tested. The sensation of facial congestion and of fullness of the head when going through the head-down position was more intense in the lower rates of rotation of 1.5 to 4 rpm, gradually reducing as the rotational rate was increased, and was minimal at 12 to 16 rpm. Tensing of body musculature when the subject went through the head-down position was minimized when the subjects were repeatedly instructed to stay relaxed and when they had gained experience.

The *heart rate response* occurring during the first 40 to 60 seconds was not used in the analysis as this was the period when the RFS accelerated to its final desired rate and the subject was "adjusting" to the rotation. Generally, the heart rate changes, particularly bradycardia, was more pronounced at the first rotational cycle (fig. 2A). Figure 2B shows the heart rate response at the end of a rotation. To study the remainder of the flight, the

¹Owing to channel limitation, accelerometer and rate gyros were used alternately in different experiments. Usually the 4 channels chosen were 3 rate gyros and Z accelerometer.

instantaneous heart rate responses for each rotation are superimposed one over the other to show variation of the response from cycle to cycle. There were three general types of heart rate response observed in the 82 rotational profiles studied.

We call type I response, the response where the heart rate plotted from cycle to cycle showed minimum amount of scatter. Three representative plots of these are shown in figure 3. In each plot, six rotational cycles were picked at random and the corresponding instantaneous heart rates plotted. Superimposed also is a sine wave to indicate subject body position, where 90° corresponds to the subject being in the head-up position, and 270° corresponds to the subject being in the head-down position. First to be noted is that in spite of some degree of scatter in the points plotted, there is unmistakable tendency of the heart rate to "track" the body position curve. A comparison of plots from different subjects and different rotational rates reveals varying degrees of scatter but this "tracking" property of the heart rate response is always obvious in the type I response. Second is the more gradual increase in the heart rate when the subject was going through the 90° position and the more rapid cardiac deceleration when going through the 270° position. Also notable is the phase relationship between the heart rate maximum and the 90° position, and between the heart rate minimum and the 270° position. This is analyzed later. Type I response was seen in all the subjects and all rotational rates except in a few of the slow rpm (type II) and fast rpm (type III). Like most physiologic phenomena, a variation of the heart rate response from subject to subject was seen and this will be appreciated by examining figures 3A, B, and C.

Type II response is illustrated by figure 4. It is seen that there is more scatter in the heart rate response. This type of response was seen in some cases when the rotational rate was quite slow. Figure 4 illustrates this response at 1.5 rpm. In spite of the greater amount of scatter in the points, however, the correlation with the body position is still evident. In the head-down position, instances

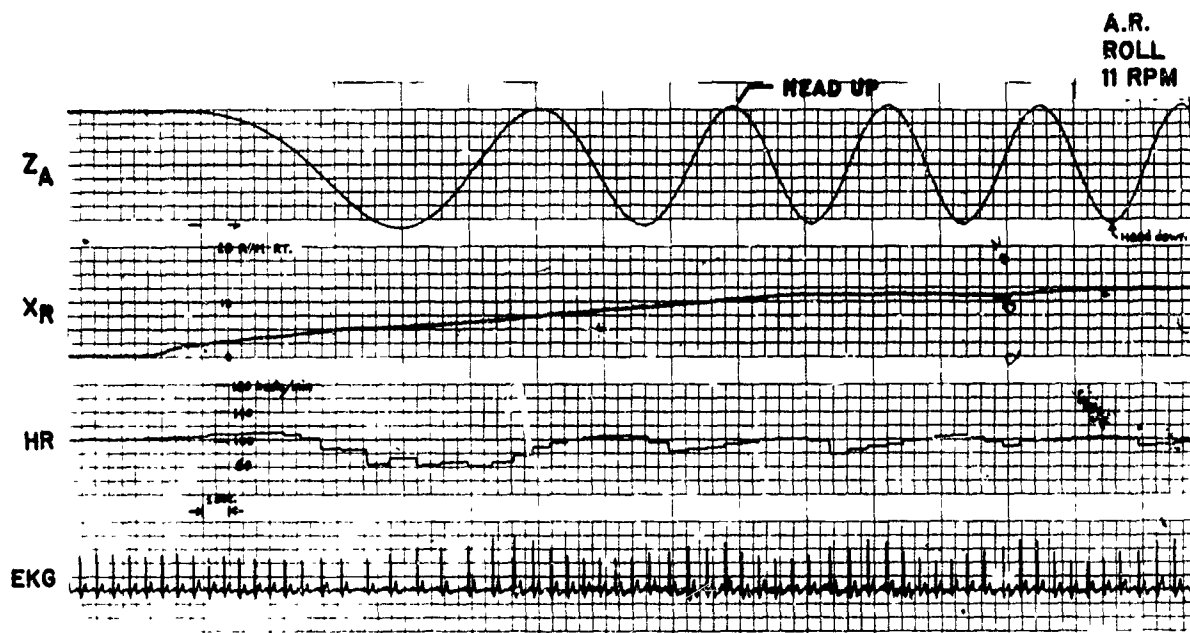
of "vagal escape" are consistently seen in different subjects, particularly in the slower rates of rotation as depicted in figure 4.

Figure 5 illustrates type III response, which is shown here at 15 rpm, pitch forward. It is seen that the cycle-to-cycle heart rate response (fig. 5B) does not appear to correlate very well with the body position. This type of response was observed in those cases where the half cycle period of the rotational rate approached the maximum heart period. If we average these heart rate values, we see a correlation with the body position (fig. 5A).

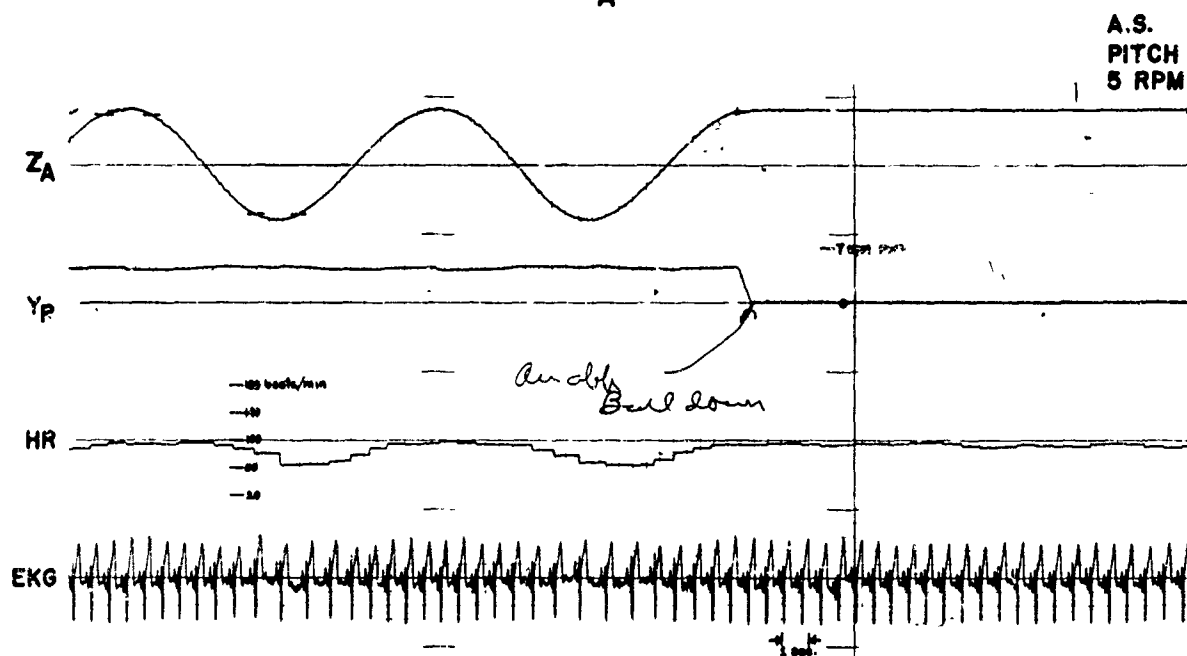
The difference in the characteristic of the cardio-acceleration and cardio-deceleration response can also be seen in a plot of the phase difference between the averaged heart rate maximum relative to the 90° position, and the average heart rate minimum relative to the 270° position as a function of rotational frequency (fig. 6).² A rotational rate dependence of these phase angles can be readily seen. The solid points in each plot correspond to phase relationship of cardiac acceleration. It is seen that the maximum heart rate lags the 90° position and the lag gets larger as the rotational rate increases.

The phase relationship of cardio-deceleration in each plot is represented by the group of clear points. Not only is there less lag in the heart rate minimum relative to the 270° position, but at the slower rotational rates the heart rate minimum could occur at the 270° position, or lead the 270° position. Again subject-to-subject variation was seen, but in all subjects tested, a similar direction in the rotational rate dependence was seen, and the cardio-deceleration points were closer to the 0 degree phase angle than the cardio-acceleration which tended to lag more (examine figures 6A, B, and C). Figure 6D plots the averaged phase angles of cardio-acceleration and cardio-deceleration as a function of rotational frequency.

²We have plotted phase relationship of cardio-acceleration and cardio-deceleration and the difference between heart rate maximum and minimum as a function of rotation frequency ω for the sake of displaying data in a convenient way. In fact, we know that the heart rate control system is a nonlinear system (2, 8). It appears, though, that we can learn something about the system we have at hand by plotting these "pseudo-Bode" diagrams.



A



B

FIGURE 2

A. Initial heart rate (HR) and electrocardiogram (ECG) response to 11 rpm rotation in the roll axis in subject A.R. B. Final heart rate (HR) and electrocardiogram (ECG) response to 5 rpm rotation in the pitch axis in subject A.S. Z_A , G force in subject vertical axis, maximum point when subject is in head-up position (or +1 G in the foot area) and minimum point when subject is in head-down position (or -1 G in the foot area). X_R , rate gyro output in the roll axis. Y_R , rate gyro output in the pitch axis.

As may be expected, it was found that the differences between the averaged heart rate maxima and minima (Δ HR) were greater during rotation than when not rotating. Figures 7A, B, and C illustrate the maximum and the minimum heart rate as a function of rotational rate in three different profiles. The averaged heart rate before the rotation and during the rotation is also represented by the solid line and dotted line, respectively. The variation from subject to subject is evident by examining closely the three graphs presented. In general, the Δ HR tend to be greater in the slower rotational rates as revealed by figure 7D which is a plot of the averaged Δ HR during rotations as a function of rotational rate.

Tables IIa and IIb tabulate, respectively, the average heart rates in the roll and pitch axes before, during, and after rotation. Examination of the heart rate values show that in the majority of cases (85%) the heart rates immediately before and after (within one minute) were higher than during rotation. The average heart rates before, during and after rotation were 88.8, 80.9, and 86.5 beats per minute, respectively.

The blood pressures taken immediately before and after each run are also presented in tables IIIa and IIIb in the roll and pitch axis, respectively. It is evident that there was no reproducible trend either in the systolic or diastolic level. The blood pressure after the run at times was higher than the prerun level, at times unchanged, and at times lower.

The ECG tracing also changed as a result of the rotation in both the pitch, roll, and random axes rotation. Most outstanding was the change in the QRS complex amplitudes. In figures 8A and B are plotted the R wave amplitude variations as a function of body position during pitch and roll rotations in subject T.S. at 6 rpm. Actual ECG tracings during pitch, roll, and random axes are shown in figure 2 and figure 9. The variation is different in the pitch, the roll, and the random rotations, different from one subject to another, but reproducible for the same subject.

The changes of the ECG pattern during slow and fast random rotation are very strikingly illustrated in C, D, and E of figure 9.

Hot and cold temperatures

The results of the hot and cold runs are summarized in table IV. In the *hot temperature runs*, the subjects during the exposure sweated moderately after about 20 minutes of exposure. The rise of about 3° C. in skin temperature indicates marked degree of cutaneous vasodilation. The heart rates showed a rise of about 10 beats per minute before rotation was started. In general, the heart rate variations relative to body position at 6 rpm, pitch forward were essentially similar when subjects A.S. and T.S. were exposed to 38° C. as when the temperature was at 25° C; both showed a type I response. The response of subject J.N. showed more scatter in the heart rate response from cycle to cycle than in the control run, especially in the onset of bradycardia.

When the RFS was *pre-cooled*, the subjects felt chilly and intermittently experienced very mild shivering of the hands and legs. The skin temperature showed a drop of 3.1° in subject T. S. and 2.5° C. in subject A.S. In subject T.S. after 55 minutes' exposure to cold the heart rate showed a drop of 8 beats per minute; whereas, it dropped by about 12 beats per minute in subject A.S. When the "cold temperature" runs are compared with the "normal temperature" runs under otherwise equal conditions, the bradycardia (relative to 270° position) apparently occurred earlier and was more variable. The indirect blood pressure readings before the hot or cold exposure and before and after rotation were apparently unchanged.

Water immersion

Within the bath, the systolic blood pressure was 98 to 110 mm. Hg and diastolic between 50 and 76 mm. Hg. In air on the stretcher, the value was 110/58. When subject took the erect position in the RFS, values rose to 125/75 (control value 120/80). The blood pressure after tumbling was 106/80 (see table IV).

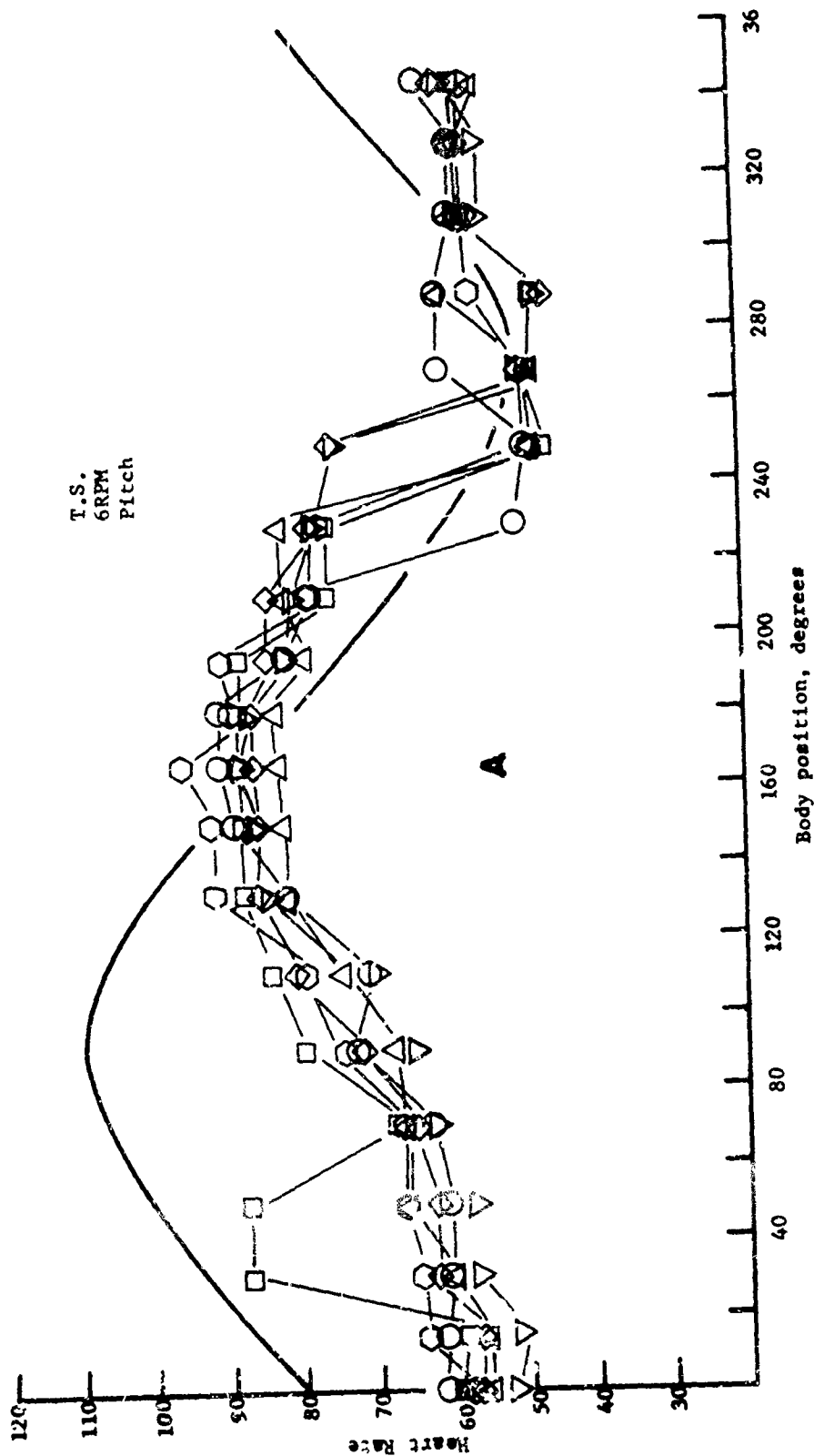


FIGURE 3

Type 1 heart rate response to rotation in axis perpendicular to earth's G field plotted as function of body position. A. Subject T.S. at 6 rpm in pitch axis. B. Subject V.R. at same profile. C. Subject J.N. at same profile. Six rotational cycles are superimposed one over another. In B, the points came very close to each other so that only four cycles were traced. Sine wave in these figures and subsequent ones corresponds to Z_A output or G force ± 1 G when in the head-up position, and -1 G when in the head-down position.

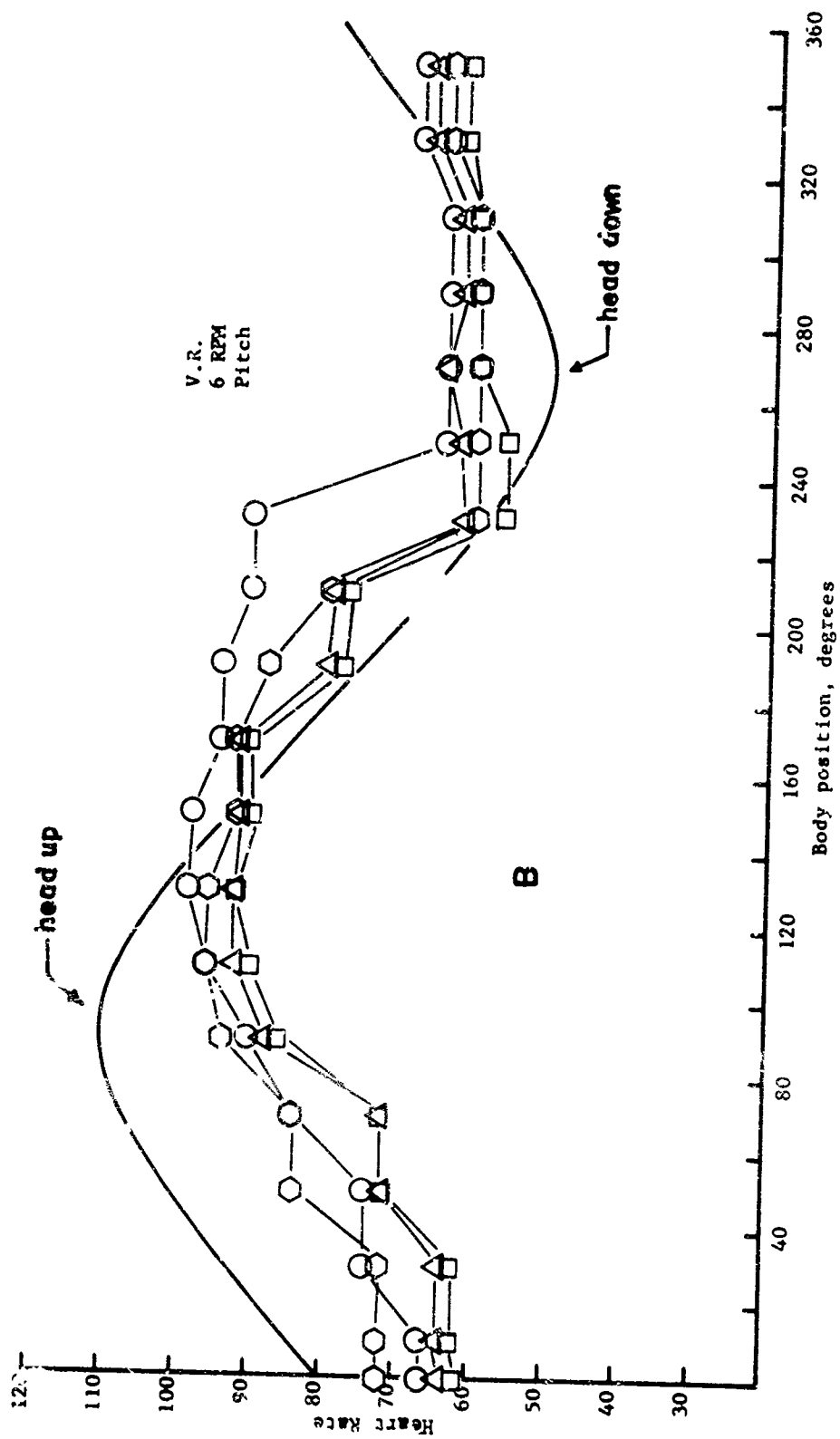


FIGURE 3

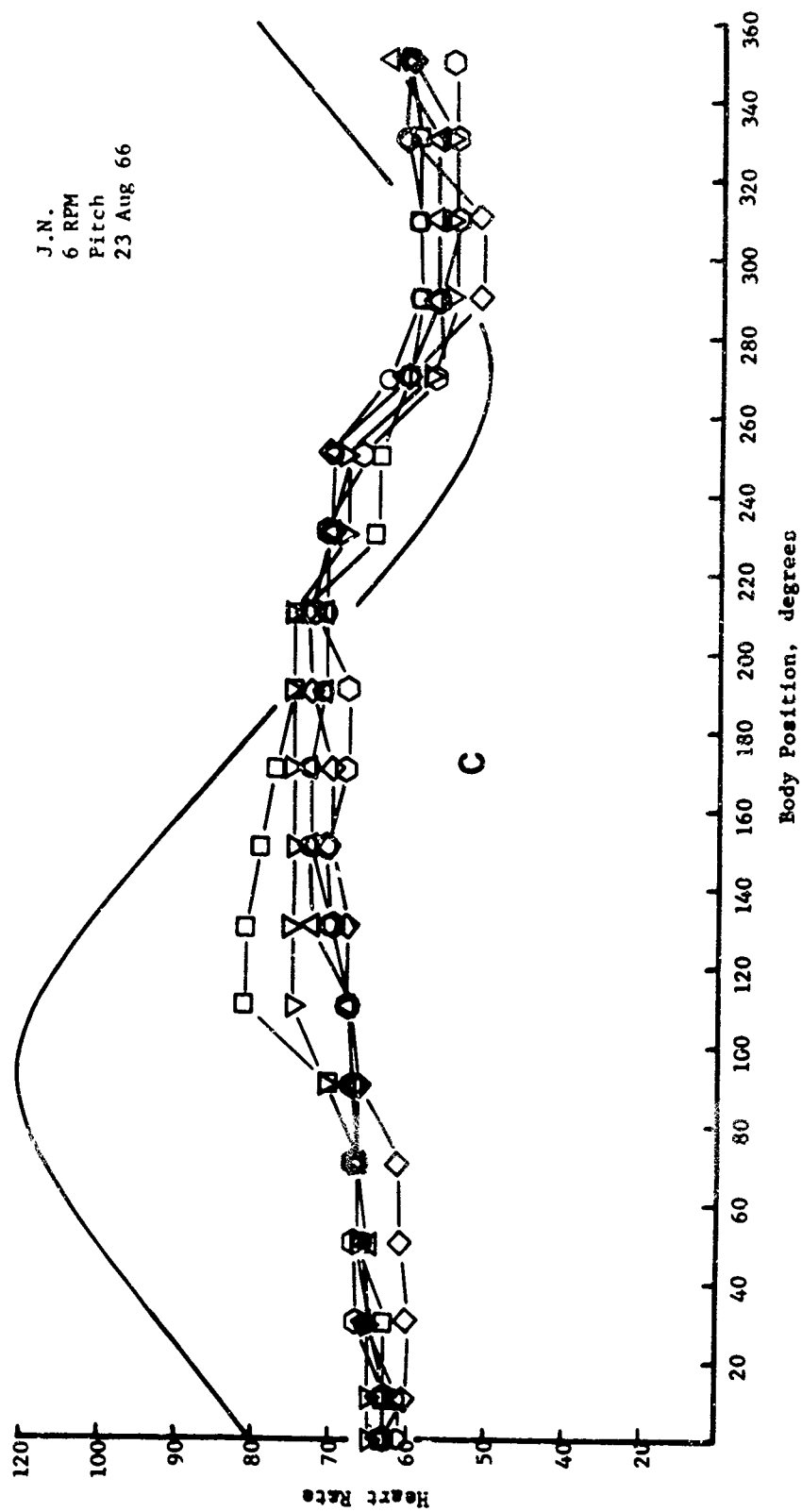


FIGURE 3

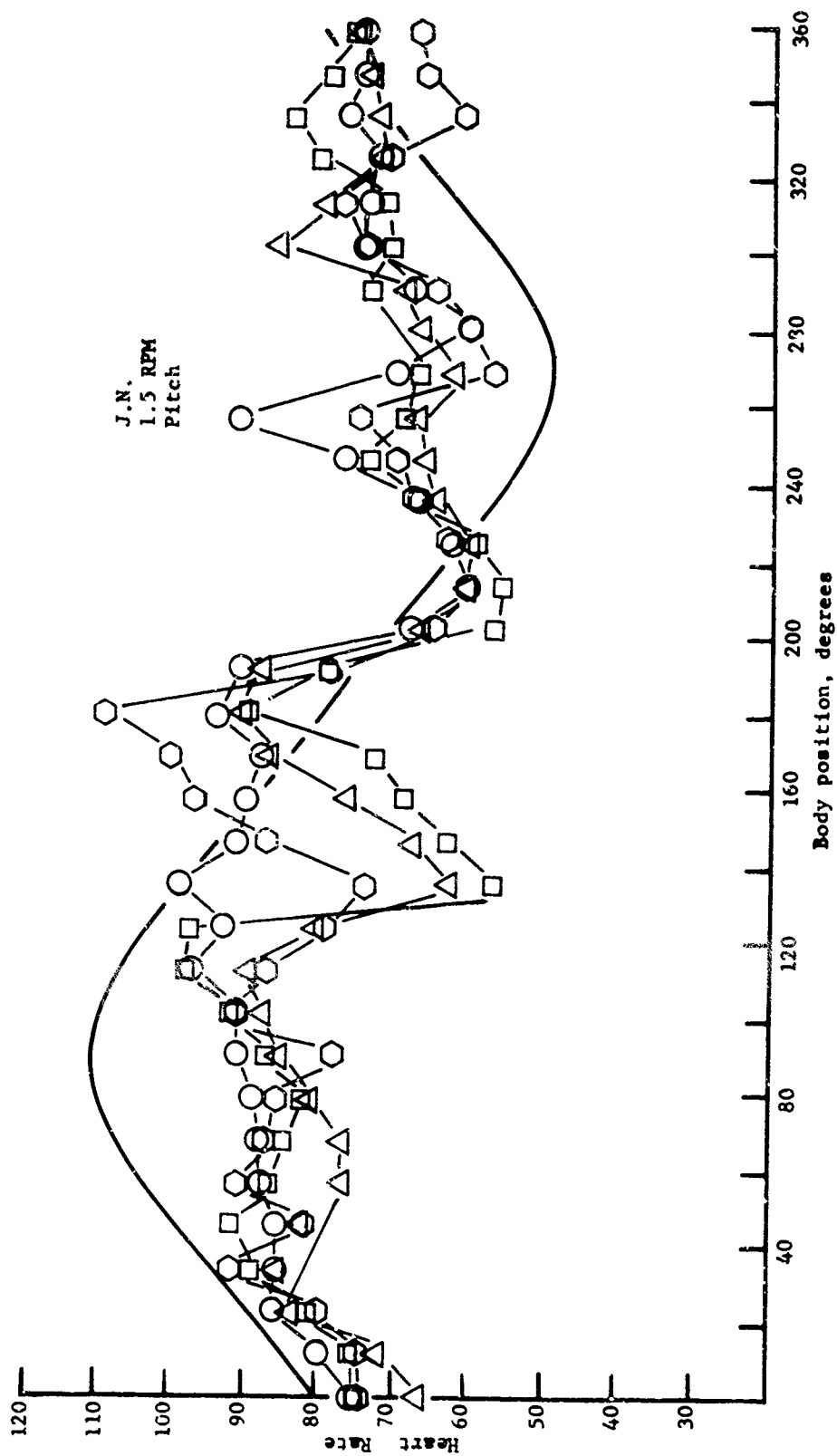


FIGURE 4

Type II heart rate response to slow rotation in an axis perpendicular to earth's gravitational field plotted as a function of body position. Shown is the response of subject J.N. at 1.5 rpm, pitch axis.

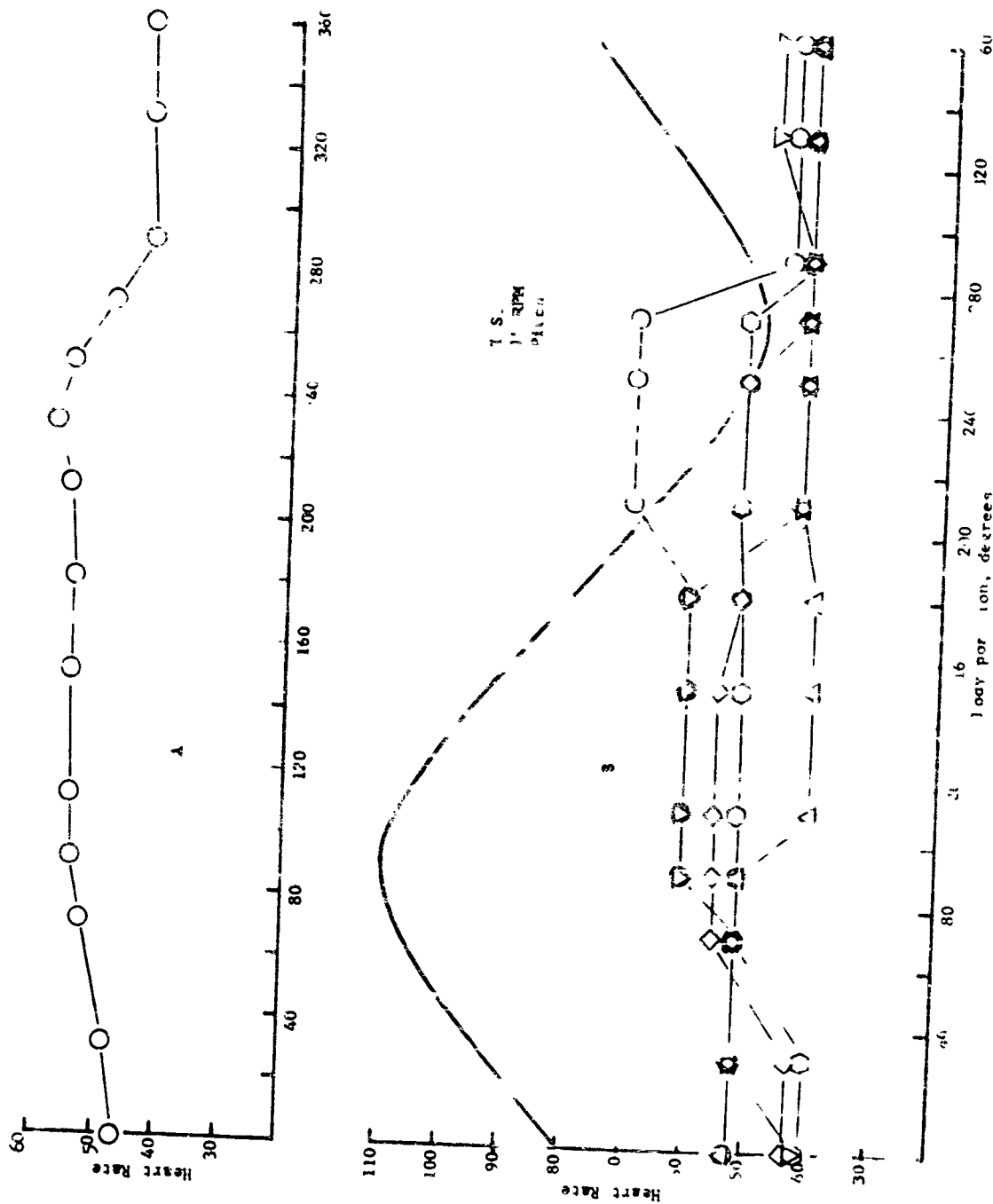


Figure 11. heart rate response to fast pitch vocatum at 15 mm in subject T.A. A. Heart rate response of 6 cycles averaged at each body position. B. Cycle to cycle heart rate variation.

The heart rate within the bath was stable at 74 to 76 beats per minute, rising to 88 as the subject anticipated leaving the water. When subject was lying on the stretcher, the rate rose to 84. On raising himself to the erect posture, the heart rate rose to 100 beats per minute. The effect of tumbling after immersion is shown in figure 10A; figure 10B shows the response to the same profile without previous immersion. The difference in the response in this one subject is very striking. The average peak-to-peak heart rate difference while tumbling after water immersion is 50 beats per minute as compared to 20 beats per minute without water immersion. The maximum heart rate lagged the 90° position by 60° in the control but only 30° after water immersion. The minimum heart rate lagged the 270° position by 20° in the control run, whereas during rotation after water immersion the minimum heart rate had a lead of 60°. The heart rate after rotation was 94 and during rotation it averaged 74 beats per minute.

Disorientation and performance decrement

Subject E.O. Figures 11A, B, and C show, respectively, the learning curve, the effect of random tumbling at slow (4 ± 2 rpm), and the effect at fast (12 ± 4 rpm) rates for different durations in subject E.O. After four trials the subject was able to right the RFS in 5 or 6 seconds from the "right side" position using the internal "joy stick." In figure 11B is seen an increase to 8 seconds in the time the subject required to right the RFS, after 16 minutes and 30 minutes of random rotation at 4 ± 2 rpm. The subject reported momentary "confusion" when the RFS was stopped after the 30-minute rotation but regained his orientation in a few seconds. Figure 11C illustrates the result after the fast random rotation at 12 ± 4 rpm. The time required to right the RFS was consistently longer than control levels, and when the duration of tumbling was 8 minutes or longer there were consistently signs of increased sweatiness and momentary disorientation. The duration was not tested at longer than 20 minutes of fast random tumbling.

Subject A.R. The learning curve depicted by figure 12A for subject A.R. reveals more scatter than that shown in figure 11A. The average of the "righting time" from the head-down position for the 5th to the 11th trial is 28 seconds. After slow random rotation for scheduled durations of 2, 4, 6, 8, and 16 minutes, the ability to right the RFS remained in the range of the control levels. When this duration was scheduled to extend 30 minutes in two trials, the subject experienced nausea after 27 minutes of rotation in the first trial and the RFS was stopped in the upright position. In the second trial he reported to be confused and disoriented after 30 minutes' tumbling. It took him 45 seconds to bring the RFS to the upright position from the head-down position. The RFS was actually still tilted after 45 seconds, but for fear that the subject might experience nausea if allowed to control the RFS further, the run was then stopped. In the first trial when nausea was reported, the run was stopped and the subject not allowed to control the RFS. With fast random tumbling, the subject in two trials experienced nausea after 3 minutes of tumbling in the first trial and "queasiness" of the stomach also after 3 minutes of tumbling in the second trial (figures 12B and C). In both trials, the subject was stopped in the head-up position and not allowed to right the RFS.

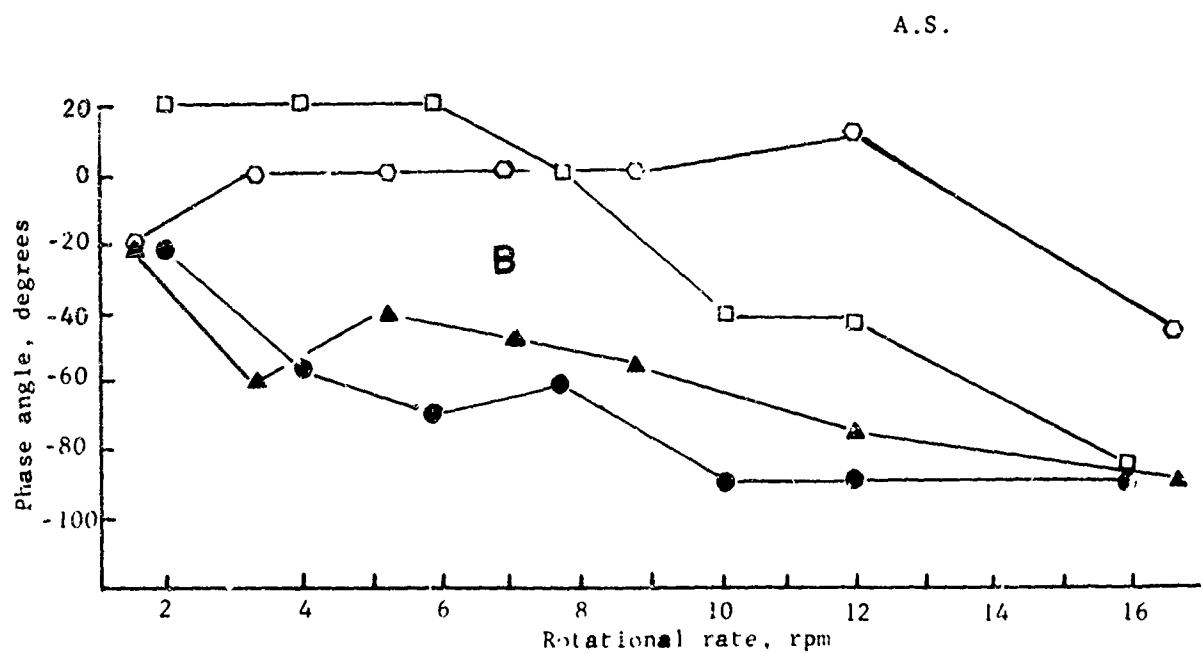
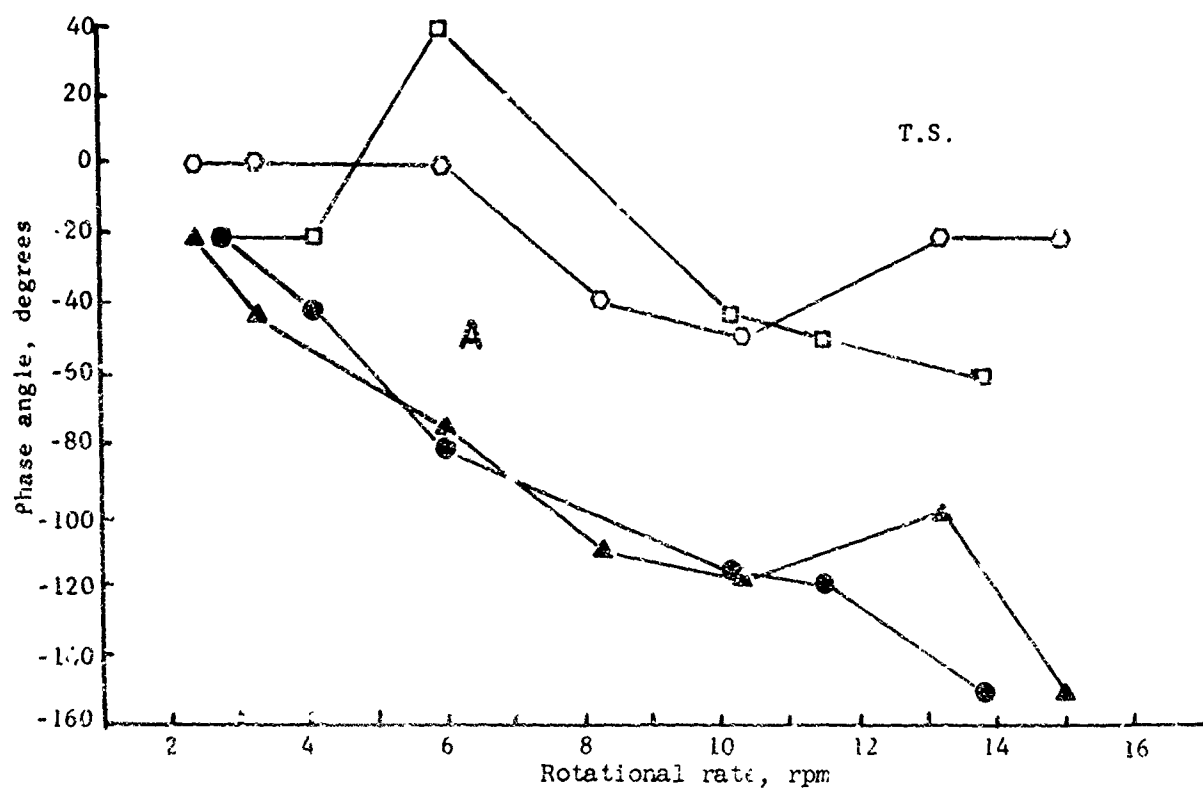
Subject J.N. Figures 13A and B depict, respectively, the learning curve and the "righting time" after fast random tumbling of a third subject. Nausea was experienced after 14 minutes of tumbling in the first trial and after 15 minutes in the second trial. The onset of nausea as experienced by subjects J.N. and A.R. was characterized by a sudden onset and associated with varying amounts of sweatiness, momentary disorientation, and slight headache.

Nystagmogram. Representative tracings of the eyeball movements as measured by our nystagmogram channels during random rotation are shown in figures 14A, B, C, and D. As can be seen, the waveform is complex, showing a fast frequency sawtooth-like waveform superimposed on a slower frequency waveform. The arrow at figure 14A indicates one of



FIGURE 6

Phase relation of heart rate maximum to 90° position and of heart rate minimum to 270° position as a function of rotational rate. A. Subject T.S. B. Subject A.S. C. Subject E.O. \blacktriangle — \blacktriangle heart rate maximum phase angle in pitch rotation; \circ — \circ heart rate minimum phase angle in pitch rotation; \bullet — \bullet heart rate maximum phase angle in roll rotation; \square — \square heart rate minimum phase angle in roll rotation. Negative angle corresponds to a lag and positive angle to a lead. D. Averaged phase angle of heart rate maximum \blacktriangle — \blacktriangle and of heart rate minimum \circ — \circ . Number of subjects tested and cycles counted are identical to those given in figure 7D.



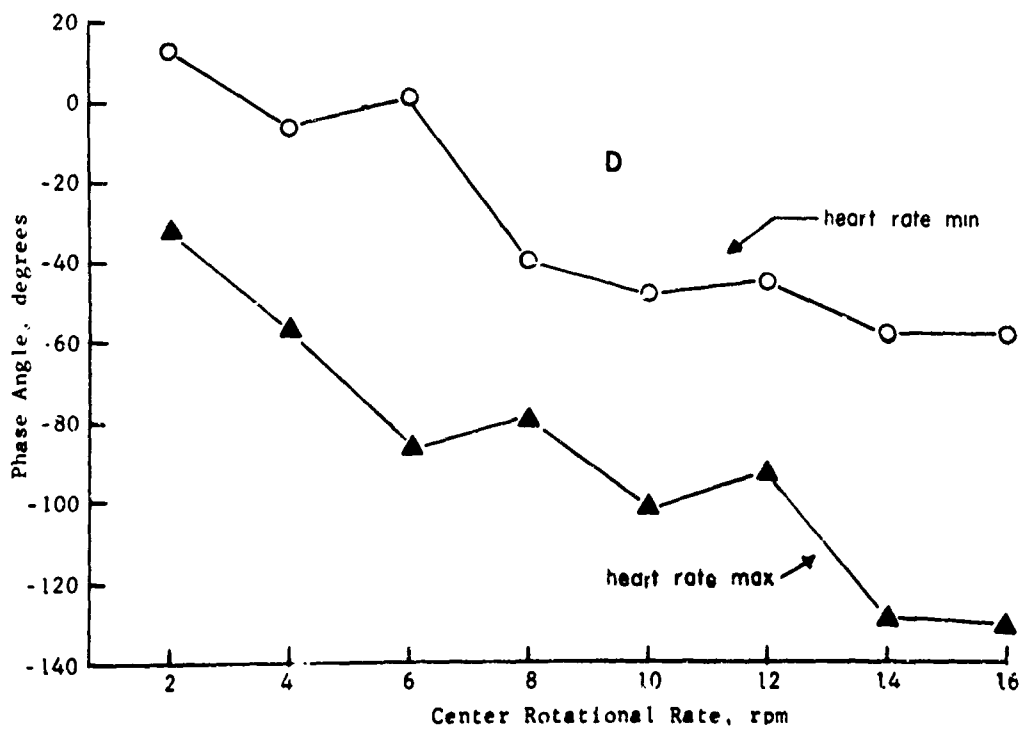
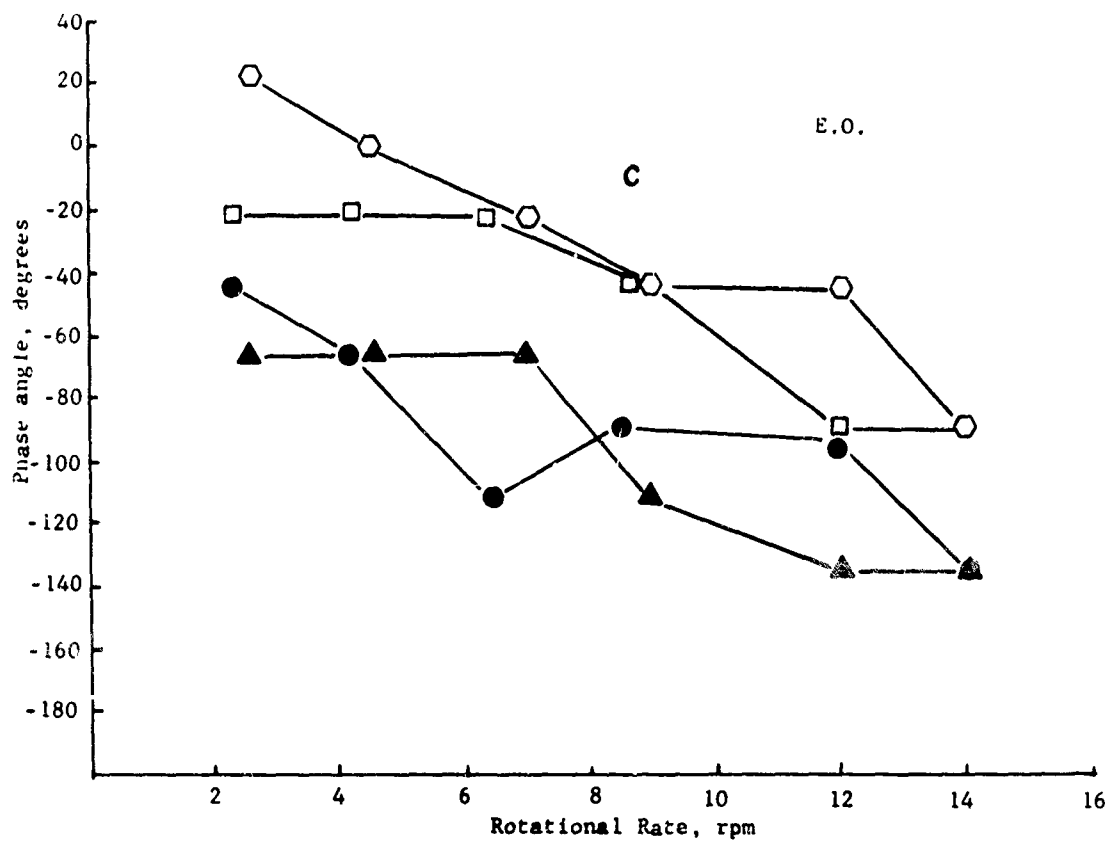


FIGURE 6

several instances when subject A.R. reported subjective nystagmus. The tracings, obtained immediately during and after random rotation when subjects A.R. and J.N. complained of nausea and tumbling was stopped, are depicted in figures 14C and D. For comparison, reference may be made to figure 2 (appendix 2), which shows a tracing of lateral nystagmus (with eyes closed) obtained after stopping 15 rpm yaw rotation in $1\frac{1}{2}$ seconds.

V. DISCUSSION

Cardiovascular system

The type of heart rate response obtained in our experiments is probably due to a combination of different factors. In the low rates of rotation used in this study, the predominant force field that the subject experiences is earth's gravitational field. At the maximum rate of 16 rpm, the centrifugal force component at the neck level (from the center of rotation) is less than 0.2 G. This study is, therefore, different in its implication from studies at high rates of rotation where the centrifugal force approaches and exceeds 1 G. Under our experimental conditions, the cardiovascular response would be mostly secondary to the hydrostatic pressure gradient variation felt along the body column brought about by body rotation through an axis perpendicular to earth's G field, and the attendant physiologic reflexes and responses brought about by this variation.

Figure 15 illustrates a simplified model of the hydrostatic pressure values along the blood column. The reference point (RP) is here assumed to be at about the diaphragmatic level of a man 67 inches in height. As before, we call the upright position the 90° position, and the head-down position the 270° position. We assume the mean arterial pressure at the reference level to be 100 mm. Hg (see figure 15A) and the venous pressure to be 2 mm. Hg (see figure 15B). In the 90° position, the pressures in the neck level will be less by an amount equal to the hydrostatic component from the RP to the neck level, which in our example would be -26 mm. Hg. The pressures in the foot level will be augmented by an amount equal to the hydrostatic component from the

RP to the foot level, which in our example is calculated to be 58 mm. Hg when taken in the seated position. As the subject rotates through the Y or X axes, the Z axis component will change as a sine function as indicated in figure 15G. As illustrated, the head hydrostatic pressure variation lags the foot variation by $(180^\circ - \theta)$ where θ is due to the subject's being in the seated position. The circled line in figure 15G corresponds to body position of subject.

In summary, in the 90° position because of the hydrostatic pressure change, there is a tendency for the arterial pressure in the carotid sinus to fall and for blood to pool in the lower extremities. In the 270° position, there is a tendency for an increased pressure in the neck area and for increased venous return from the lower half of the body. The effect of these potential hydrostatic changes on the pumping action of the heart will be discussed shortly.

As mentioned earlier this is a simplified model, where we have assumed that the reference point is the same for the head part and leg part of the body, and that this reference point does not shift. In fact, evidence has been published to show that in the anesthetized dog, the head part and leg part of the body may behave like separate hydrostatic compartments and so may have different hydrostatic pressure reference points (7, 57); also that the reference point in human subjects may shift to some degree during changes of position (1). This shifting of the reference point may be caused by a nonlinear pressure-volume curve of the blood vessels or a time-dependent vascular impedance. The latter could be due to reflex mechanisms brought about by postural changes. In spite of this complication, the hydrostatic pressure variation will follow in a general way the type of variation we have assumed in our simplified model, provided that, if there is a shift in the reference point, it is small and has the same frequency as the rotation of the subject. It is hoped, nevertheless, that the model presented would be useful in visualizing the events occurring secondary to an oscillating G force.

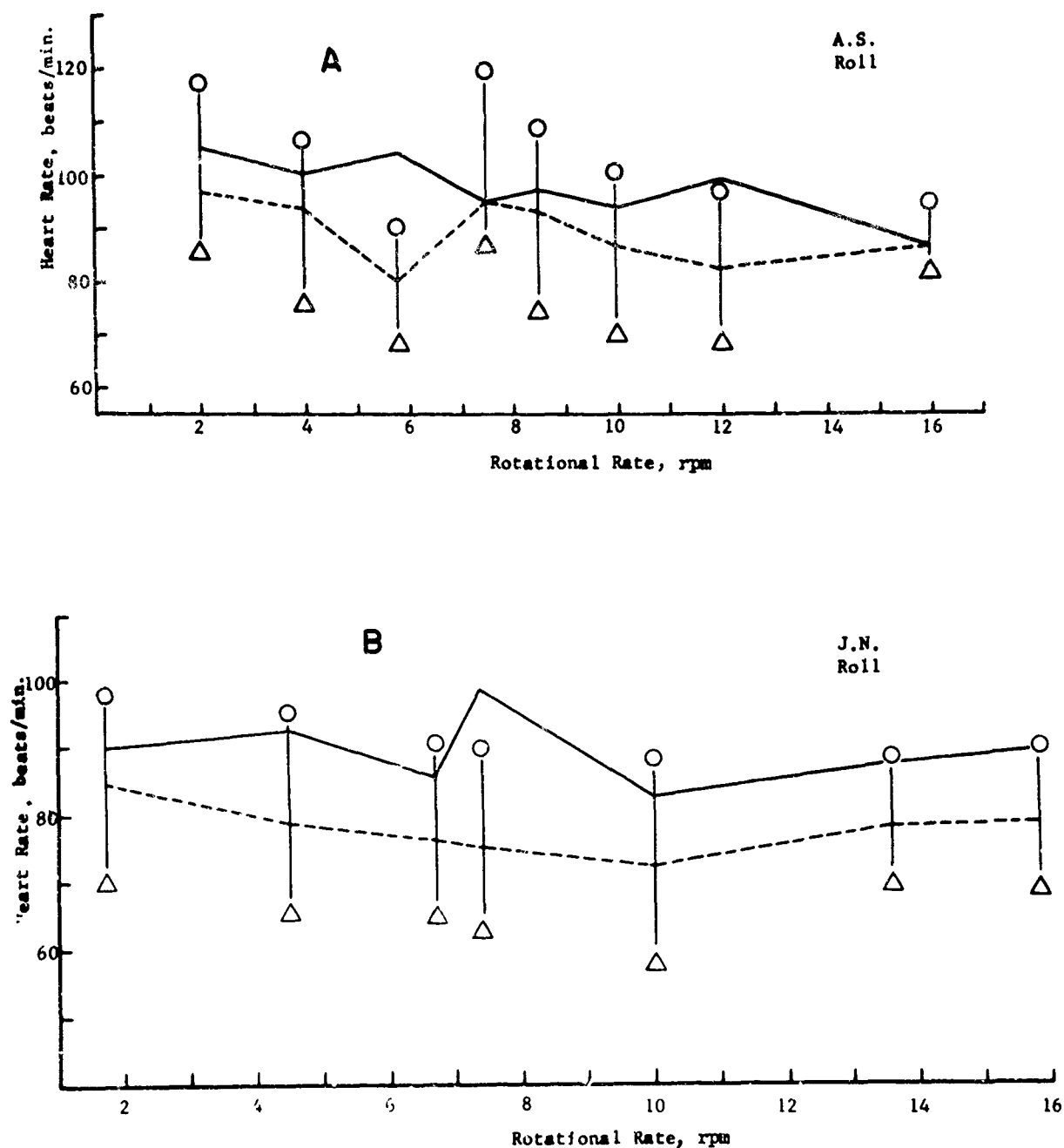


FIGURE 7

Peak-to-peak averaged heart rates as a function of rotational rates. A. Subject A.S. in roll axis. B. Subject J.N. in roll axis. C. Subject A.S. in pitch axis. O - peak heart rate. Δ - minimum heart rate. Solid line - average heart rate before rotation. Dotted line - average heart rate during rotation. D. Averaged difference between maximum heart rate and minimum heart rate as a function of center rotational frequency. The first number at top of each bar refers to the number of subjects tested, and the second number refers to the number of rotational cycles counted, in both pitch and roll profiles. Center rotational rate is the midpoint of the rotational rate class intervals; for example, 2 rpm includes rates of 1 to 2.9 rpm, 4 rpm includes rates of 3 to 4.9 rpm, etc.

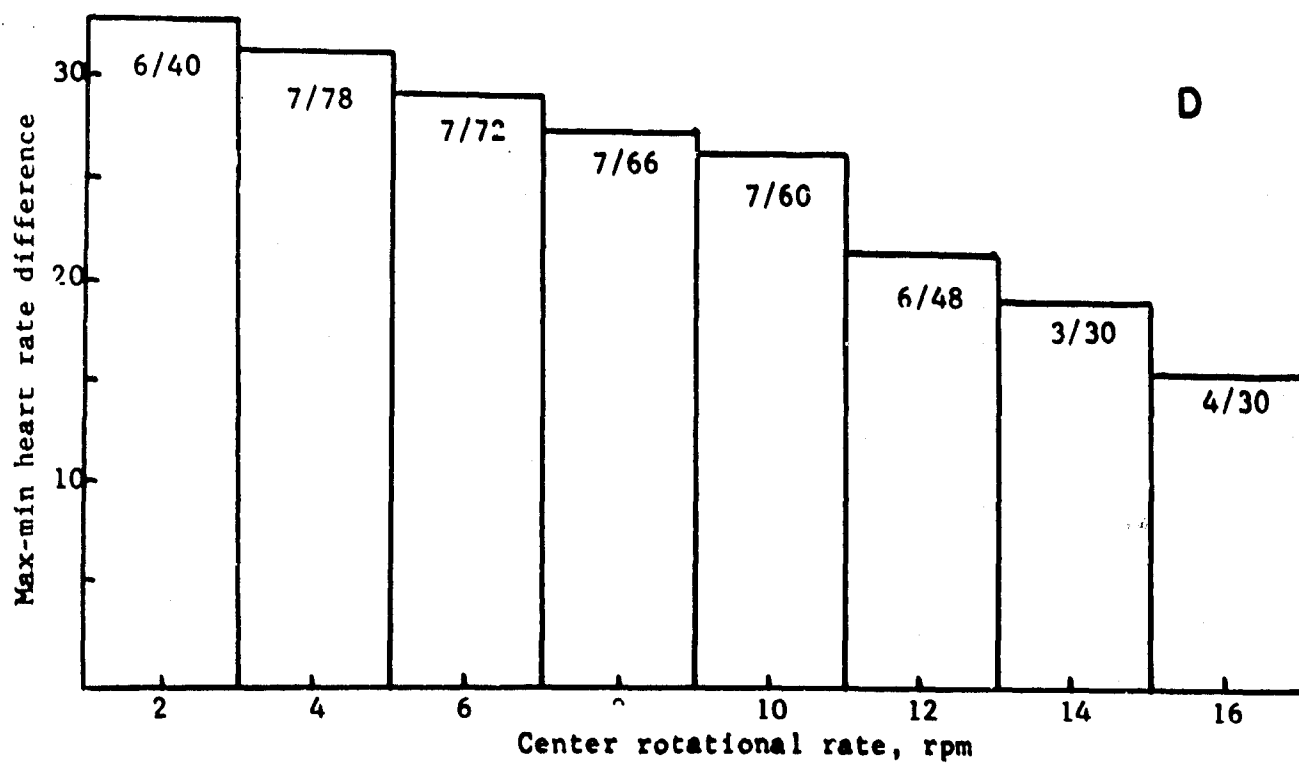
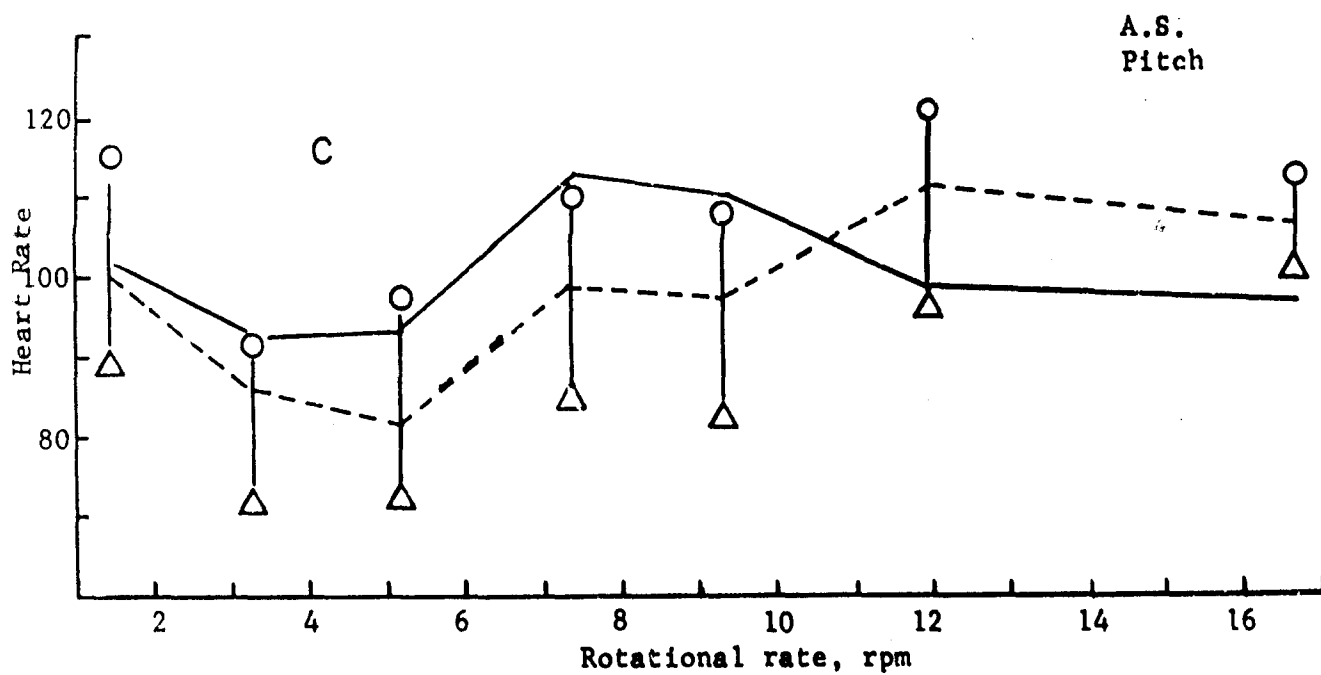


TABLE IIa

Average heart rates before, during, and after rotations in the roll axis

Subject		RPM†							
		2	4	6	8	10	12	14	16
J.N.	E*	90	92.3	85.2	98.9	82.8	—	87.8	90.0
	D*	84.5	78.7	76.3	75.2	72.4	—	78.4	79.0
	A*	89.2	90.8	89.4	98.35	92.6	—	86.7	88.6
E.O.	B	93.8	91.9	95.2	90.5	—	82.4	90.0	96.0
	D	83.7	86.0	82.5	80.1	—	81.6	89.5	90.9
	A	93.1	90.8	86.1	87.3	—	93.2	92.1	98.8
A.R.	B	101.8	99.8	98.5	101.2	92.9	97.8	—	—
	D	92.2	90.7	91.1	92.2	90.0	92.1	—	—
	A	106.6	100.0	98.0	99.3	100.0	99.0	—	—
A.S.	B	105.3	100.2	104.7	97.8	94.5	99.2	—	87.0
	D	97.0	93.6	79.9	93.5	86.7	82.8	—	88.4
	A	102.9	104.8	98.2	97.1	89.5	93.2	—	84.0
T.S.	B	57.8	59.4	58.1	—	96.4	84.8	88.7	—
	D	56.7	60.6	54.7	—	79.8	75.0	70.2	—
	A	63.5	55.8	50.8	—	82.4	95.5	92.1	—
R.D.	B	88.8	93.4	91.0	72.2	81.8	—	—	—
	D	89.2	80.7	76.7	71.6	69.7	—	—	—
	A	84.0	87.9	93.6	78.5	76.4	—	—	—
V.R.	B	—	89.0	92.6	88.6	83.0	87.0	—	—
	D	—	81.6	77.5	76.7	81.9	81.0	—	—
	A	—	83.8	91.0	90.7	88.2	81.2	—	—

°B — Before rotation.

D — During rotation.

A — After rotation.

†Revolutions per minute are midpoint rotational rate of class intervals as explained in legend of figure 7D.

TABLE IIb

Average heart rates before, during, and after rotations in the pitch axis

Subject		RPM†							
		2	4	6	8	10	12	14	16
J.N.	B*	91.4	84.6	89.3	91.3	91.4	85.9	93.6	—
	D*	77.5	71.5	69.4	73.2	73.0	73.0	75.4	—
	A*	93.9	81.1	88.0	89.1	87.0	87.7	87.0	—
E.O.	B	96.1	95.9	98.4	91.2	—	92.0	86.7	—
	D	86.6	85.4	84.9	83.4	—	80.5	79.4	—
	A	98.6	90.0	91.5	89.3	—	83.8	80.1	—
A.R.	B	93.2	87.2	92.1	86.1	—	—	—	—
	D	76.4	71.5	75.3	75.6	—	—	—	—
	A	80.6	75.7	80.7	85.7	—	—	—	—
A.S.	B	102.2	92.6	93.4	110.2	110.4	99.5	—	97.7
	D	100.2	86.6	81.9	99.5	97.8	112.6	—	107.5
	A	98.0	92.0	89.9	113.3	96.2	106.5	—	97.6
T.S.	B	101.6	71.5	80.2	68.0	60.4	—	63.1	50.0
	D	81.6	74.6	69.1	73.3	70.9	—	50.6	50.5
	A	81.2	76.6	69.5	58.4	55.3	—	52.1	48.0
V.R.	B	—	80.5	73.2	—	—	—	—	—
	D	—	78.1	75.9	—	—	—	—	—
	A	—	81.9	62.8	—	—	—	—	—

*B — Before rotation.

D — During rotation.

A — After rotation.

†Revolutions per minute are midpoint rotational rate of class intervals as explained in legend of figure 7D

TABLE IIIa

Blood pressure values before and after rotations in the roll axis

Subject		RPM†								BP reading
		2	4	6	8	10	12	14	16	
J.N.	Pre-run	130	125	125	105	120	—	125	115	S*
		80	70	75	70	75	—	70	75	D*
	Post-run	125	120	105	130	105	—	115	—	S
		80	75	70	80	70	—	75	—	D
E.O.	Pre-run	125	135	125	125	—	110	115	110	S
		80	75	75	75	—	80	75	70	D
	Post-run	—	125	125	120	—	110	115	125	S
		—	80	75	70	—	70	75	80	D
A.R.	Pre-run	110	115	105	110	120	120	—	—	S
		70	70	75	80	75	75	—	—	D
	Post-run	115	130	115	110	120	120	—	—	S
		70	70	70	70	75	70	—	—	D
A.S.	Pre-run	130	130	130	—	135	130	—	140	S
		85	75	70	—	80	80	—	70	D
	Post-run	130	135	140	130	130	135	—	140	S
		70	65	70	75	70	70	—	80	D
T.S.	Pre-run	115	110	110	110	125	130	135	—	S
		65	65	80	70	80	—	70	—	D
	Post-run	115	115	110	120	115	130	135	—	S
		75	75	65	75	70	80	80	—	D
R.D.	Pre-run	110	—	120	125	125	105	—	—	S
		70	—	75	75	75	75	—	—	D
	Post-run	130	125	125	110	105	120	—	—	S
		80	80	70	75	75	80	—	—	D
V.R.	Pre-run	—	135	125	130	—	125	—	—	S
		—	65	80	70	—	70	—	—	D
	Post-run	—	125	125	135	125	125	—	—	S
		—	75	75	70	70	70	—	—	D

*S — Systolic.

D — Diastolic.

†Revolutions per minute are midpoint rotational rate of class intervals as explained in legend of figure 7D.

TABLE IIIb

Blood pressure values before and after rotations in the pitch axis

Subject		RPM†								BP reading
		2	4	6	8	10	12	14	16	
J.N.	Pre-run	130	115	110	110	120	115	125	—	S*
		70	75	80	75	80	80	70	—	D*
	Post-run	110	110	115	115	125	—	115	—	S
		80	80	80	80	70	—	70	—	D
E.O.	Pre-run	115	115	115	105	130	110	115	—	S
		70	75	65	80	85	80	75	—	D
	Post-run	120	115	105	120	125	120	115	—	S
		65	75	80	70	75	75	75	—	D
A.R.	Pre-run	130	115	115	130	130	128	120	—	S
		65	65	70	75	80	80	75	—	D
	Post-run	120	105	115	125	130	130	120	—	S
		70	60	70	70	75	80	75	—	D
A.S.	Pre-run	120	125	120	120	125	130	—	120	S
		70	80	80	85	30	80	—	90	D
	Post-run	120	115	115	125	130	130	—	125	S
		80	70	75	80	80	70	—	80	D
T.S.	Pre-run	140	125	135	140	—	—	115	120	S
		75	75	75	85	—	—	75	75	D
	Post-run	150	130	130	—	124	—	115	125	S
		70	75	75	—	75	—	80	75	D
V.R.	Pre-run	130	120	110	—	—	—	—	—	S
		75	75	75	—	—	—	—	—	D
	Post-run	125	110	110	—	—	—	—	—	S
		75	75	75	—	—	—	—	—	D

*S — Systolic.

D — Diastolic.

†Revolutions per minute are midpoint rotational rate of class intervals as explained in legend of figure 1D.



FIGURE 8

Electrocardiogram R wave amplitude plotted from cycle to cycle as a function of body position in subject T.S. while rotating in pitch and roll axis at 6 rpm. As usual, sine wave corresponds to G force in caudal portion of body with maximum point when in the head-up position, and minimum in the head-down position.

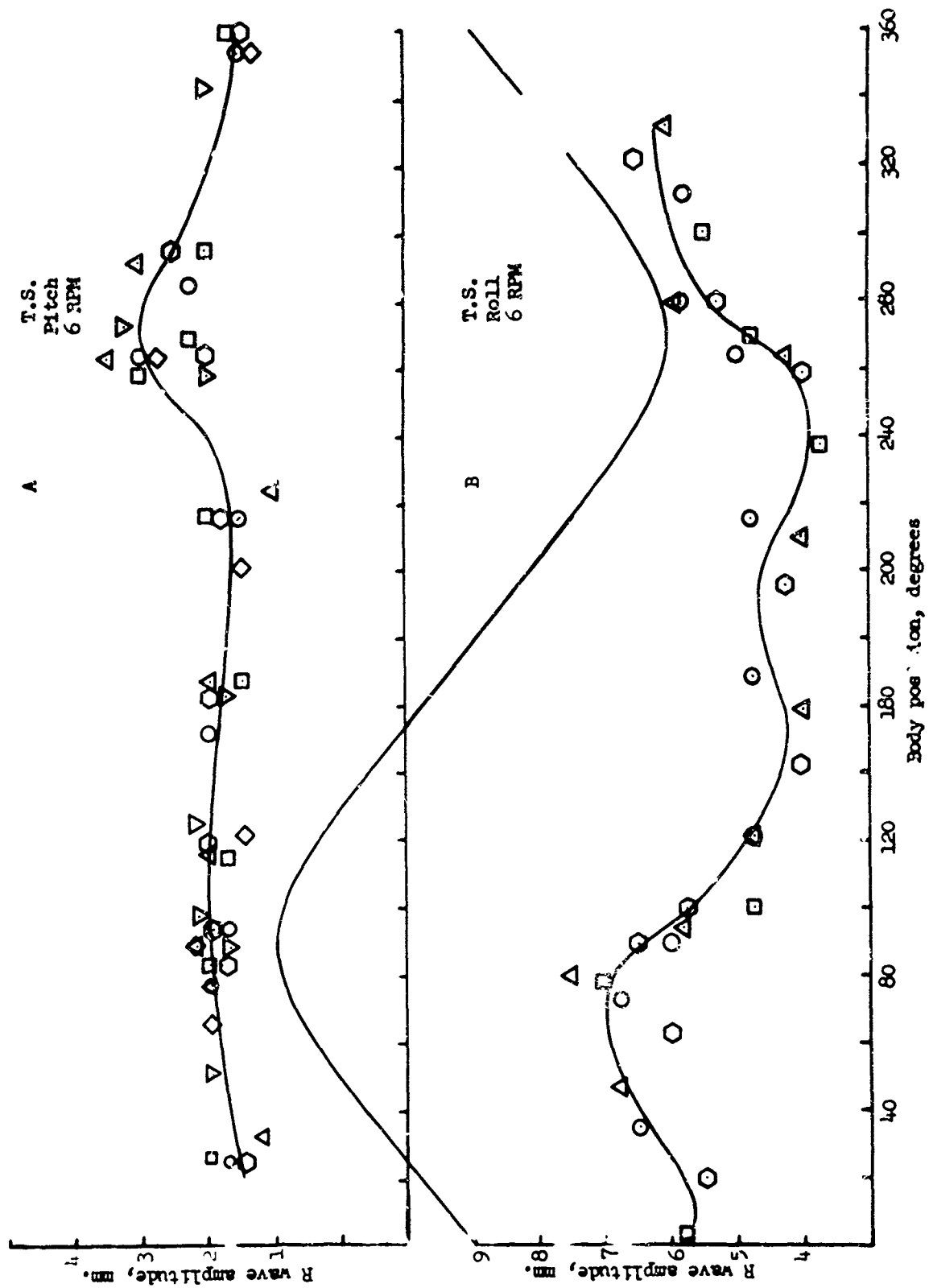




FIGURE 9

Electrocardiogram tracing from actual experiment. a, Subject V.R. in roll axis rotation at 10 rpm. b, Subject E.O. in pitch axis rotation : 7 rpm. c, Subject E.O. during slow random rotation. d, Subject E.O. during fast random rotation. e, Subject A.R. during slow random rotation. Arrows in a and b indicate head-down position.

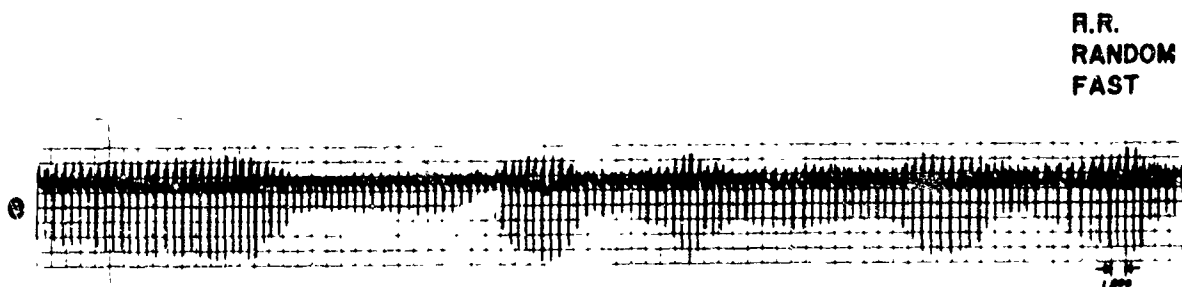
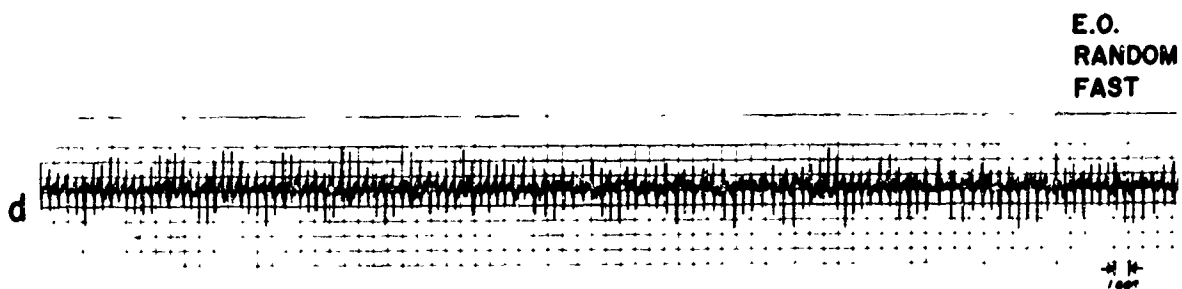
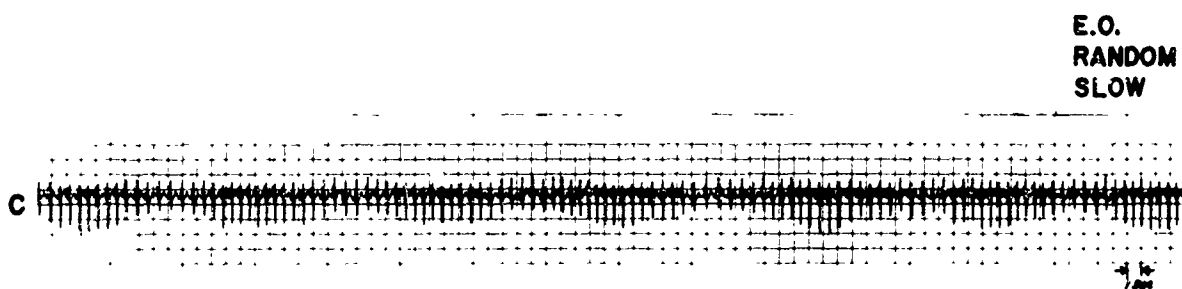
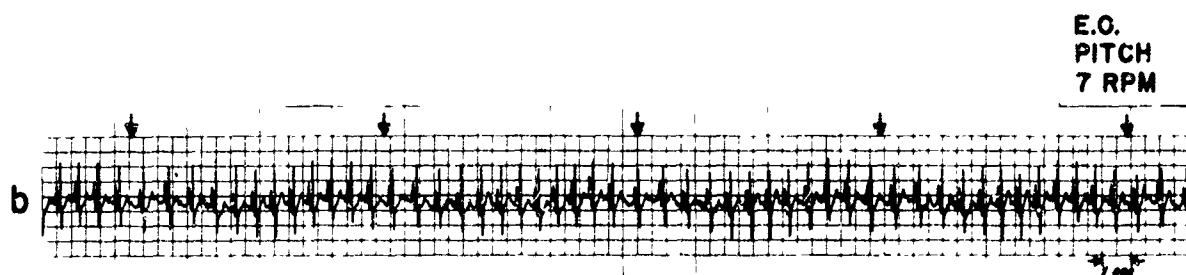
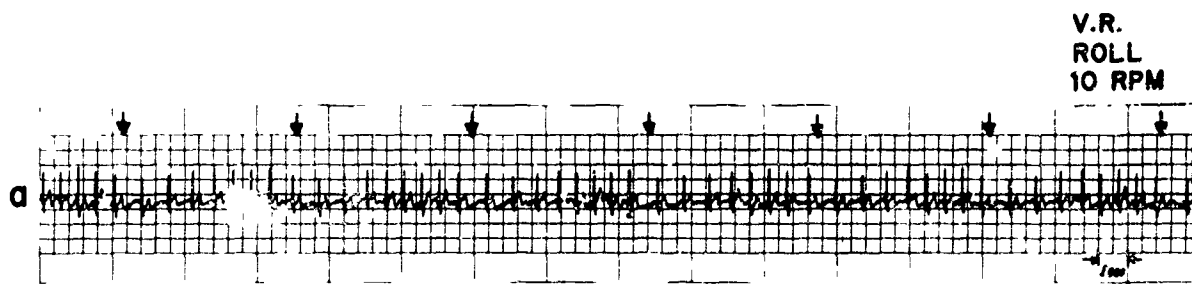


TABLE IV
Summary of hot and cold environment and of water immersion experiments

Subject	Conditions	Sequence of events	RFS temp. (°C.)	Time of exposure (min.)	Skin temp. (°C.)	Rectal temp. (°C.)	Heart rate	BP
T.S.	Hot environment	I*	—	—	33.6°	36.8°	60.0	110/70
		II	38°	50	36.8°	36.8°	71.9	110/75
		III	—	3	—	—	67.7	—
		IV	36.5°	—	36.9°	36.8°	76.2	110/70
	Cold environment	I	—	—	34.1°	37.1°	60.0	115/70
		II	12.5°	55	31.0°	37.0°	52.0	115/65
		III	—	3	—	—	52.4	—
		IV	15.5°	—	30.5°	37.0°	48.0	110/85
A.S.	Hot environment	I	—	—	34.0°	37.1°	86.0	110/70
		II	38°	63	36.4°	37.3°	96.6	110/75
		III	—	3	—	—	80.6	—
		IV	36.5°	—	36.6°	37.45°	95.3	110/80
	Cold environment	I	—	—	35.5°	37.35°	82.0	120/80
		II	11.5°	60	33.0°	37.35°	70.3	115/80
		III	—	3	—	—	75.2	—
		IV	14.5°	—	33.0°	37.5°	65.2	112/80
J.N.	Hot environment	I	—	—	34.0°	37.6°	72.0	115/80
		II	38°	72	36.4°	37.62°	83.4	110/80
		III	—	3	—	—	70.4	—
		IV	36.5°	—	36.5°	37.62°	85.1	110/75
	Water immersion	I	—	—	—	—	82.1	120/80
		II	25°	360	—	—	100.0	110/75
		III	—	4	—	—	77.7	—
		IV	25°	—	—	—	94.0	106/80

*I — Before exposure.
II — Before rotation.
III — During rotation.
IV — After rotation.

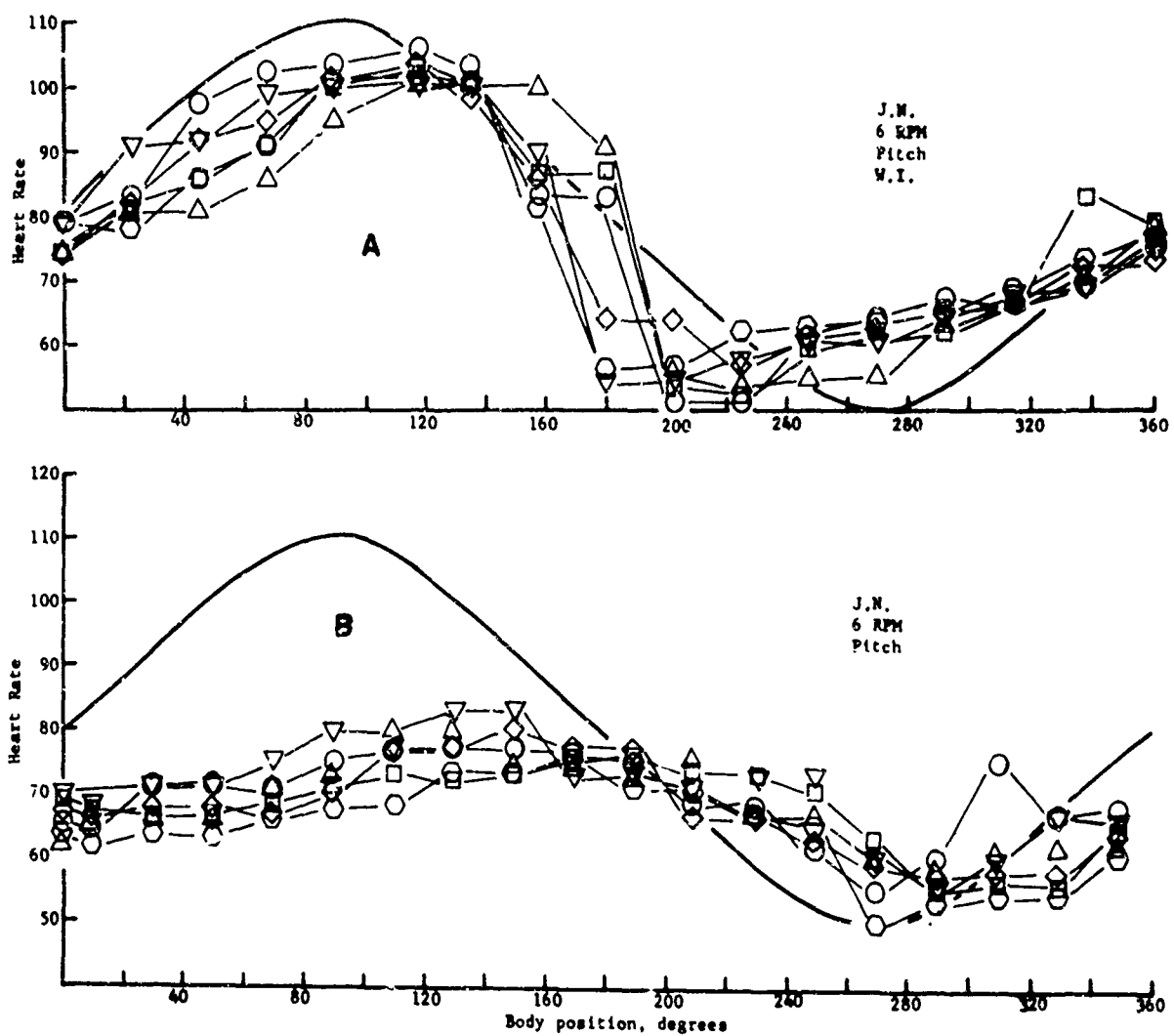


FIGURE 10

A. Heart rate response of subject J.N. during 6 rpm, pitch forward rotation 22 minutes after 8-hour water immersion. B. Heart rate response of same subject to same profiles without previous water immersion.



FIGURE 11

- A. Time required by subject E.O. to bring back RFS to upright position ("righting time") from initial position of RFS on the right side are plotted against trial numbers.
- B. "Righting time" plotted as a function of duration of random tumbling at slow rate.
- C. "Righting time" plotted as a function of duration of random tumbling at a fast rate.

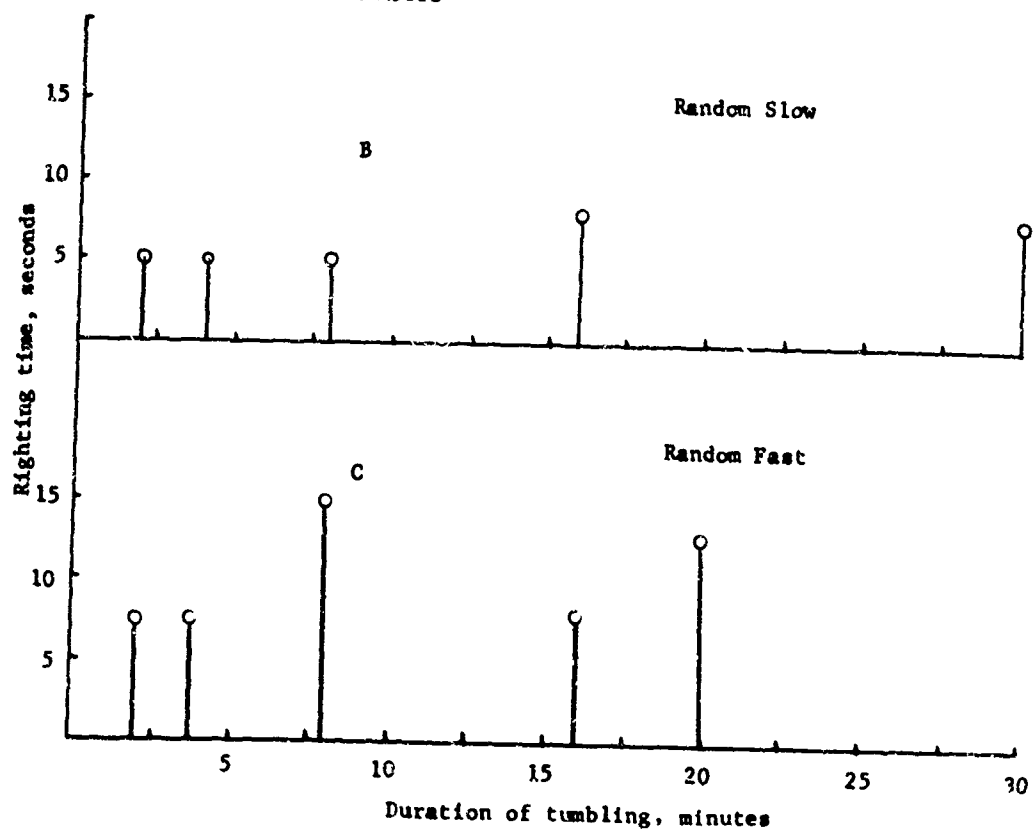
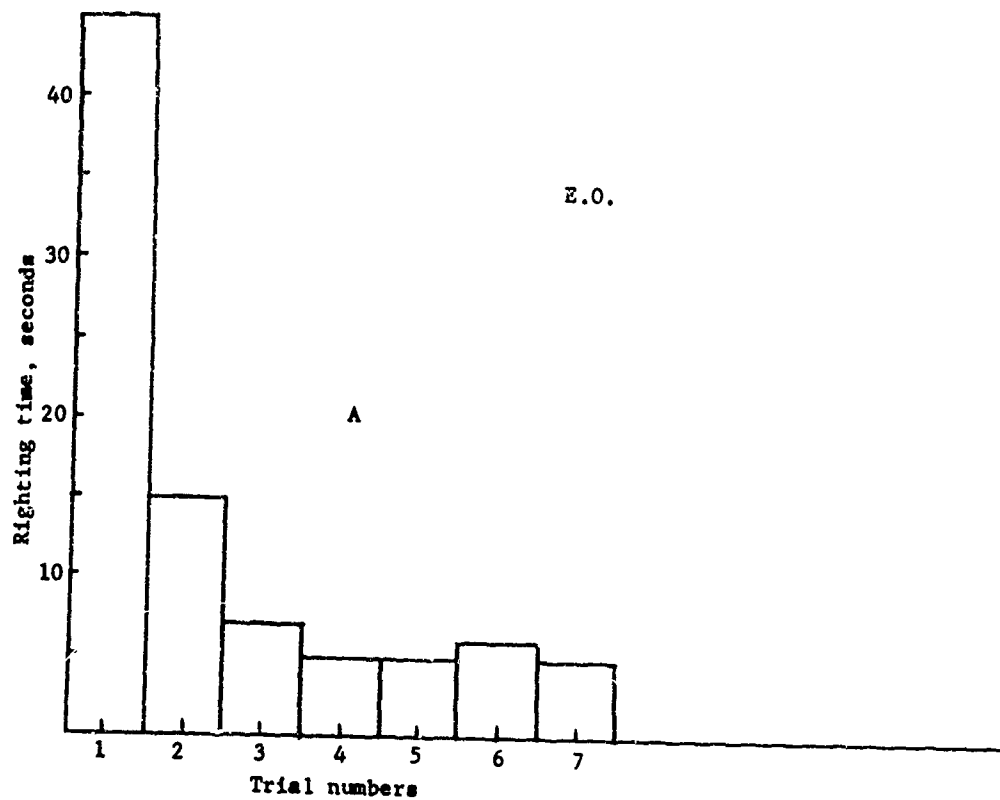




FIGURE 12

A. "Righting time" plotted against trial numbers in subject A.S. righting RFS from head-down position. B. "Righting time" plotted as a function of duration of tumbling at a slow rate. C. "Righting time" plotted as a function of duration of random tumbling at a fast rate. Arrows indicate time when queasy stomach or nausea was experienced and tumbling was discontinued.

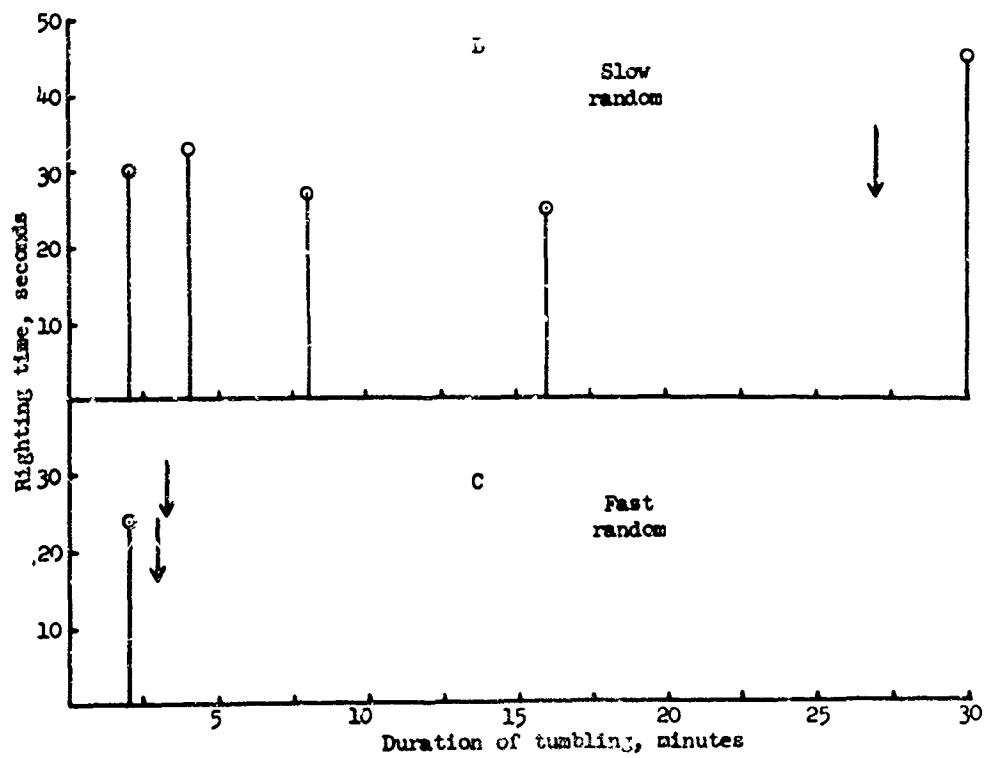
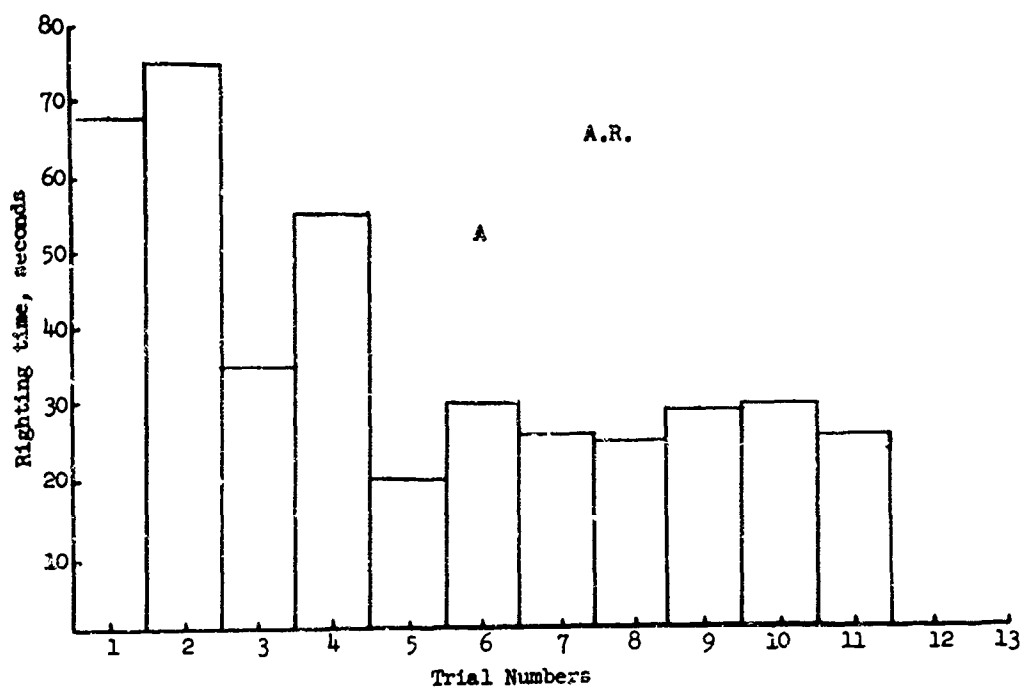




FIGURE 13

A. "Righting time" plotted against trial numbers in subject J.N. righting RFS from head-down position. B. "Righting time" plotted as a function of duration of tumbling at a fast rate. Arrows indicate times when queasiness of stomach or nausea was experienced.

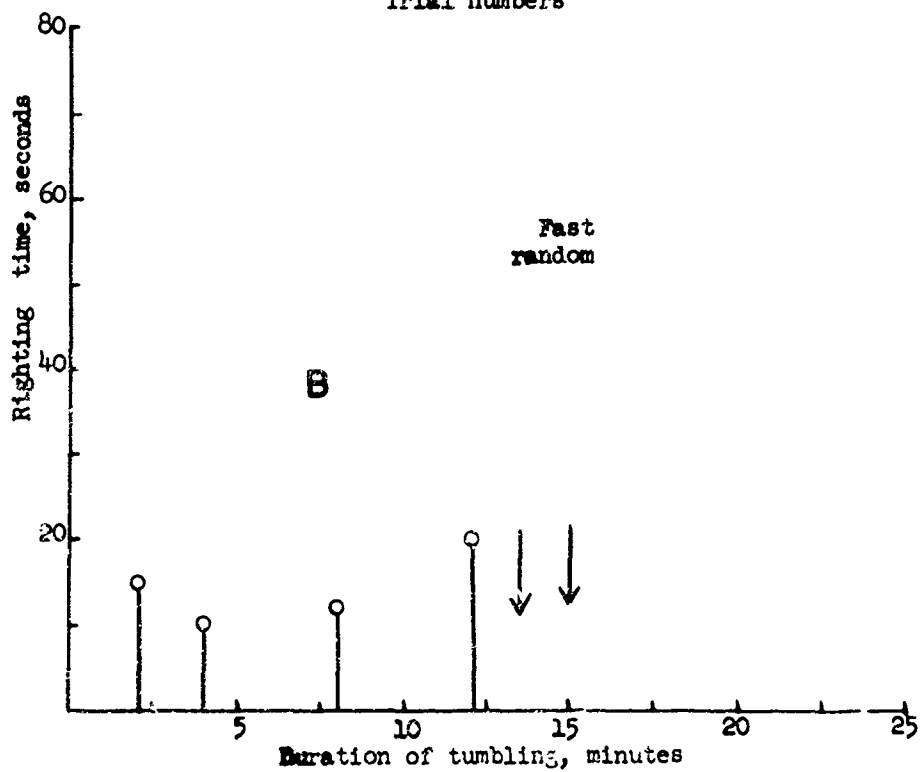
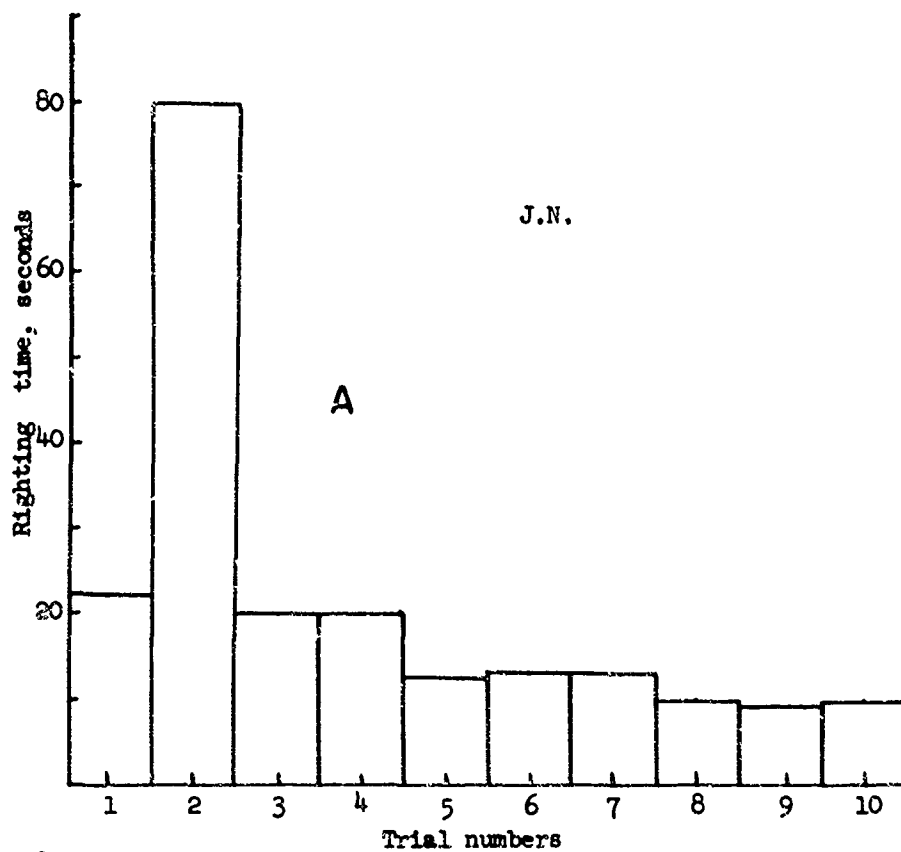
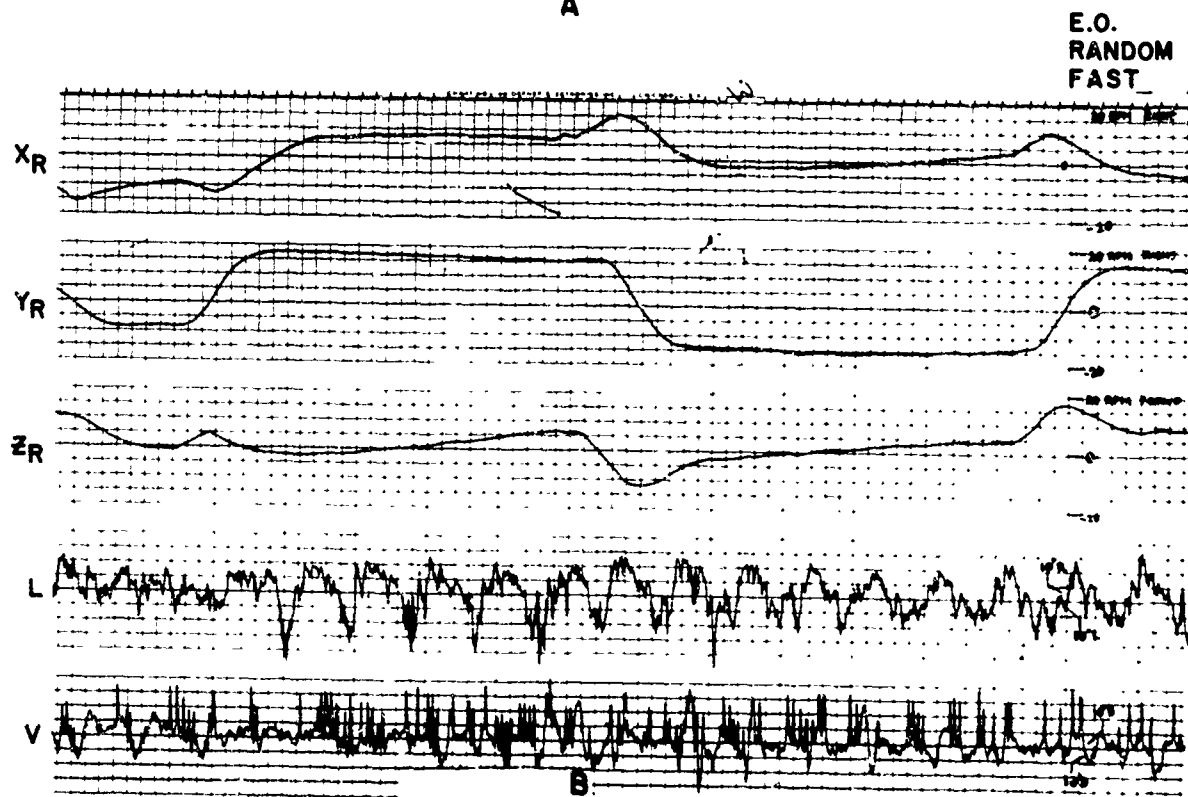
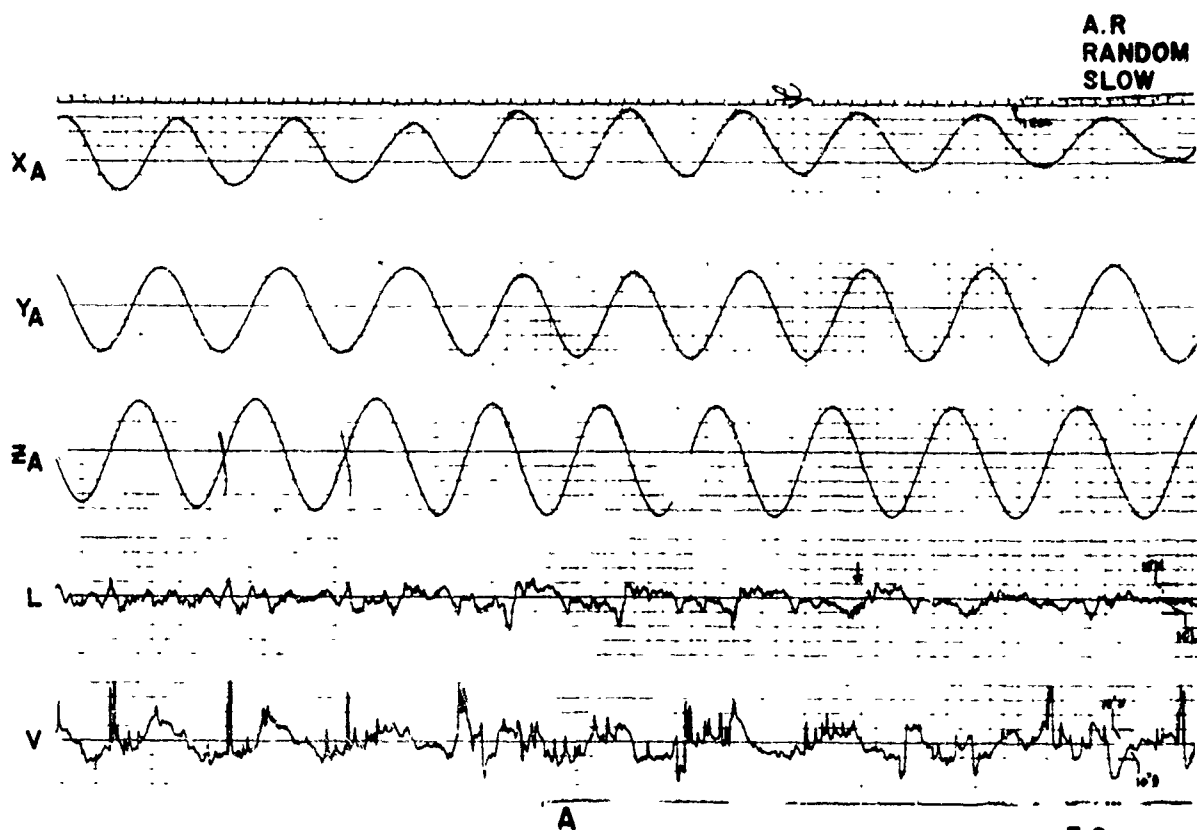
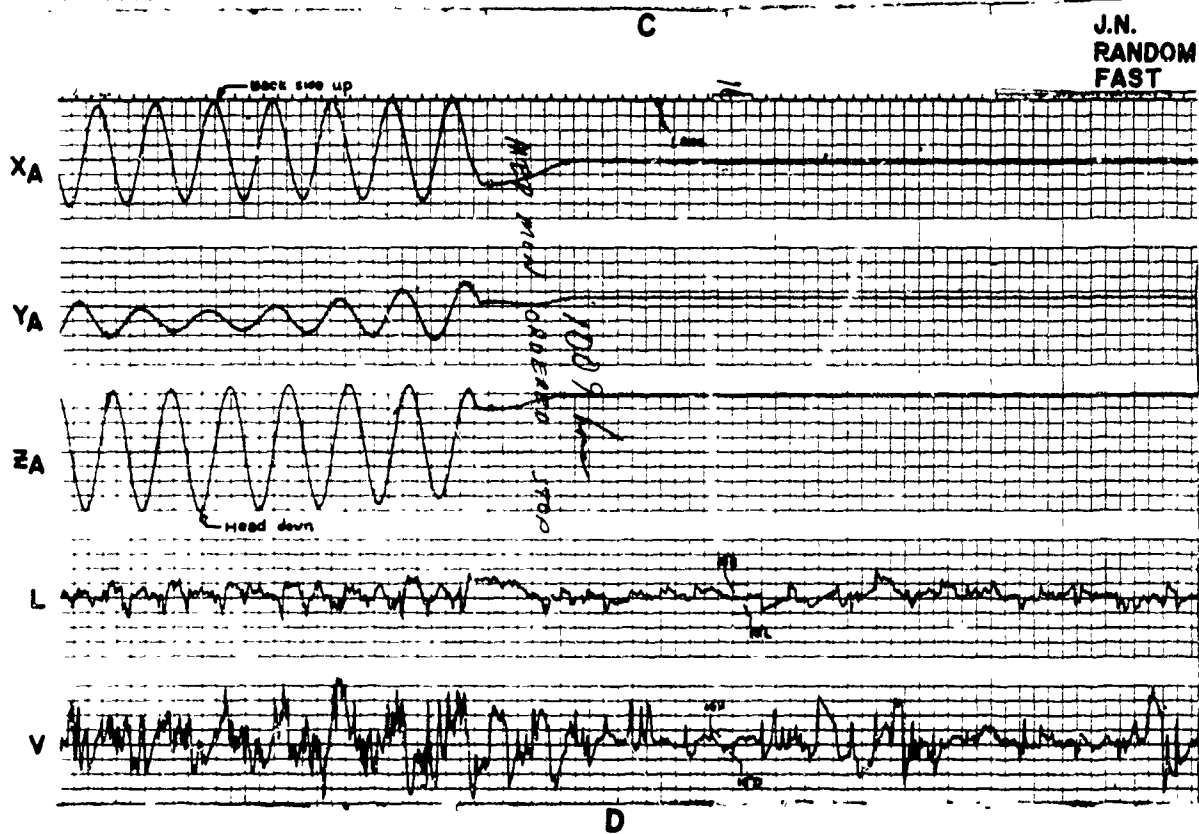
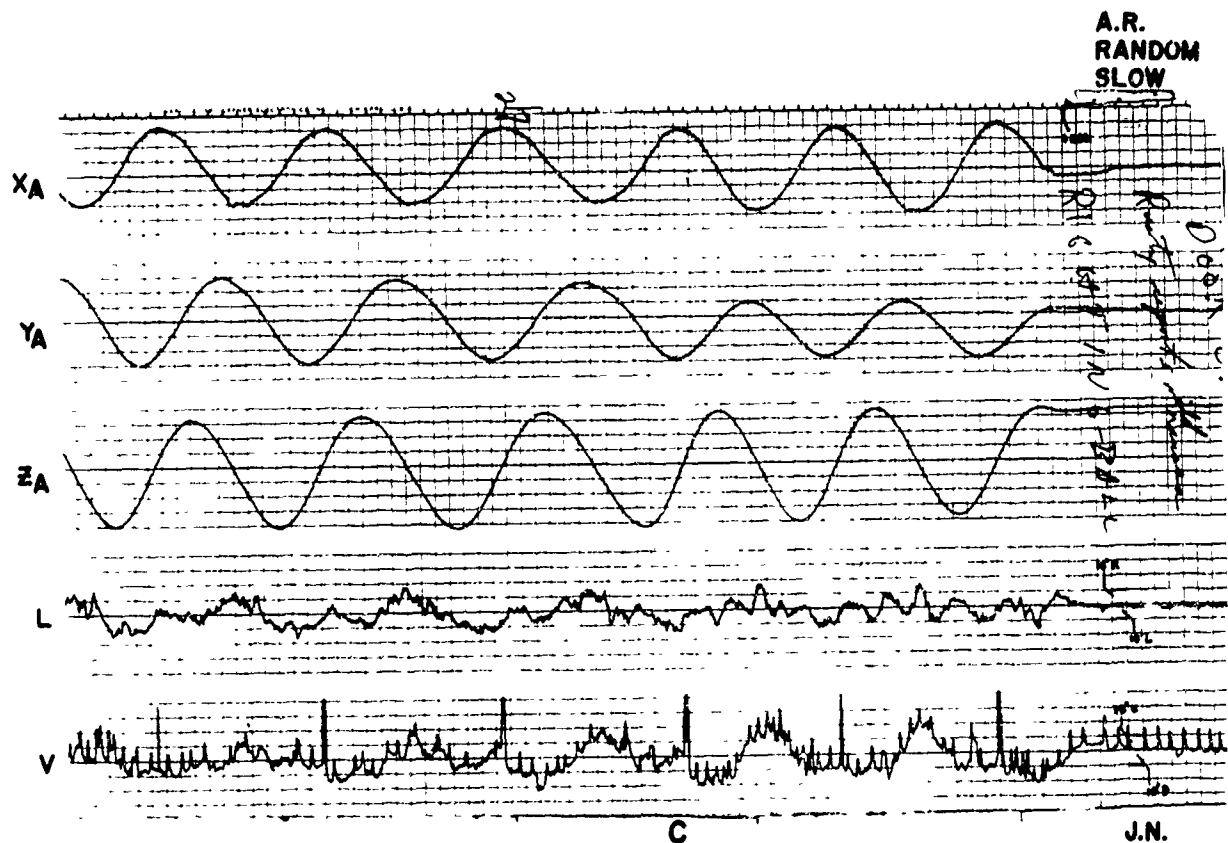




FIGURE 14

A. Lateral and vertical nystagmogram tracings shown with three channels of accelerometer in the roll (X_A), pitch (Y_A), and yaw (Z_A) axis in subject A.R. during random tumbling at a slow rate. Arrow indicates one of several occasions when subject reported subjective nystagmus. B. Same as A shown with three channels of rate gyros corresponding to roll (X_R), pitch (Y_R), and yaw (Z_R) in subject E.O. during random tumbling at a fast rate. C. Same subject and experiment as in A during the latter part of 27 minutes of slow random tumbling. Nausea was experienced and so the RFS was stopped and RFS door opened immediately. D. Subject J.N. random tumbling at fast rate, showing outputs of three channels of accelerometer, lateral and vertical nystagmogram. Subject was sick after 15 minutes of tumbling and RFS was stopped. Observation for possible nystagmus was continued, tracings of which are shown here. Sharp spikes in the vertical nystagmogram channel correspond to eye blinking.





The actual pressure variation and the actual shift of blood volume secondary to this potential variation of hydrostatic pressure are very hard to ascertain. We cannot yet measure blood pooling during slow rotation, but from studying the initial responses (first few seconds) seen in tilt table and postural change studies (1, 50, 51, 57) it may be assumed that in the slow rotation we performed, blood shifting occurred. It is generally accepted that in tilt table studies (tilting to the head-up or head-down position), the shift in arterial blood volume is minimal, but the shift in venous blood distribution could be considerable in view of the greater distensibility of the veins (4, 15). Moreover, the distensibility of the veins caudal to the heart are probably greater than that rostral to the heart. If this is so, the variation of cardiac filling during rotation would be dominated by the effect of the cyclic "pooling" and "collapsing" of the veins of the caudal portion of the body. The changes in the cardiac filling bring about corresponding changes in the cardiac output (Frank-Starling mechanism). The heart rate oscillation, therefore, is probably due to the arterial pressure changes brought about by the changes in cardiac return, and to the changes in the hydrostatic pressure component *per se* felt at the carotico-aortic sinuses level. Both factors would give a heart response in the same direction, but a differentiation of the effects of each factor cannot be made in the experiment we have done.

The frequency dependence of the heart rate response to rotation is a complex one. We have seen that cardio-acceleration is a gradual process, that there is a lag in reaching the maximum pulse rate (relative to the 90° position), and that this lag gets more pronounced as rotational frequency is increased. These characteristics are explained here as being due to a combination of different factors: (1) A response characteristic of the sympathetic system and of the accompanying synergistic depression of vagal impulses, because of a decreasing pressure in the carotid sinus level. Qualitatively, our results imply a longer time constant of the cardio-acceleration response curve as compared to cardio-deceleration response curve. (2) A lag in the occurrence of

the arterial pressure reduction felt at the pressoreceptor sites—secondary to blood pooling in the lower half of the body. This lag may be due to a complex interrelationship of blood vessel impedance, blood fluid inertia, and reflex vasomotor responses. Changes in peripheral vascular resistance secondary to postural change probably occur in slow rotation, since the response time of the changes of vessel is about 0.6 to 1.2 seconds (41).

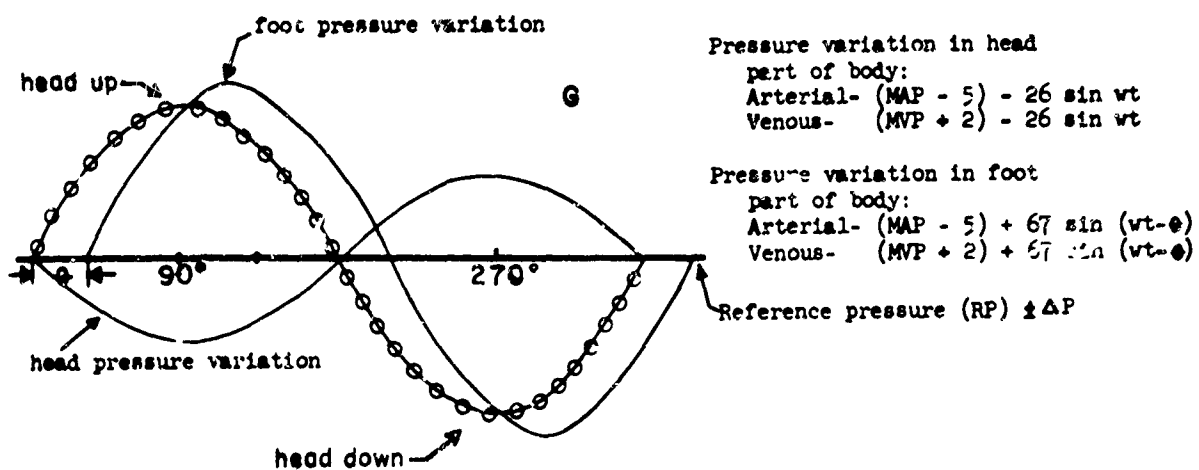
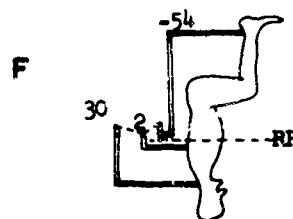
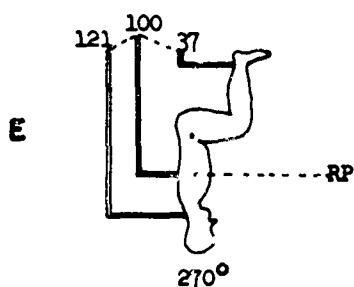
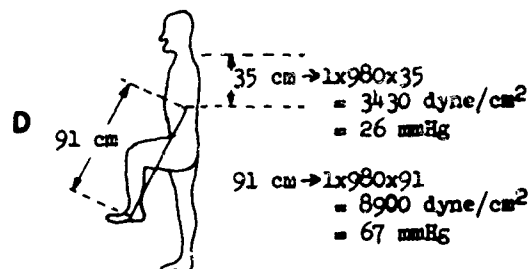
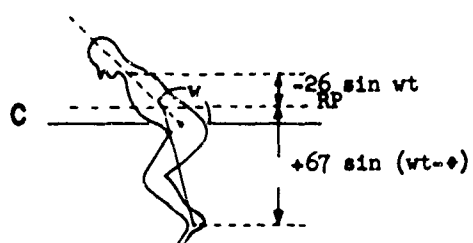
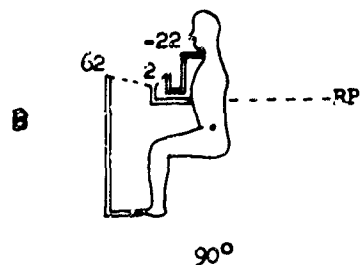
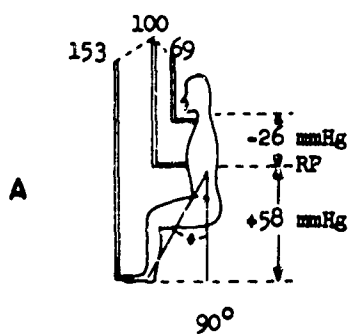
In contrast, cardio-deceleration is a more rapid process; there is a smaller phase lag in the bradycardia trough (relative to the 270° position) which sometimes leads the 270° position, and this lag gets larger with increase of rotational frequency. This complex response again is probably due to a combination of different mechanisms: (1) The known dominance of vagal influence on the heart rate control. (2) A response characteristic of the vagal system and the accompanying inhibition of the sympathetic impulses, in which our results imply a shorter response time of the composite cardio-deceleration response curve. (3) Greater pressure stimulus sensitivity of the carotid sinus in response to the unaccustomed head-down posture. (4) The resultant interrelationship of blood vessel impedances, blood fluid inertia, and reflex vasomotor responses (going in the opposite direction to that induced by the 90° position). The points enumerated here necessarily overlap because our knowledge of the system is incomplete. The complex combination of these factors resulting in the synthesis of the type of heart rate response observed indeed defies present analytical tools. The fact that the subject was in the sitting position, with the foot in front of the heart vertical axis that forms about a 30° angle with the body axis (see figure 15), may contribute to a delay in heart rate maxima and minima relative to body position; but this alone will not account for the frequency dependence observed.

A knowledge of the instantaneous blood pressures in the different parts of the circulatory system would be most important in analyzing further our results, but the technical difficulties of doing this in the RFS at present



FIGURE 15

Simplified model of hydrostatic pressure variation secondary to rotation in an axis perpendicular to earth's gravitational field is illustrated here in the pitch axis. In A, B, E, and F are indicated the expected mean arterial pressures (A and E) and venous pressures (B and F) in the neck, diaphragm, and feet levels when subject is at 90° and 270° positions. C and D illustrate the calculation of the hydrostatic pressure components from anatomical considerations and their sinusoidal variations. In G is shown a schematic plot of the expected hydrostatic pressure variation in the head and feet. The circled sine wave refers to body position where the maximum point corresponds to the head-up position and the minimum point to the head-down position. The maximum hydrostatic pressure at the foot area lags the head-up position by angle θ since the subject is in the sitting position. In the expressions for pressure variations in the head and foot part of body, MAP refers to mean arterial pressure; MVP refers to mean venous pressure; and δ and ϵ are hypothetical pressure drops along the arterial and venous vessels, respectively.



are formidable. The measurements by catheterization done on tilt table studies in men (57), nevertheless, support the essential parts of the assumption we have made earlier as regards the blood pressure variation in the head and foot part of the cardiovascular system. The indirect blood pressures we have taken before and after each run are limited in physiologic value since the most interesting blood pressure changes probably occur during the rotation, and are probably rapid and transient.

Most of the discussion above would apply to the type I response. Type II response, as seen in the very low rotational rates and which exhibits more scatter with minor heart rate peaks and troughs, is possibly due to attempts of the system to adapt to instantaneous body position. In other words, since the body rotates slowly, the circulatory reflex mechanisms attempt to adjust to specific body positions, but are thwarted because the body position continues to change. The type III response, seen when the half-cycle period of the rotation approaches the period of the lowest pulse rate, is possibly due to a finite decay time particularly of the parasympathetic response. If so, as a result of a response to reflexes excited by the head-down position, the heart may still be under predominantly vagal control and the sympathetic system still partially depressed when the subject starts to come to the head-up position at a fast rate.

The Δ HR appear to be greatest (32 beats per minute) when the subjects were rotating at 1 to 3 rpm (0.017 — 0.05 cps) and smallest (17 beats per minute) when rotating at 14 to 16 rpm (0.23 — 0.25 cps). A significant part of this difference is probably due to a greater pressure amplitude variation imposed on the pressoreceptors at the slow rotational rate as there is greater time for blood shifting to occur so that heart rate variation would correspondingly be greater. Some part of this, however, may be due to the rectifying property of the blood pressure control mechanism as the frequency of pressure variation increases beyond 0.1 cps (10, 39).

In spite of the complex type of stimulus by which we are exciting the pressoreceptors, and

the undefined location of the pressoreceptors involved, it is interesting to note that the heart rate response we observed bears some analogy with results obtained in animal experiments when the isolated carotid sinus is exposed to a sinusoidal pressure input. Stegemann (41) in 1957 studied the blood pressure and heart rate response to sinusoidal forcing pressure in the isolated carotid sinus. He reported that the femoral artery pressure response was not exactly sinusoidal, but decreases faster than it rises. Further, that the increase of the slope of the "sympathetic sensor phase lag" (angle between carotid sinus pressure minimum and femoral artery maximum) with increasing stimulus frequency was steeper than the corresponding slope of the "parasympathetic sensor phase lag" (angle between carotid sinus pressure maximum and femoral artery minimum). The analogous results in our experiments in humans are: (1) the heart rate response was asymmetrical, falling faster than it increased; and (2) the phase lag between heart rate maximum and 90° position was always larger than the phase lag between the heart rate minimum and the 270° position. This interesting correspondence, however, can only be a very rough one. In our experiments the control loop was not opened, so that all the reflexes were active in a closed loop mode of operation. In our analysis we assumed that the carotid sinus pressoreceptors are predominantly involved, although in our experiments receptors in the atria, ventricles, pulmonary vessels, and perhaps in the splanchnic circulation are probably also active. We do not have instantaneous blood pressure measurements which Stegemann had, and the heart rate probably does not always parallel the blood pressure changes. Furthermore, our forcing pressure function may not be sinusoidal because of the undefined effect of changing venous return and its dynamic effect on the cardiac output. Despite these reservations, our results show characteristics of the sympathetic and parasympathetic system response in human heart rate control analogous to Stegemann's findings.

The absence of a striking difference in the heart rate response between the roll and pitch

axes is because the hydrostatic pressure variation is similar in both profiles. The variation of the ECG pattern in the pitch, roll, and random profiles is here interpreted as being due to some motion of the heart within its attachments, so that the heart vector changes in direction and magnitude not only because of depolarization but also because of its movement within the thorax. The difference from subject to subject is probably predominantly due to differences in the mobility of the heart in its asymmetric elastic suspensions, differences in the attachment points of connective tissue, and differences in mechanical properties of these tissues. Variations in QRS amplitude in the random axis rotations are more pronounced than in the pure axes rotations. This is expected on account of the randomly changing angular momentum imposed on the heart structures so that the torques imposed on the heart structure probably would be more severe. This suggests to us that the mechanical strain on the heart and its attachments is greater in random axes tumbling than in pure axes rotation. The consequences of this on circulatory dynamics may be an interesting problem to pursue.

Effects of ambient air temperature

On the basis of the heart rate and indirect blood pressure response, it appears that the 3 subjects tested did not show very severe circulatory system stress as a result of a combined exposure of 38° C. environment for 50 to 72 minutes and subsequent rotation at 6 rpm, pitch axis for 3 minutes. The skin temperature rise of about 3° C. observed and the sweating at the end of the heat exposure, however, indicate that a large amount of cutaneous vasodilatation was probably present. Because of the complex response of the circulatory system to hot environment, more experiments are necessary to study in greater depth this aspect of the response to tumbling. In addition, environmental humidity needs to be defined.

The exposure of 2 subjects to RFS temperature of 11.5° to 15.5° C. followed by 3 minutes' rotation at 6 rpm in the pitch axis resulted in greater scatter in the bradycardia response and

more occurrences of earlier bradycardia; this finding suggests the possibility of a reduced peripheral vascular resistance, which may be due to some vasodilatation resulting from local heat production which could occur secondary to intermittent shivering of the legs. Another factor may be shunting of blood into low resistance deep veins secondary to cutaneous vasoconstriction, which is suggested by the drop of skin temperature of 2.5° and 3.2° C. Owing to the limited number of experiments, no definitive conclusions can be drawn here.

Effects of water immersion

It is known from the work of Hunt (26) that a 6-hour period of water immersion can produce significant orthostatic deconditioning. The type of heart rate response observed during 6 rpm pitch rotation after 6-hour water immersion suggests a shift of blood volume to a greater degree. This could be brought about by a decreased peripheral vascular resistance and increased venous capacitance, and perhaps a concomitant change in blood pressure regulatory mechanism induced by water immersion. In any case, this single study points out certain important properties of the response to slow tumbling in a G field after some degree of orthostatic deconditioning has occurred. Extension of this study to greater number of subjects would be of great value.

Pilot performance and motion sickness

From the studies made in 3 subjects, the following conclusions are suggested: (1) the 3 subjects had different abilities in "righting" the RFS from a chosen initial static position; (2) learning to "right" the RFS from some chosen static position showed fast improvement with repetitive trials; (3) the "righting time" was increased with longer duration of random tumbling and even more increased when rate of random rotation was increased; (4) the time of onset of queasiness of stomach or nausea secondary to random tumbling varied from subject to subject; (5) faster rate of rotation in the random axis produced more nausea than slower rate of rotation; and (6) in the subjects who experienced nausea, the time of onset was reproducible in two trials.

It is not intended that a detailed discussion of pilot performance and motion sickness be made here since the number of experiments performed was limited. It should be noted, however, that in contrast to the experiments where the rotational rate was constant, in random tumbling the semicircular canals and the otoliths are most certainly stimulated. By virtue of the complex nature of the rotational profile it becomes an intractable problem to trace the angular accelerations to which the vestibular system is exposed. The fact that it was whenever a new axis was introduced that seemed to give the subjects motion sickness perhaps points to Coriolis stimulation of a complex pattern (9, 17, 32) as an important factor in the causation of motion sickness. Our "fast random tumbling" actually is fairly slow compared to the work of Useller and Algranti (45), but in our subjects a relatively shorter period was required to induce motion sickness, whereas in Useller's studies, up to 50 rpm for one hour was required. The

difference between our profile and theirs is, of course, that we introduced new axes dynamically, whereas they started at some initial resultant axis.

The nystagmogram we obtained shows a very complex waveform. In general, a faster frequency saw-tooth wave was superimposed on a slower frequency waveform, the latter being in the range of the RFS rotational rate. Although there are momentary waveforms that appear like classical nystagmus tracings, the overall complex behavior of the tracing precludes interpretation of these waveforms at the present time. Undoubtedly, noise due to some electrode motion is occasionally also superimposed in the nystagmogram tracing. In any case, the tracings obtained seem to indicate that random tumbling produces a slow eyeball rolling at a rate correlating with RFS rotational rate and a faster frequency saw-tooth waveform of 2 to 6 pulses per second which may be due to true vestibular nystagmus.

BIBLIOGRAPHY

1. Asmussen, E., E. H. Christensen, and M. Nielsen. The regulation of circulation in different postures. *Surgery* 8:604 (1940).
2. Bevegard, B. S., and J. T. Shepherd. Circulatory effects of stimulating the carotid arterial stretch receptors in man at rest and during exercise. *J. Clin. Invest.* 45:132 (1966).
3. Blair, E., R. A. Cowley, S. Attar, and W. Esmond. The effect of hypothermia on circulatory reflexes in human. *Surg. Gynec. Obstet.* 117:553 (1963).
4. Burton, A. C. *Physiology and biophysics of the circulation*. Chicago: Year Book Publishers, 1965.
5. Celander, O. The range of control exercised by the sympathico-adrenal system. A quantitative study on blood vessels and other smooth muscle effectors in the cat. *Acta Physiol. Scand.* 32, Suppl. 116 (1954).
6. Clark, B., and A. Graybiel. Human performance during adaptation to stress in the Pensacola slow rotation room. *Aerospace Med.* 32:93 (1961).
7. Clark, J. H., D. R. Hooker, and L. H. Weed. The hydrostatic factor in venous pressure measurements. *Amer. J. Physiol.* 109:166 (1934).
8. Colehour, J. K., and A. Graybiel. Biochemical changes occurring with adaptation to accelerative forces during rotation. *Aerospace Med.* 37:1205 (1966).
9. Dowd, P. J. Induction of resistance to motion sickness through repeated exposure to Coriolis stimulation. *Aerospace Med.* 36:452 (1965).
10. Ead, H. W., J. H. Green, and E. Neil. A comparison of the effects of pulsatile and non-pulsatile blood flow through the carotid sinus on the reflexogenic activity of the sinus baroreceptors in the cat. *J. Physiol.* 118:509 (1952).

11. Edelberg, R., and H. S. Weiss. Centrifugation of animals about an axis through the body. (Abstract) Fed. Proc. 11:40 (1952).
12. Edelberg, R., H. S. Weiss, and P. V. Charland. Hydrostatic behavior of the vascular column during tumbling. (Abstract) Fed. Proc. 12:37 (1953).
13. Edelberg, R., H. S. Weiss, P. V. Charland, and J. I. Rosenbaum. The physiology of simple tumbling. Part I-Animal Studies. 172/53-139 USAF Wright-Patterson AFB, Ohio, Jan. 1954.
14. Folkow, B., B. Lofving, and S. Mellander. Quantitative aspects of the sympathetic neuro-hormone control of the heart rate. Acta Physiol. Scand. 37:363 (1956).
15. Gauer, O. H., and J. P. Henry. Circulatory basis of fluid volume control. Physiol. Rev. 43:423 (1963).
16. Gauer, O. H., and W. Hull. Paradoxical fall of pressures in the right and left auricles and the pulmonary artery in a head down tilt. (Abstract) Fed. Proc. 13:52 (1954).
17. Gillingham, K. K. Training the vestibule for aerospace operations: I. Using Coriolis acceleration to assess rotation. Aerospace Med. 36:170 (1965).
18. Graveline, D. E. Effects of posture on cardiovascular changes induced by prolonged water immersion. 172/TR 61:563 (1961).
19. Graybiel, A., B. Clark, and J. J. Zarriello. Observations on human subjects living in a "slow rotating room" for a period of two days. Arch. Neurol. 3:55 (1960).
20. Graybiel, A., R. S. Kennedy, E. C. Knoblock, F. E. Guedry, W. Mertz, M. E. Mcleod, J. K. Colchour, E. F. Miller, and A. R. Fregley. The effects of exposure to a rotating environment (10 rpm) on four aviators for a period of 12 days. Aerospace Med. 36:733 (1965).
21. Green, R. S., A. Iglaier, and J. McGuire. Alterations of radial or brachial intra-arterial blood pressure and of the EKG induced by tilting. J. Lab. Clin. Med. 33:951 (1948).
22. Grodins, F. S. Control theory and biological systems. New York: Columbia University Press, 1963.
23. Hardy, J. D. (ed.). Temperature, its measurement and control in science and industry. Biology and medicine, vol. 3, part 3. New York: Reinhold, 1963.
24. Henderson, Y., and H. W. Haggard. The circulation in man in the head-down position and a method for measuring the venous return to the heart. J. Pharmacol. Exp. Ther. 11:189 (1918).
25. Heymans, C., and E. Neil. Reflexo-genic areas of the cardiovascular system. Boston: Little, Brown and Co., 1958.
26. Hunt, N. C., III. Immersion diuresis. Aerospace Med. 38:176 (1967).
27. Katona, P. G. Computer simulation of the blood pressure control of heart period. Proc. of 18th Annual Conference of Engineering in Medicine and Biology, Philadelphia, 1965.
28. Katona, P. G. The cardiovascular system. In Stark, L., et al. (eds.). Biological control systems. 3500/CR-577:344 (1966).
29. Lawton, R. W., L. C. Green, G. H. Kydd, L. H. Peterson, and R. J. Crosbie. Arterial blood pressure responses to G forces in the monkey. I. Sinusoidal positive G. J. Aviat. Med. 29:97 (1958).
30. Mayerson, H. S., and W. D. Davis, Jr. The influence of posture on the EKG. Amer. Heart J. 24:593 (1942).
31. Meek, W. J., and A. Wilson. The effect of position of heart on QRS complex of the EKG. Arch. Intern. Med. 36:614 (1925).
32. Moore, E. W., and R. L. Cramer. Speed of recovery from Coriolis stimulus and its relationship to motion sickness. Proceedings of the 73d Annual Convention of the American Psychological Association, Chicago, 3-7 Sept. 1965.
33. Nielsen, M., L. P. Harrington, and C. E. A. Winslow. The effect of posture on skin circulation. Amer. J. Physiol. 127:573 (1939).
34. Rosenbleuth, A., and F. A. Simeone. The interrelations of vagal and accelerator effects on the cardiac rate. Amer. J. Physiol. 110:42 (1934).
35. Roston, S. The cardiovascular effects of the carotid sinus mechanism. Bull. Math. Biophys. 27:167 (1965).
36. Sancetta, S. M., D. B. Hackell, E. Tracks, and B. Wittels. The effect of dry heat on the circulation of man. Coronary hemodynamics. Amer. Heart J. 67:593 (1964).

37. Sarnoff, S. J., and S. I. Yamada. Evidence for reflex control of arterial pressure from abdominal receptors with special reference to the pancreas. *Circ. Res.* 7:325 (1959).
38. Schaefer, H. Central control of cardiac function. *Physiol. Rev.*, Suppl. 4, 40:213 (1960).
39. Scher, A. M., and A. C. Young. Servoanalysis of carotid sinus reflex effects on peripheral resistance. *Circ. Res.* 12:152 (1963).
40. Sigler, L. H. EKG changes occurring with alterations of posture from recumbent to standing positions. *Amer. Heart J.* 15:146 (1938).
41. Stegemann, J. Der Einfluss sinusformiger Druckänderungen in isolierten Karotissinus auf Blutdruck und Pulsfrequenz beim Hund. *Deutsch. Ges. Kreislaufforsch* 23:392 (1957).
42. Stephens, O. Z. Blood pressure and pulse rate as influenced by different positions of the body. *J.A.M.A.* 43:955 (1904).
43. Tuckman, J., S. R. Slater, and M. Mendlowitz. The carotid sinus reflexes. *Amer. Heart J.* 70:119 (1965).
44. Urschel, C. W., and W. B. Hood, Jr. Cardiovascular effects of rotation in z axis. *Aerospace Med.* 37:254 (1966).
45. Useller, J. W., and J. S. Algrant. Pilot reaction to high speed rotation. *Aerospace Med.* 34:501 (1963).
46. Vogt, F. B. Effect of extremity cuff tourniquet on tilt table tolerance after water immersion. *Aerospace Med.* 36:442 (1965).
47. Wakim, K. G. Bodily reactions to high temperature. *Anesthesiology* 25:532 (1964).
48. Wald, H., M. Guernsey, and F. H. Scott. Some effects of alteration of posture on arterial blood pressure. *Amer. Heart J.* 14:219 (1937).
49. Wang, S. C., and H. L. Botison. An analysis of the carotid sinus cardiovascular reflex mechanism. *Amer. J. Physiol.* 150:712 (1947).
50. Wang, Y., R. J. Marshall, and J. T. Shepherd. The effects of changes in posture and of graded exercise on stroke volume in man. *J. Clin. Invest.* 39:1051 (1960).
51. Ward, R. J., F. Danziger, J. J. Bonica, G. D. Allen, and A. G. Tolas. Cardiovascular effect of change in posture. *Aerospace Med.* 37:257 (1966).
52. Warner, H. R., and A. Cox. A mathematical model of heart rate controlled by sympathetic and vagus efferent information. *J. Appl. Physiol.* 17:349 (1962).
53. Weiss, H. S. The human electrocardiogram during tumbling. *J. Aviation Med.* 26:206 (1955).
54. Weiss, H. S., R. Edelberg, P. V. Charland, and J. I. Rosenbaum. Animal and human reactions to rapid tumbling. *J. Aviation Med.* 25:5 (1954).
55. Weiss, H. S., R. Edelberg, P. V. Charland, and J. I. Rosenbaum. The physiology of simple tumbling. Part II—Human Studies 172/53-139. USAF Wright-Patterson AFB, Ohio, Jan. 1954.
56. Wilkins, R. W., M. H. Halperin, and J. R. Litter. The effect of the dependent position upon blood flow in the limbs. *Circulation* 2:3 (1950).
57. Wilkins, R. W., S. E. Bradley, and C. K. Friedland. The acute circulatory effects of the head-down position (neg. G) in normal man. *J. Clin. Invest.* 29:940 (1950).

APPENDIX 1
PERSONAL DATA

All 7 subjects used in this experiment were experienced in the centrifuge. The following table summarizes their vital statistics:

Subject	Sex	Age (yr.)	Height (in.)	Weight (lb.)
R.D.	M	24	68	145
J.N.	M	30	71.5	194
E.O.	M	31	61.5	184
A.R.	M	23	67	132
V.R.	M	25	71	170
A.S.	M	22	61.25	121
T.S.	M	24	76	189

APPENDIX 2

METHODS FOR INSTRUMENTING SUBJECTS

This section describes the technic followed in instrumenting the subjects. It does not include a discussion of the operating principles of the instruments employed, which are discussed in the engineering section.

I. Electrocardiogram (ECG)

A set of six silver-silver chloride electrode ECG leads supplied by SAM was used to record sternal and axillary ECG. The sternal leads were placed midsternally on the manubrium and xiphisternal area, whereas the axillary leads were located on the right and left midaxillary lines, about the 5th or 6th intercostal space. The two ground leads, one each for the sternal and axillary pickups were placed midsternally at about the 3d and 4th rib level (fig. 1B).

The method of applying the skin electrode described here was adapted from the technics currently employed by the SAM subject instrumentation personnel in their centrifuge experiments.

To prepare the subject, the skin area to which the electrode was to be applied was first rubbed with alcohol until it appeared slightly reddish or pinkish in color. The superficial cornified layer of the same area was then removed using either a fine grit sandpaper or small burring tool. The latter was a light hand-held electric drill, with an attached spherical fine dental drill (fig. 1A). When using the sandpaper method a few strokes over the skin to be prepared were required, and the end point was usually a very slight tenderness. The burring method was faster and seemed less traumatic. The area was marked with a felt pen, and the drill tip lightly touched the marked area which would then show a whitish shiny spot. A spot of about 2 mm. was usually adequate.

To apply the electrodes, the standard Beckman 2-face adhesive discs cut to the size of Beckman electrodes were used. After one face of the adhesive disc had been applied to the electrode, NASA electrode paste was introduced into the electrode cavity through the four holes on the electrode face by means of a blunt needle and syringe. Great care was taken not to leave any bubbles inside the electrode cavity as they increase the electrode impedance. After excess paste was leveled off and discarded, the remaining protective paper was peeled off from the adhesive discs, and the electrode pressed on the prepared skin.

Electrode impedance was checked by an ohmmeter set to the $\times 100$ scale. An upper limit of 1.5 K was used and if the impedance exceeded this, the skin and electrode were reprepared. At the conclusion of the run, the electrodes were washed thoroughly with soap and water before the electrode paste had a chance to dry and cake. The subject's skin was cleaned and treated with an antiseptic ointment or tincture.

II. Indirect Blood Pressure Measurement

The blood pressure measuring device consisted of a small piezoelectric contact microphone, a regular blood pressure cuff, and the SAM automatic blood pressure inflation-deflation device. The microphone was placed over the strongest brachial pulse felt on the inner aspect of the lower third of the upper arm. The cuff was then applied around the upper third of the upper arm. It was often necessary to reposition the microphone and cuff and several blood pressure readings taken before the best blood pressure recording could be obtained. Blood pressure reading was initiated by pressing a button at the physiologist's console which remotely actuated the RF-controlled SAM blood pressure measuring device. Muscle artifacts in the blood pressure recording were minimized by instructing the subject to relax before the

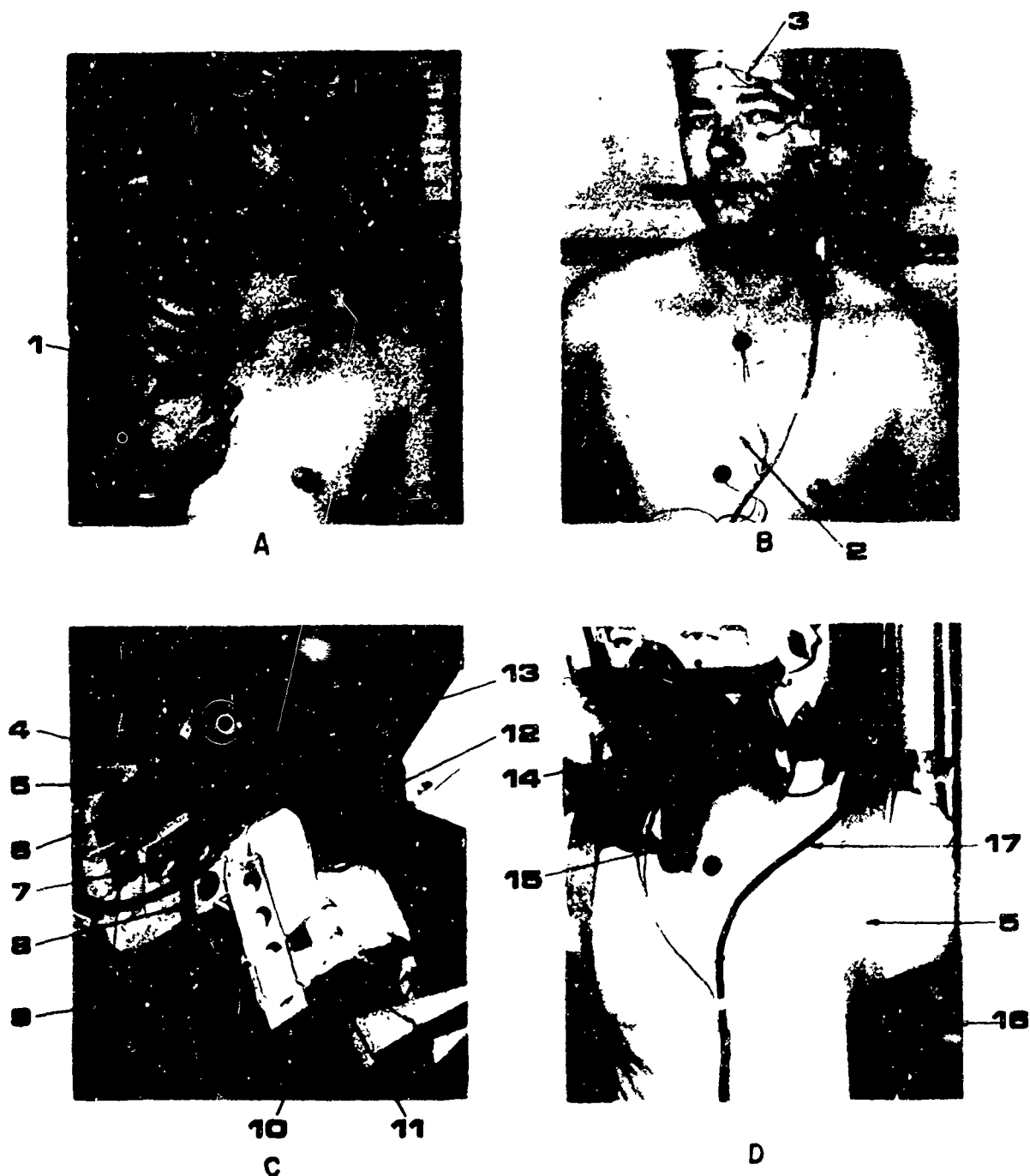


FIGURE 1

Photograph illustrating subject preparation: 1, burring tool; 2, electrocardiogram leads; 3, electronystagmogram leads; 4, shoulder pad; 5, shoulder and chest strap; 6, "joy-stick" control; 7, waist strap; 8, hip strap; 9, strap single release mechanism; 10, blood pressure gas tank; 11, feet strap; 12, roll inertia ring; 13, subject transceiver; 14, microphone and respiration thermistor housing; 15, respiration thermistor attachment; 16, blood pressure cuff; 17, intercom connection.

button was pressed. Full scale on the blood pressure recording was 250 mm. Hg which was calibrated against a mercury manometer.

III. Respiration

Respiratory rate was measured by using a sensitive thermistor situated in the respiratory air path. At first the thermistor was housed on a light plastic piece which clipped onto the nasal septum. This caused much discomfort and pain to the subject especially when he was in the head-down position as the weight of the mouth-piece (mike) pressed on the clip and nose. The thermistor was then housed in the airflow path of a standard Air Force altitude oxygen mask (breathing ambient air) which also housed the subject intercom microphone. This had the advantage over the nose clip in that air flow due to the subject's talking or breathing through the mouth was also picked up. During the experiments, the subject was asked to snap the mask onto the helmet attachment.

During the "hot temperature" runs the respiration recording only showed spikes corresponding to inspiration. This can be explained by noting that, at RFS cabin temperature of 100° F., the air breathed in and out had temperatures very close to each other, and the spike was caused by transient cooling caused by faster air velocity during initial inspiration. The thermistor then warmed up immediately even before expiration started.

IV. Nystagmogram (ENG)

Six silver-silver chloride electrodes were used to pick up eyeball movement (Mennen-Greatbatch Electronics model 407 electrodes). The skin and electrodes were prepared in an identical manner as the ECG electrodes. The electrodes were placed around the eye as shown in figure 1B. Lateral and vertical eyeball movements of 10° and 20° were used to calibrate eyeball motion by requesting the subject to look, with the head held still, at correspondingly marked points on the RFS wall in front of the subject's chair. The strip chart output was labeled accordingly for 10° and 20° arc gaze. This was done before each run where ENG was recorded.

V. Body Temperature

Yellow Spring Instruments (Ohio) skin and rectal temperature probes were used. The skin temperature probe was taped by means of regular adhesive tape on the skin about 2 in. inferior to the junction of the medial and middle third of the inguinal line taking care to avoid contact with the scrotum. The rectal probe (covered with petrolatum) was inserted about 3 in. into the rectum by the subject himself and kept in place by a rubber ball (of about 1/4-in. diameter through which the probe has been cemented at the 3-in point). After probe placement, 10 minutes were allowed for temperature equilibration before temperature was read, using YSI telethermometer readout, and prior to letting the subject enter the RFS. In the RFS the two subject temperatures were telemetered, the readouts of which were checked and calibrated against the YSI telethermometer.

VI. Safety Harness

The subject harness provided support of the shoulders and chest, the waist, the hips, and the feet. The original "across-chest" strapping was modified so that the straps came over the shoulders alongside the chest without crossing. This minimized chest cage pressure and eliminated ECG artifacts arising from the straps rubbing over the leads. The strapping method featured a single release mechanism for all the straps, except for an independent waist safety strap. Straps were released by pulling a metal handle located between the subject's thighs. Size of subject presented some problem as the seat was designed for a certain percentile of Air Force men. For smaller sized subjects we had to use two layers of foam rubber (each 2 in. thick) in the seat and a layer at the back in order to fit the straps to them.

VII. Instrument Calibration

After the subject was strapped, instrument calibrations were done. The *accelerometer outputs* were calibrated by means of a calibrate button inside the RFS. With the button unpressed, the Z accelerometer on the strip chart was calibrated to full-scale (2 cm.) positive deflection corresponding to 1 G and the X and Y accelerometer outputs zeroed to the midline. When the button was pressed, the X and Y accelerometer outputs were calibrated full-scale (2 cm.) positive deflection corresponding to 1 G, and the Z output zeroed to the midline. A calibrate button for the *rate gyro* was also provided. The calibrate signal was equivalent to 10 rpm. With the button unpressed, the strip chart pens for the X, Y, and Z rate gyros were zeroed to the midline. When the button was pressed, the pens were calibrated to either full positive deflection or one half of this distance, depending upon the gain setting of the chart amplifier. The less sensitive gain setting was used when the rotation was expected to go beyond 10 rpm. For pure axis rotation, a tachometer on the external drive also gave out RFS rotational rate.

After the single subject cannon plug was mated into the socket at the center of the outer edge of the subject seat, the telemetered subject variables were checked by two technicians—one inside the RFS and the other at the physiologist's console. The *ECG amplifiers* were adjusted so that the peak-to-peak QRS tracing registered 4 to 6 cm., the peak-to-peak *respiration* tracing about 2 or 3 cm., and the blood pressure peak inflation pressure (corresponding to 200 mm. Hg) registering full positive scale. The *Beckman tachometer* was also calibrated by the calibration knob provided in the tachometer.

For the subject temperature signal, a 38° and 30° C. calibration signal was provided by pressing two buttons in the RFS alternately. The strip chart pens were then calibrated to full maximum and full minimum excursion. In all the calibration operations, the step gain settings of the strip chart recorder had been pre-set by the engineers according to the known signal voltage levels such that during experimental days, the technician had only to calibrate using the continuous zero and calibrate knobs. For the *ENG*, the 10° calibration mark point was usually used. This was calibrated to register ½ cm. excursion from the midline as the subject was requested to look at the 10° marks to the left and right and up and down. Figure 2 illustrates the calibration signals and specimen tracings from actual RFS runs.

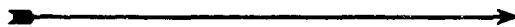
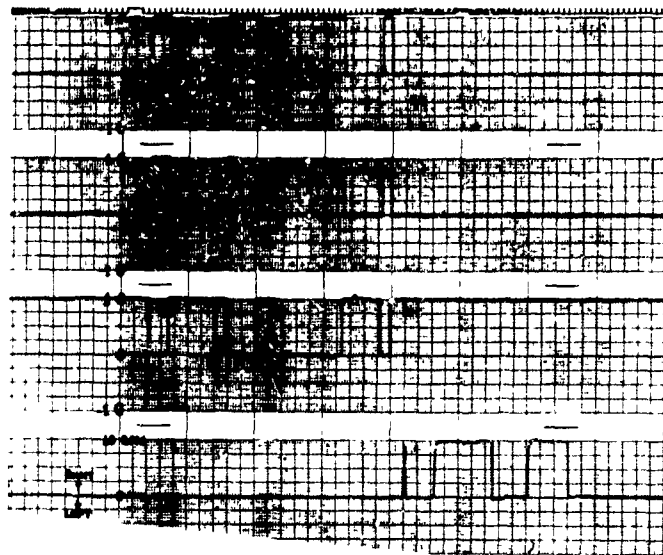


FIGURE 2

Sample channel tracings, calibration signals on the left column and actual run signals on the right column. The lateral nystagmus tracing was obtained with subject's eyes closed after stopping 15 rpm yaw rotation in 1½ seconds.

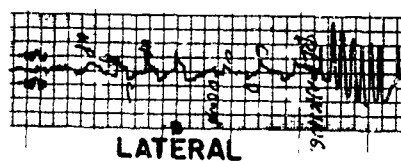
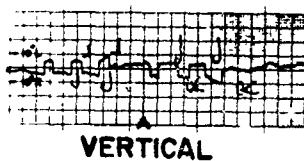


← X ACCELE

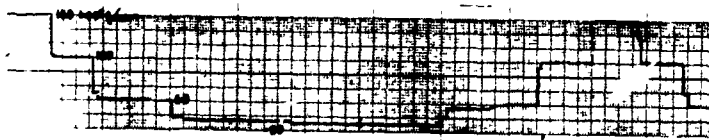
← Y ACCELE

← Z ACCELER

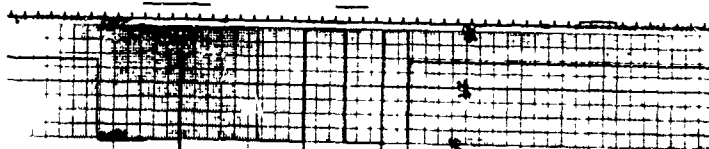
← Y AXIS RA



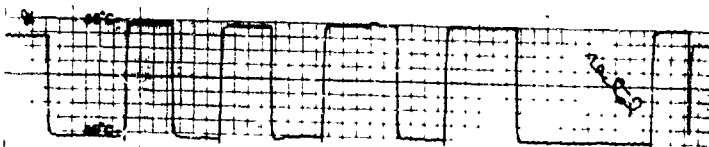
← LATERAL N



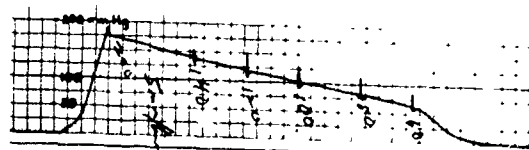
← CARDIOT



← SKIN TEMP



← RECTAL TEM
RESPIR

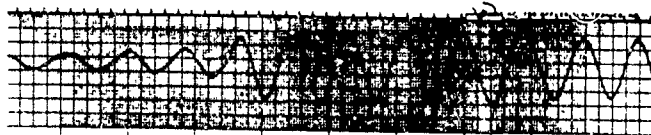


← BLOOD P

CALIBRATION

A

← X ACCELEROMETER →



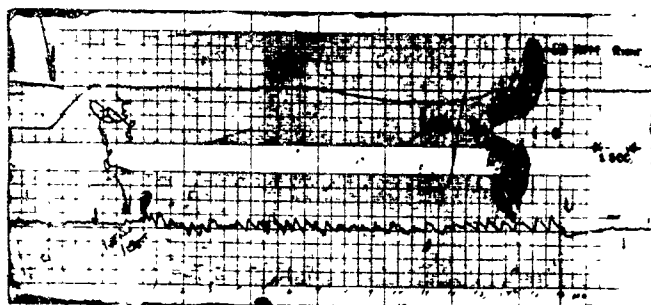
← Y ACCELEROMETER →



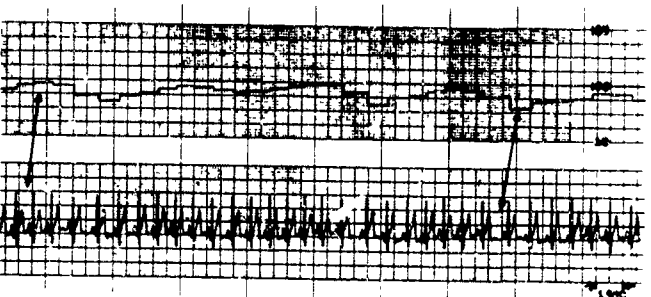
← Z ACCELEROMETER →



← Y AXIS RATE GYRO →



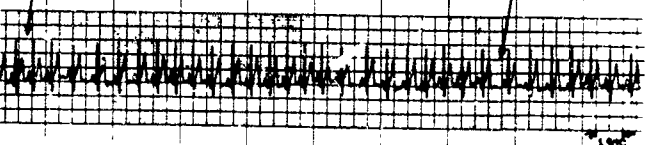
← LATERAL NYSTAGMUS →



← CARDIOTACHOGRAM →

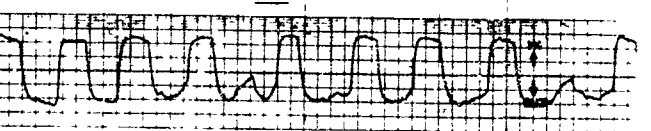


EKG →

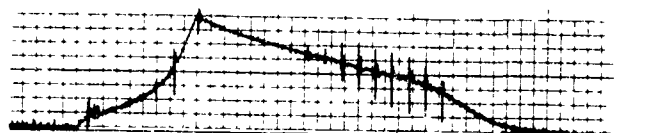


← SKIN TEMPERATURE

← RECTAL TEMPERATURE
RESPIRATION →



← BLOOD PRESSURE →



ACTUAL RUN

B

APPENDIX 3

SCHEME OF EXPERIMENTS

- I. *Subject J.N.*
Random axis
Roll axis
Pitch axis
Hot ambient temperature
Water immersion
- II. *Subject E.O.*
Random axis
Roll axis
Pitch axis
- III. *Subject A.S.*
Yaw axis
Roll axis
Pitch axis
Hot ambient temperature
Cold ambient temperature
- IV. *Subject T.S.*
Pitch axis
Roll axis
Hot ambient temperature
Cold ambient temperature
- V. *Subject A.R.*
Random axis
Pitch axis
Roll axis
- VI. *Subject V.R.*
Roll axis
Pitch axis
- VII. *Subject R.D.*
Roll axis

Results are given in protocol form in appendix 4.

APPENDIX 4
EXPERIMENT PROTOCOLS

Subject J.N.

Date	Time in (hours)	Time out (hours)	Scheduled profile	Run time* (min.)	Medical monitor	Comments
7-29	1430	1450	Random axes, 16 min.	20	Leverett	Demonstration to group of visitors.
8-4	1400	1430	Learning control, righting RFS from head-down position. Random 12 \pm 4 rpm, duration of 2 min., 4 min.	30	Brown	Learning curve from head-down position to upright. Report of dust getting into eyes.
	1600	1620	Random axes, 8 min.	8	Brown	Right RFS from head-down position to upright after each random rotation.
8-5	1030	1100	Random axes, 16 min.	13	Brown	Nausea reported after 14 min. rotation. Run aborted.
8-9	0930	1000	Random axes, 16 min.	15	Brown	Severe nausea after 15 min. rotation. Run aborted.
	1300	1400	Random axes, 12 min.	12	Brown	Right RFS from head-down position to upright after random rotation.
8-19	0950	1015	Roll, right, 2, 4, 8 rpm, 3 min.	25	Stegall	TV fuses out consistently. Experiments canceled until TV is checked out.
8-23	0900	0920	Roll, right 12 pm. Pitch forward 2, 4, 6 rpm, 3 min.	20	Stegall	Impossible to control axis at 12 rpm.
	1100	1120	Roll, right 8, 10 rpm, 3 min.	12	Stegall	Axes wavered slightly.
						— SUCTION CUPS USED —
9-6	1420	1445	Roll, right, 2, 4, 6, 8 rpm, 3 min.	24	Olson	Pure axis with cups.
	1555	1615	Roll, right, 10, 12, 14 rpm, 3 min.	18	Olson	
10-13	1425	1550	Pitch, forward, 2, 4, 6, 3 rpm, 3 min	36	Stegall	
	1450	1620	Pitch, 10, 12, 14 rpm, 3 min.	25	Stegall	14 rpm canceled because of battery discharge.
10-21	0920	0930	Pitch, forward, 14 rpm, 3 min.	3	Meyer	

10-21	1825	1855	Thermal stress testing. No rotation.	30	Meyer	RFS at 100° F. Sweating, skin temperature at beginning — 36.1° C.; after 30 min. exposure — 37.4° C. Rectal temperature — 37.8° C.
10-31	1027	1142	Hot temperature run, pitch, forward, 6 rpm, 3 min.	8	Meyer	RFS at 100° F. Subject exposure before rotation — 72 min.
11-10	0845	1537	After water immersion, pitch, forward, 6 rpm, 4 min.	4	Olson	Water immersion, 6 hr., 0910 - 1510.
Subject E.O.						
8-1	1130	1150	Learning control, righting RFS from right side to upright position.	10	Rogge	Obtain learning curve.
	1430	1845	Random axes, 4 ± 2 rpm, 2, 4, 8, 16 min.	45	Rogge	Ability to right RFS from right side position timed.
8-5	1500	1530	Random axes, 4 ± 2 rpm, 30 min.	30	Rogge	Sweatiness. Slight momentary confusion. No nausea.
8-8	1400	1430	Random axes, 12 ± 4 rpm, 2, 4, 8 min.	30	Rogge	Slight sweating but no nausea.
	1600	1530	Random axes, 16 min.	16	Rogge	TV and ECG signal bad. Subject asked to be excused after 2 min. rotation.
8-10	1530	1600	Random axes, 12 ± 4 rpm, 30 min.	2	Rogge	Alternator came loose. Run stopped.
8-12	0960	1020	Random axes, 12 ± 4 rpm, 30 min.	20	Rogge	Pushed from outside—axis mixed.
8-18	0910	0940	Roll, right, 2, 4, 8, 10 rpm, 8 min.	30	Rogge	— SUCTION CUPS USED —
10-10	1425	1540	Roll, right, 2, 4, 6, 8 rpm, 3 min.	45	Brown	TV poor during second group of runs.
	1500	1600	Roll, right, 10, 12, 14 rpm, 3 min.	30	Brown	
10-14	1405	1435	Pitch, forward, 2, 4, 6, 8 rpm, 8 min.	30	Olson	
	1530	1650	Pitch, forward, 10, 12, 14 rpm, 3 min.	20	Olson	

*Includes rest period between runs.

Subject A.S.

Date	Time in (hours)	Time out (hours)	Scheduled profile	Run time* (min.)	Medical monitor	Comments
8-16	1100	1200	Yaw — 8 rpm, 15 rpm, right then left, 2 min. duration each.	15	Rogge	Test of nystagmus record. Lateral nystagmus exhibited with eyes closed after RFS is stopped.
8-17	1400	1430	Roll, right, 2, 4, 8 rpm, 3 min.	25	Stegall	Without suction cups. Roll axis mixed with yaw.
	1300	1630	Pitch, forward, 2, 4, 8 rpm, 3 min.	20		— SUCTION CUPS USED —
8-25	1330	1400	Pitch, forward, 10, 12, rpm, 3 min.	15	Rogge	Successful runs canceled because of interference with com. ability.
9-22	1530	1630	Pitch, forward, 2, 4, 6 rpm, 3 min.	20	Olson	NASA Med. Adv. Comm. visit.
9-30	0915	0920	Roll, right, 2 rpm, 3 min.	5	Brown	10 rpm stopped because of sparks caused by wire stripper shorting 60-v. system in attic.
10-4	0915	1130	Roll, right, 8, 10, 12, 14 rpm, 3 min.	25	Stegall	Battery charging in between 10 and 12 rpm run, 1 hour.
10-11	1420	1435	Pitch, forward, 8, 14 rpm, 3 min.	10	Olson	Suction cups went off 3 times. Repositioned each time.
10-17	0930	0950	Roll, right, 2, 4, 6 rpm, 3 min.	18	Olson	
10-26	0920	1030	Hot temperature run. Pitch, forward, 6 rpm, 3 min.	3	Olson	RFS at 100° F., subject exposure before rotation — 63 min.
11-1	1350	1500	Cold temperature run. Pitch, forward, 6 rpm, 3 min.	3	Stegall	53° F. initially, 58° at end of experiment. Subject exposure before rotation — 60 min.

Subject A.R.

8-2	1000	1030	Learning control, righting RFS from head-down position. Random axes, 4 \pm 2 rpm, 2 min.	30	Rogge	Learning curve from head-down to upright. "Righting time" time after random rotation.
	1400	1430	Random axes, 4 \pm 2 rpm, 4, 8 min.	20	Rogge	Ran out of fuel; run terminated after 8 min. rotation.
8-3	1400	1430	Random axes, 4 \pm 2 rpm, 16 min.	20	Brown	Sparking of battery terminals; overheating of motor; run stopped.
	1600	1628	Random axes, 4 \pm 2 rpm, 30 min.	27	Brown	Nausea at 27 min.
8-8	0950	1030	Random axes, 4 \pm 2 rpm, 30 min.	30	Brown	"Slightly confused."
8-11	1100	1130	Random axes, 12 \pm 4 rpm, 2, 4 min.	20	Rogge	Nausea and retching.
8-17	1000	1010	Random axes, 12 \pm 4 rpm, 4 min.	3' 10"	Stegall	Queasiness of stomach; bumpy inertial rings due to dirt in roll ring; run stopped.
8-24	0950	1010	Roll, right, 2, 4, 6 rpm, 3 min.	9	Stegall	Axes very good; used suction cups.
	1100	1130	Roll, right, 8, 10, 12 rpm, 3 min.	9	Stegall	
9-26	1000	1030	Pitch, forward, 2, 4, 6 rpm, 3 min.	30	Stegall	Voice communication with subject not very good; afternoon run canceled for intercom checkout.
	1100	1130	Pitch, forward, 8, 10, 12 rpm, 3 min.	30	Stegall	

*Includes rest period between runs.

Subject T.S.

Date	Time in (hours)	Time out (hours)	Scheduled profile	Run time* (min.)	Medical monitor	Comments
8-23	1400	1415	Pitch, forward, 2, 4, 6 rpm, 3 min.	11	Brown	Use of polar suction cups to hold axis steady. Jet fuel out during 6 rpm.
	1600	1625	Pitch, forward, 6, 8, 10 rpm, 3 min.	9	Brown	Axes very good.
9-22	1015	1100	Roll, right, 2, 4, 6, 8 rpm, 3 min.	21	Meyer	
10-5	1415	1500	Roll, right, 10, 12, 14 rpm, 3 min.	18	Rogge	
10-7	0925	1000	Pitch, forward 12, 14 rpm, 3 min.	12	Meyer	Suction cups became loose twice, repositioned each time.
10-21	1407	1531	Thermal stress testing. No rotation.	1 hr. 24 min.	Brown	Test of RFS at 95° F. No rotation.
10-25	1006	1100	Pitch, forward, 6 rpm, 3 min.	3	Stegall	RFS at 100° F., subject exposure before rotation — 50 min.
11-7	1355	1455	Pitch, forward, 6 rpm, 3 min.	3	Meyer	RFS at 84° F. initially; 61° at end of experiment; subject exposure before rotation — 85 min.
11-15	1415	1425	Pitch, forward, 6 rpm, 3 min.	½	Rogge	For Col. Nuttall and company.
11-17	1415	1425	Pitch, forward, 6 rpm, 3 min.	½	Meyer	For Gen. Roadman and company.
11-31	0900	0915	Pitch, forward, 6 rpm, 3 min.	½	Meyer	For a group of generals.

Subject V.R.

8-15	0920	1000	Learning control, righting RFS from head-down position.	20	Brown	7th trial — low hydraulic pressure warning light, clutch out of order, experiment stopped.
8-22	0920	0950	Roll, left, 2, 4 rpm, 3 min. duration; 6 rpm, 3 min.	10	Brown	TV out after 1½ min. of 2 rpm; fuse changed. Axes had considerable yaw.
	1330	1430	Roll, left, 8 rpm, 3 min. duration; 10 rpm, 3 min.	15	Brown	Axis not good. Nausea after 1½ min. canceled subsequent runs.
						— SUCTION CUPS USED —
8-25	0920	1000	Roll, left, 10, 12 rpm, 3 min.	15	Rogge	Slight stomach fullness at end of 12 rpm run.
	1100	1130	Pitch, forward 2, 4, 6 rpm, 3 min.	20	Rogge	

Subject R.D.

8-28	1350	1430	Roll, right, 2, 4, 6, 8 rpm, 3 min.	30	Meyer
	1600	1630	Roll, right, 10, 12 rpm, 3 min.	15	Meyer

*includes rest period between runs.

Unclassified

Security Classification

DOCUMENT CONTROL DATA - R&D		
(Security classification of title, body of abstract and indexing annotation must be entered when the overall report is classified)		
1 ORIGINATING ACTIVITY (Corporate author) Systems Research Laboratories, Inc. 432 E. Josephine Street San Antonio, Texas		2a REPORT SECURITY CLASSIFICATION Unclassified
		2b GROUP
3 REPORT TITLE RESEARCH ON THE HUMAN PHYSIOLOGIC RESPONSE TO PROLONGED ROTATION AND ANGULAR ACCELERATION, A. ENGINEERING ACTIVITIES. B. PHYSIOLOGIC ACTIVITIES		
4 DESCRIPTIVE NOTES (Type of report and inclusive dates) Jan. - Dec. 1966		
5 AUTHOR(S) (Last name, first name, initial) Rothe, W. E. Lim, Samuel T. Pope, Edward E. Fletcher, John G.		
6 REPORT DATE Sept. 1967	7a TOTAL NO. OF PAGES 95	7b NO. OF REFS A-3; B-57
8a CONTRACT OR GRANT NO AF41(609)2897	9a ORIGINATOR'S REPORT NUMBER(S) SAM-TR-67-69	
b. PROJECT NO 7930		
c Task No. 793003		
d.	9b OTHER REPORT NO(S) (Any other numbers that may be assigned this report)	
10. AVAILABILITY/LIMITATION NOTICES This document has been approved for public release and sale; its distribution is unlimited.		
11. SUPPLEMENTARY NOTES	12. SPONSORING MILITARY ACTIVITY USAF School of Aerospace Medicine Aerospace Medical Division (AFSC) Brooks Air Force Base, Texas	
13 ABSTRACT Physiologic research has explored the responses of humans to rotation and acceleration. The test vehicle was the Rotational Flight Simulator, an air bearing suspended sphere with unrestricted rotational freedom propelled by internally mounted inertia rings and, later, by a single axis external drive assembly. Engineering efforts established the dynamics and improved the control of the vehicle. Instrumentation was provided for the readout, display, and recording of significant data serving for physiologic evaluation and medical monitoring. The data were telemetered; pictorial display of the subject and two-way communication links were provided. A total of 138 experiments yielded valid physiologic and human performance information in a rotational environment from fractional to 16 rpm and for several minutes to a maximum of 30 minutes. The subjects consisted of 7 young, healthy males. Results indicated that the RFS properly used and instrumented represents a valuable and unique test vehicle; that changes in heart rate, and ECG readings depended on body position with respect to gravity; that electro-oculogram, subjective sensations, incipient nausea, and ability of the pilot to right the stationary sphere after tumbling--all depended on the rate, duration, and axis pattern of rotation.		

DD FORM 1473
1 JAN 64

Unclassified

Security Classification

Unclassified

Security Classification

14 KEY WORDS	LINK A		LINK B		LINK C	
	ROLE	WT	ROLE	WT	ROLE	WT
Physiology Bioinstrumentation Rotational Flight Simulator Rotation, physiologic effects Acceleration, physiologic effects						

INSTRUCTIONS

1. **ORIGINATING ACTIVITY:** Enter the name and address of the contractor, subcontractor, grantee, Department of Defense activity or other organization (*corporate author*) issuing the report.

2a. **REPORT SECURITY CLASSIFICATION:** Enter the overall security classification of the report. Indicate whether "Restricted Data" is included. Marking is to be in accordance with appropriate security regulations.

2b. **GROUP:** Automatic downgrading is specified in DoD Directive 5200.10 and Armed Forces Industrial Manual. Enter the group number. Also, when applicable, show that optional markings have been used for Group 3 and Group 4 as authorized.

3. **REPORT TITLE:** Enter the complete report title in all capital letters. Titles in all cases should be unclassified. If a meaningful title cannot be selected without classification, show title classification in all capitals in parenthesis immediately following the title.

4. **DESCRIPTIVE NOTES:** If appropriate, enter the type of report, e.g., interim, progress, summary, annual, or final. Give the inclusive dates when a specific reporting period is covered.

5. **AUTHOR(S):** Enter the name(s) of author(s) as shown on or in the report. Enter last name, first name, middle initial. If military, show rank and branch of service. The name of the principal author is an absolute minimum requirement.

6. **REPORT DATE:** Enter the date of the report as day, month, year; or month, year. If more than one date appears on the report, use date of publication.

7a. **TOTAL NUMBER OF PAGES:** The total page count should follow normal pagination procedures, i.e., enter the number of pages containing information.

7b. **NUMBER OF REFERENCES:** Enter the total number of references cited in the report.

8a. **CONTRACT OR GRANT NUMBER:** If appropriate, enter the applicable number of the contract or grant under which the report was written.

8b, 8c, & 8d. **PROJECT NUMBER:** Enter the appropriate military department identification, such as project number, subproject number, system numbers, task number, etc.

9a. **ORIGINATOR'S REPORT NUMBER(S):** Enter the official report number by which the document will be identified and controlled by the originating activity. This number must be unique to this report.

9b. **OTHER REPORT NUMBER(S):** If the report has been assigned any other report numbers (*either by the originator or by the sponsor*), also enter this number(s).

10. **AVAILABILITY/LIMITATION NOTICES:** Enter any limitations on further dissemination of the report, other than those imposed by security classification, using standard statements such as:

- (1) "Qualified requesters may obtain copies of this report from DDC."
- (2) "Foreign announcement and dissemination of this report by DDC is not authorized."
- (3) "U. S. Government agencies may obtain copies of this report directly from DDC. Other qualified DDC users shall request through _____."
- (4) "U. S. military agencies may obtain copies of this report directly from DDC. Other qualified users shall request through _____."
- (5) "All distribution of this report is controlled. Qualified DDC users shall request through _____."

If the report has been furnished to the Office of Technical Services, Department of Commerce, for sale to the public, indicate this fact and enter the price, if known.

11. **SUPPLEMENTARY NOTES:** Use for additional explanatory notes.

12. **SPONSORING MILITARY ACTIVITY:** Enter the name of the departmental project office or laboratory sponsoring (*paying for*) the research and development. Include address.

13. **ABSTRACT:** Enter an abstract giving a brief and factual summary of the document indicative of the report, even though it may also appear elsewhere in the body of the technical report. If additional space is required, a continuation sheet shall be attached.

It is highly desirable that the abstract of classified reports be unclassified. Each paragraph of the abstract shall end with an indication of the military security classification of the information in the paragraph, represented as (TS) (S) (C), or (U).

There is no limitation on the length of the abstract. However, the suggested length is from 150 to 225 words.

14. **KEY WORDS:** Key words are technically meaningful terms or short phrases that characterize a report and may be used as index entries for cataloging the report. Key words must be selected so that no security classification is required. Identifiers, such as equipment model designation, trade name, military project code name, geographic location, may be used as key words but will be followed by an indication of technical context. The assignment of links, rules, and weights is optional.

GPO 886-551

Unclassified

Security Classification